Title
Cysteine Protease Function in Trypanosoma brucei

Author
O'Brien, Theresa Cunningham

Publication Date
2007-12-20

Peer reviewed|Thesis/dissertation

CYSTEINE PROTEASE FUNCTION IN TRYPANOSOMA BRUCEI

by

THERESA CUNNINGHAM O'BRIEN

DISSERTATION

Submitted in partial satisfaction of the requirements for the degree of

DOCTOR OF PHILOSOPHY

in

BIOCHEMISTRY AND MOLECULAR BIOLOGY

in the

GRADUATE DIVISION

of the

UNIVERSITY OF CALIFORNIA, SAN FRANCISCO

ACKNOWLEDGEMENTS

I am indebted to my family, friends, and labmates for their support. I would like to thank my advisor, Jim McKerrow, for his guidance and enthusiasm throughout the past 5 years. Zachary Mackey served as a daily mentor to me, especially during the first phase of this project, and I have appreciated his honesty and dedication to teaching and training students, myself included. I am especially grateful for the encouragement and perspective provided by my parents, Audrey and Leo, and brother, Sean. Without their support, my graduate school experience would not have been as productive or enjoyable.

The text of this dissertation is, in part (Chapter 1), a reprint of the material as it appears in the Journal of Biological Chemistry, 279(46): 48426-33. The Journal of Biological Chemistry is copyrighted by the American Society for Biochemistry and Molecular Biology, Inc. Permission granted for publication.

Chapters 2 and 3 include material that will be submitted for review to Molecular and Biochemical Parasitology (with Maha-Hamadien Abdulla, Theresa C. O'Brien, Zachary B. Mackey, and James H. McKerrow as co-authors) and the Journal of Biological Chemistry (with Theresa C. O'Brien, Zachary B. Mackey, Richard D. Fetter, Conor R. Caffrey, Youngchool Choe, Charles S. Craik and James H. McKerrow as co-authors), respectively.

CYSTEINE PROTEASE FUNCTION IN *TRYPANOSOMA BRUCEI*

Theresa Cunningham O'Brien

Abstract

Treatment of *Trypanosoma brucei* with cysteine protease inhibitors demonstrated that clan CA cysteine protease activity was essential for parasite viability in culture and infection in mice. However, the identity and biological function of the essential protease or proteases targeted by these inhibitors was not known. Biochemical, molecular biology, and proteomics techniques were used to identify potential targets of inhibition and to investigate the biological function of cysteine proteases in *T. brucei.*

A search of the *T. brucei* genome revealed two cysteine proteases: the previously characterized cathepsin L-like cysteine protease, rhodesain, and a newly-identified cathepsin B-like cysteine protease, tbcatB. Rhodesain is expressed at high levels in procyclic and bloodstream form parasites. TbcatB was found to be expressed at low levels relative to rhodesain, but was more abundant in bloodstream form parasites. RNA interference (RNAi) of rhodesain in cultured parasites did not produce a phenotype. In contrast, a modest decrease in tbcatB mRNA and protein caused by RNAi produced a marked phenotype, with swollen endosomes, accumulation of fluorescein isothiocyanate-transferrin, and a block in cytokinesis, resulting in death. Induction of RNAi against tbcatB in a mouse model of infection confirmed that tbcatB is essential for parasite survival *in vivo*. The *in vivo* induction of RNAi against rhodesain did not cure infection, although it extended the survival of five out of ten mice beyond 60 days post-infection. TbcatB-deficiency produced by either *TBCATB* heterozygosity or RNAi caused

morphological abnormalities similar to those seen with cysteine protease inhibitors. TbcatB-deficient parasites exhibited swollen flagellar pockets and accumulated unprocessed or undegraded host and parasite proteins, including transferrin, p67, and rhodesain. Expression and biochemical purification of active, recombinant tbcatB from *Pichia pastoris* allowed for the determination of the P1-P4 substrate specificity profile. Both results of transferrin cleavage assays and predictions of host substrates based on substrate specificity support the hypothesis that a key function for tbcatB is the degradation of host transferrin. Transferrin receptor expression is specifically upregulated in tbcatB-deficient parasites, consistent with iron starvation.

TbcatB is therefore critical to the survival of *T. brucei* and a logical drug target for the development of new anti-trypanosomal chemotherapy.

TABLE OF CONTENTS

CHAPTER 2: RNAi OF *TRYPANOSOMA BRUCEI* CYSTEINE PROTEASES *IN VIVO* CLARIFIES THEIR CONTRIBUTION TO DISEASE PROGRESSION

CHAPTER 3: A PARSITE CYSTEINE PROTEASE IS KEY TO HOST PROTEIN DEGRADATION AND IRON ACQUISITION

CHAPTER 4: UNPUBLISHED DATA

ABBREVIATIONS

ACC	7-amino-4-carbamoylmethylcoumarin
AMC	7-amino-4-carbamoylmethylcoumarin
BBB	blood brain barrier
BCEM's	human brain microvascular endothelial cells
CA074	N-(L-3-trans-propylcarbamoyloxirane-2-carbonyl)-L-isoleucyl-L-proline
ConA	Conconavalin A
DAPI	4,6-diamidino-2-phenylindole
D-PBS	Dulbecco's phosphate buffered saline
dsRNA	double-stranded RNA
DTT	dithiothreitol
E-64	N-[N-(L-trans-carboxyoxiran-2-carbonyl)-L-leucyl]-agmatine
ER	endoplasmic reticulum
FACS	fluorescence-activated cell sorter
FITC	fluorescein isothiocyanate
FP	flagellar pocket
FR	flanking region
gPGK	glycosomal 3-phosphoglycerate kinase
GPI	glycosylphospatidylinosotiol
HAT	Human African Trypanosomisis
HPLC	high performance liquid chromatography

ABBREVIATIONS

IFA	immunflourescence microscopy
Immuno-EM	immunoelectron microscopy
K11777	*N*-Pip-phenylalanine-homophenylalanine-vinyl sulphone phenyl
K_{cat}	enzyme turnover number
kDa	kilodaltons
K_m	Michaelis constant
LDL	low density lipoprotein
PAGE	polyacrylamide gel electrophoresis
PBS	phosphate buffered saline
PCR	polymerase chain reaction
PMSF	phenylmethylsulfonyl fluoride
PS-SCL	positional scanning synthetic combinatorial peptide library
PVDF	polyvinylidene difluoride)
RNAi	RNA interference
rRNA	ribosomal RNA
SCCA1	quamous cell carcinoma antigen 1
SDS	sodium dodecyl sulfate
TbcatB	*T. brucei* cathepsin B
TetR	Tet repressor
Tf-R	transferrin receptor
TLF	trypanosome lystic factor
U	uridylate
VSG	variant surface glycoprotein

ABBREVIATIONS

Z-Phe-Ala-CHN_2	benzyloxycarbonylphenylalanine diazomethane

LIST OF TABLES

LIST OF FIGURES

LIST OF FIGURES

INTRODUCTION

HUMAN AFRICAN TRYPANOSOMIASIS: AN OVERVIEW

Causative Agent and Disease Burden

Trypanosoma brucei is the causative agent of Human African Trypanosomiasis (HAT) (also known as sleeping sickness), a fatal disease that is transmitted by the tsetse fly. Disease distribution is restricted to areas where the tsetse is endemic, and cases have been reported in 36 countries in sub-Saharan Africa. In 2000, the WHO estimated that 300,000 to 500,000 people suffered from the disease, while an additional 50-60 million people were at risk (meaning that they were exposed to the bit of the tsetse fly) (1,2). Global health experts have calculated that HAT contributes 1,525,000 DALYs, which is a measure of the number of healthy years of life lost due to premature death and disability, to the total global health burden (3). Recent outbreaks of HAT in villages in the Democratic Republic of Congo, Angola, and Southern Sudan have been so severe that disease prevalence levels reached 50%, surpassing HIV/AIDS as the greatest cause of mortality (2). Improved disease surveillance has lead to a decrease in the number of current cases (estimated currently at 50, 000-70,000) (2). However, it is impossible to know the real number of current HAT cases because surveillance programs are lacking in many rural and politically-unstable regions.

Pathology and Life-Cycle of *T. brucei*

Two sub-species of *T. brucei* infect humans, *T. brucei gambiense*, found in western and central Africa, and *T. brucei rhodesiense*, found in eastern and southern Africa. The geographical distribution of the *T. brucei* sub-species is determined by the species of

Glossina (or tsetse fly) that it infects: *T. brucei gambiense* infects *G. palpalis* and *T. brucei rhodesiense* infects *G. morsitans*. Animals are known to serve as a reservoir for *T. brucei rhodesiense*, while other *T. brucei* subspecies are pathogenic only to animals (2). Those *T. brucei* that are pathogenic only to animals cannot infect humans because normal human serum contains a "trypanosome lytic factor", identified as the human-specific serum protein apolipoprotein L-I, that lyses the parasites (4) (5) (6). Sleeping sickness in domesticated animals, particularly in cattle, poses a major obstacle to economic development in rural areas that are affected by the disease. The primary subspecies that infects cattle is *T. brucei brucei* and the disease in cattle is called "nagana" (a Zulu word meaning "to be depressed").

Humans become infected with *T. brucei* when an infected tsetse fly takes a blood meal. In the initial stage of the disease, parasites proliferate in the blood. Patients experience headaches, fever, itching, aches and pains in their joints and can present with Winterbottom's sign, which is a pronounced swelling of the lymph nodes along the back of the neck. In the second, neurological stage of the disease, parasites cross the blood brain barrier and establish infection in the central nervous system, causing irreversible neurological damage. Patients exhibit sensory disturbances, confusion, irritability, alerted sleep/wake patterns, and eventually coma. It is the sleep disturbances that give the disease the name "sleeping sickness". If untreated, HAT is fatal.

The speed of progression from the initial stage of the disease to the second, neurological stage varies depending on the sub-species of *T. brucei*. *T. brucei gambiense* causes a chronic form of HAT, in which progression takes from months to years. In contrast, HAT caused by *T. brucei rhodesiense* is an acute disease, with neurological

symptoms presenting several weeks after infection. Evolutionary studies indicate that *T. brucei gambiense* has been associated with humans for a longer period of time than *T. brucei rhodesiense*, a fact that may explain why the later is less virulent (7).

The *T. brucei* life cycle alternates between a mammalian host and the tsetse fly vector. When in the mammalian host, *T. brucei* are in their bloodstream form, while in the tsetse fly vector, the parasites are in their procyclic form. The main difference between these forms is the character of the surface coat proteins expressed by the parasite. Bloodstream form *T. brucei* express a coat of variant surface glycoproteins (VSGs) and procyclic *T. brucei* exhibit a coat of procyclins (EP and GPEET proteins (8)). When an infected tsetse fly takes a blood meal, it transmits metacyclic trypomastigotes, which proliferate in the bloodstream as morphologically "long slender" bloodstream forms. The metacyclic trypomastigotes are later replaced with non-proliferative "short stumpy" bloodstream forms as parasite numbers increase. It is the short stumpy parasites that are infective to tsetse flies. Upon uptake by the tsetse, procyclic form parasites are generated. The parasites, called procyclic trypomastigotes at this stage, first proliferate in the fly midgut, then arrest in division and migrate to the salivary glands where they attach as epimastigotes. After further proliferation in the salivary glands, the epimastigotes are replaced with non-proliferative metacyclic trypomastigotes, which are infective to humans.

Diagnosis and Treatments

Since neurological damage is inevitable once parasites have crossed the blood brain barrier of the mammalian host, it is crucial that a *T. brucei* infection is diagnosed as early as possible. Diagnosis of HAT requires identifying parasites in the patient. Serological

tests are commonly used to screen patients, but health care workers may also screen for clinical manifestations, such as the Winterbottom's sign. If parasites are identified in the blood or serum, a lumbar puncture is then carried out and the cerebrospinal fluid is examined for parasites. Diagnosis of the initial stage of the disease is hampered by the fact that many patients are asymptomatic. Diagnosis is further complicated when parasite numbers in the serum are low, which is often the case in *gambiense* infections (*rhodesiense* infections, in contrast, yield high parasite loads). Since *gambiense* infections are chronic, frequent screening is required to reduce transmission, and effort that requires significant financial and human capital to implement. There is a clear need to develop new, low cost, minimally-invasive diagnosis techniques that will allow for the detection of a small number of parasites.

Treatment of HAT is limited to four drugs, all of which have serious side effects in patients. Suramin and pentamidine are used to treat the initial stage of the disease, while melarsoprol and eflornithine are used to treat the neurological stage of HAT. Drug resistance, drug toxicity, and the cost of manufacturing and administering these drugs further complicate treatment, especially in the neurological stage of disease. The following offers a short description of each drug (2,9):

- Suramin (discovered in 1921) is used to treat the initial stage of *gambiense* infections. Side effects of suramin treatment include nausea, vomiting, tingling skin, rash, and adrenal cortical damage. Suramin is administered intravenously.
- Pentamidine (1937) is used to treat the initial stage of *rhodesiense* infections. Treatment with pentamidine can cause allergic reactions, kidney damage,

hypotension (arrhythmias and heart failure), nausea, skin irritation, and anemia in patients. Pentamidine is administered parenterally.

- Melarsoprol (1941), which is an arsenic derivative, is extremely toxic. It is used to treat the neurological stage of both *gambiense* and *rhodesiense* infections. Melarsoprol treatment is associated with mortality rates of up to 10% and relapse occurs in up to 20% of cases. Side effects of melarsoprol treatment include reactive encephalopathy, convulsions, loss of consciousness, and death. The drug is administered intravenously and is too irritant for intramuscular administration. Reports of resistance to melarsoprol are on the rise in certain areas in central Africa.
- Eflornithine (1990), or DFMO, is used to treat the neurological stage of *gambiense* infections (although, it is also effective against the initial stage). It is the only drug used to treat HAT that is the product of targeted drug design. Eflornithine targets ornithine decarboxylase, a key enzyme involved in polyamine biosynthesis. The drug was originally developed to treat cancer, and was later found to be effective in treating HAT. Eflornithine has been referred to as the "resurrection drug", since it is capable of bringing patients back from coma. Although it is 95% effective, the drug is not widely used because it costly to manufacture and time-consuming to administer, requiring 4 infusions per day for 14 days. Treatment with eflornithine can cause diarrhea, anemia, and convulsions.

Given the limitations of these drugs, there is an obvious and urgent need to develop new chemotherapies.

One new drug, pafuramidine maleate, is in phase III clinical trials for the treatment of early stage HAT. The drug is an aromatic cationic compound, which was modeled after pentamidine (10 pipeline). Modifications to the pentamidine's structure decreased the drug's toxicity, while improving its binding activity and absorption in the gastrointestional tract. Importantly, pafuramidine is also orally bioavailabile and can withstand tropical conditions necessary for transport and storage. Although the drug's mechanism of action is not completely understood, pafuramidine is known to bind segments of DNA and thereby disrupt processes required for cellular growth. Development of the drug has been carried out by a consortium of more than a dozen faculty from institutions in the United States, Europe, and Africa, along with Immtech Pharmacuticals, based in Veron Hill, VA (11). The consortium is lead by Dr. Richard Tidwell at the University of North Carolina Chapel Hill and has received significant funding from the Bill and Melinda Gates Foundation. Phase III clinical trials are being carried out in the Democratic Republic of Congo, Sudan, and Angola and favorable interim analysis of the trials were announced in October, 2007 (12). The FDA has approved pregnant and lactating women for participation in the trials, since pafuramidine demonstrated a favorable safety profile in prior animal and human studies (10 pipeline). The regulatory body also granted "Orphan Drug Status" to the drug, meaning that Immtech Pharmaceuticals will receive financial and regulatory benefits in order to facilitate pafuramidine's development for the treatment of HAT (13).

The search for Drug Targets

Much of the past and present research on *T. brucei* has focused on the identification and validation of drug targets – that is, identifying genes that have essential function(s) in

T. brucei and then demonstrating that the gene product is an exploitable drug target. As mentioned above, elflornithine is the only drug currently used to treat HAT that was designed for a specific target. Suramin, pentamidine, and melarsoprol were all discovered because of their (or a related compound's) anti-typanosomal activity and mechanisms of action for the drug are still being investigated (14). The story is the same for most other tropical parasitic diseases – a limited number of drugs are available and the targets for the drugs are largely unknown (15). Furthermore, many of the drugs that have been put into use to treat tropical parasitic diseases arose as the result of veterinary and/or cancer research (15). Several broad classes of targets that are being studied for use against HAT include pentamidine analogs, enzymes involved in pyrimidine biosynthesis, enzymes required for response to oxidative stress, enzymes that function in carbohydrate metabolism, kinases, and proteases (16). Specific targets have been validated in many, but not all of these cases. While target validation is desired, failure to validate a specific target is not always a strong-enough reason to terminate drug development (16), especially given that the specific targets and mechanisms of action for current therapies are largely unknown.

The completion of the *T. brucei* genome (17) and development of high-throughput techniques for evaluating gene function by RNAi (18), has aided the process of target identification significantly. Recent efforts have been made to facilitate the validation and early drug development process as well, with publications that elucidate the characteristics of exploitable targets and demystify the drug development pipeline, consortia that bring together researchers from across the globe, and collaborations between academic institutions, non-profit organizations, and drug companies. Major

government and philanthropic organizations, such as the World Health Organization, Welcome Trust, Gates Foundation, and Sandler Family Supporting Foundation, have also contributed substantially in recent years to drug discovery and development efforts aimed at HAT and other tropical parasitic diseases (16). With a growing number of potential targets and a significant (although, far from robust) stream of funding, one of the greatest challenges facing researchers is how to identify which targets are exploitable for drug development. The ideal characteristics of a drug target may include (15):

- Essential function has been demonstrated in the appropriate parasitic lifecycle stage (bloodstream form, in *T. brucei*).
- The target is sufficiently different than homologous host enzymes.
- The target can be inhibited pharmacologically at levels high enough to ablate essential activity.
- Design of inhibitors with drug-like properties is feasible.

Once a drug target has been selected for further development, researchers face the even greater obstacle of moving the target through the time-consuming and expensive drug development pipeline. With the goal of bringing new, safer chemotherapies to patients suffering from HAT as soon as possible, researchers are currently combining their efforts at targeted-drug discovery with high-throughput screening technologies that allow for the rapid identification of compounds that have anti-trypanosomal activity and have already passed FDA-approval (19).

LABORATORY STUDY OF *TRYPANOSOMA BRUCEI*

T. brucei as a Model Organism

T. brucei has become a model system for studying cellular function in protists. The cellular structure of the parasite shares much with other eukaryotes. For example, *T. brucei* has all of the major organelles (nucleus, mitochondria, endoplasmic reticulum, and Golgi apparatus), as well a complex endocytic system that includes coated vesicular transport. The endocytic system is also highly polarized, facilitating the study of endocytic mechanisms. *T. brucei* are large enough (approximately 3 μm by 20 μm) to visualize under a light microscope and their cellular components are readily visualized using immunofluorescence and electron microscopy techniques. Furthermore, the parasites can be grown in quantities large enough to facilitate biochemical analysis, such as purification and analysis of specific organelles. *T. brucei* are also one of the earliest eukaryotes in which RNA interference (RNAi) has been discovered, making the parasite a model organism for the study of RNAi mechanisms.

Unique features of *T. brucei* also motivate investigation. Of particular interest is the parasite's mechanism for evading the host immune system, known as antigenic variation. *T. brucei* can express different, antigenically distinct VSGs, the glycoproteins that coat the surface of bloodstream form parasites. Since VSG's are on the parasite's surface, they are exposed to attack by the host's immune system and, in particular, are the target of host B cells. VSG is an abundant protein, with approximately 10^7 copies per cell. Most parasites in a population will express the same VSG. However, with each

generation, a small number of parasites switch the VSG that they express[1]. These parasites evade the host's immune defenses and multiply, while those parasites that did not switch, perish. The process leads to observed "waves" of parasitemia in the host's blood. *T. brucei* are believed to have more than 1000 distinct VSG genes and the mechanism by which they switch the gene that is expressed is an active area of research.

T. brucei have a number of unique cellular structures, namely the kinetoplast, flagellar pocket, and glycosomes. The kinetoplast contains the mitochondrial genome of *T. brucei* and its presence bestows membership in the order kinetoplastida[2]. The mitochondrial genome in *T. brucei* is made up of condensed maxi-circle and mini-circle DNA. The maxi-circle DNA encodes key mitochondrial genes, while the function of mini-circle DNA is less clear. A process known as RNA-editing occurs in some of the genes encoded in the maxi-circles. These genes contain small "errors", which are repaired after transcription, using guide RNAs that are also synthesized in the maxi-circles. RNA-editing specifically involves the insertion and (less frequently) deletion of uridylates (U's) at multiple sites in mitochondrial pre-mRNA to produce mature mRNAs. Editing can be so extensive as to add more U's to the mature transcript than nucleotides present in the pre-mRNA (21). Research has focused on understanding the complex enzymatic steps required for editing and identifying the macromolecular complex required for catalysis.

The flagellar pocket (FP) is the site of all endocytosis and exocytosis in the *T. brucei*. It is located at the base of the flagellum and is cytoskeletally-defined (although the

[1] The rate at which *T. brucei* switch the VSG expressed is 10^{-2} per cell per generation 20. Vanhamme, L., Pays, E., McCulloch, R., and Barry, J. D. (2001). An update on antigenic variation in African trypanosomes. *Trends Parasitol*. **17**(7), 338-343.

[2] Kinetoplasts are flagellated protozoan organisims. Both *Trypanosoma* and *Leishmania* species are kinetoplasts.

identity of filaments that define the FP neck is not known) (22). The flagellar pocket membrane is continuous with the surface and flagellar membranes and a good deal of research has focused on understanding what defines each of these membranes. Two membrane-bound proteins, VSG and transferrin receptor, are endocytosed at particularly high rates in *T. brucei* (23). Both proteins are involved in essential processes in *T. brucei* – that is, antigentic variation (VSG) and iron acquisition (transferrin receptor) – and are glycosylphosphatidylinisotol (GPI)-anchored. Given that GPI-anchored proteins are ubiquitous in the animal kingdom, it's no surprise that *T. brucei* is also a model organism for studying the endocytosis and trafficking of GPI-anchored proteins.

Glycosomes contain glycolytic enzymes (hence, their name) and were first discovered in *T. brucei* (24). The organelle contains all of the enzymes necessary for glycolysis and this compartmentalization is unique to kinetoplastid protozoans. Glycosomes are related to peroxisomes, although in *T. brucei* they function almost exclusively in glycolysis.

***In vitro* and *in vivo* Study**

Molecular, biochemical, genetic, cell biological, and tissue culture techniques have been developed for the study of *T. brucei in vitro*. Both procyclic and bloodstream form parasites can be stably maintained in culture, and most strains are capable of being induced to differentiate from one form to the other while in culture (although some strains differentiate more readily). Bloodstream form parasites are also capable of growing to high densities on agarose plates containing culture medium (25). *T. b. brucei* is commonly studied in the laboratory, since it is non-pathogenic to humans. However, there are cases in which it is necessary to study *rhodesiense* and *gambiense* strains, particularly when the research question involves understanding the mechanism of disease

in humans. Procyclic and bloodstream forms of *T. brucei* are cultured in different media (Cunningham's or HMI-9[3], respectively), at different temperatures (27 °C and 37 °C, respectively), and under different CO_2 conditions (without CO_2 and with 5% CO_2, respectively). To induce differentiation from bloodstream to procyclic *T. brucei*, the temperature is dropped to 27 °C and the medium switched to Differentiating Trypanosome Medium (26), which is supplemented with ≥ 3mM citrate or cis-aconitate (25). Differentiation from procyclic to bloodstream form parasites is much more difficult and no reliable protocols have been established.

Various animal models of *T. brucei* infection have also been developed, although the most common laboratory animals used are mice and rats (examples: (27) (28) (29) (30)).

Genetic Manipulations in *T. brucei*

T. brucei are genetically tractable organisms and genetic manipulations have been aided by the completion of its genome (17,31). Well-established techniques exist for transient and stable transfection, inducible expression, gene knockout, and RNA interference (RNAi) in *T. brucei*. Transfection in *T. brucei* is carried out by electroporation with circular or linearized DNA vector and recent advances in electroporation technology have increased rates of transient and stable transfection. Transient transfection requires the use of an RNA polymerase I (usually, an EP promoter in procyclics or VSG promoter in bloodstream form parasites) or ribsosomal RNA promoter (32). A linearlized vector must be used to generate stable transformants. The vector is linearized at sequences identical to those in the desired integration site and integration occurs by homologous recombination. The vector can be targeted to a region

[3] Both Cunningham's medium and HMI-9 medium are supplemented with 10% fetal bovine serum and 1x penicillin/streptomycin. In addition, 10% Serum Plus™ (JRH Bioscinces) is added to HMI-9 medium.

that is transcribed by endogenous RNA polymerase II, or to a silent region of the genome (such as the ribosomal RNA spacer) if an RNA polymerase I is present in the construct. Reporter gene transcription is greater in the latter scenario, when RNA polymerase I is used (32). Transcription efficiency can be further increased when the vector construct contains a bacteriophage T7 promoter and is transfected into a strain of *T. brucei* that stably expresses the bacteriophage T7 polymerase (33). A small number of selectable, or drug-resistance, markers can be used in *T. brucei*. They include: NEO (selection with the drug G418), HYG (hygromycin), BLE (phleomycin), SAT (nourseothricin), PUR (puromycin), and BSR (blasticidin).

T. brucei is a diploid organism, so both heterozygous and homozygous (or complete) gene knockouts can be generated. However, if the gene of interest is essential, only the heterozygote can be generated. Gene deletion constructs include a selectable marker (hygromycin resistance, for example) flanked by 5' and 3' regions from the gene to be targeted and gene deletion occurs by homologous recombination. Heterozygous knockout parasites are selected by culturing in media containing the appropriate drug (*i.e.* hygromycin). Once a heterozygous knockout is generated, a second gene deletion construct is used, which contains a different selectable marker (blasticidin resistance, for example). Parasites that survive in media containing two selectable drugs (*i.e.* hygromycin and blasticidin) have incorporated both gene deletion cassettes and are presumed to be complete gene knockouts. However, steps must be taken to confirm that both copies of the targeted gene have been deleted, since it is possible for the gene deletion vectors to be integrated upstream or downstream of the targeted gene or to be integrated elsewhere in *T. brucei* genome. Complete gene knockouts can also be

generated by culturing heterozygous knockout parasites in increasing amount of selective drug, although this process is time-consuming and there is no guarantee of success (32). The effect(s) of a complete gene knockout should be assayed in culture, as well as in an *in vivo* model of infection, since virulence phenotypes cannot be assayed in culture. Many gene knockout strategies are complicated in *T. brucei* by the fact that many genes are present in multiple copies. In these cases, RNAi strategies are often the preferred method for assessing gene function.

The preferred system for inducible expression in *T. brucei* utilizes the Tet repressor (TetR). TetR functions in *E. coli* (and other gram-negative bacteria) to repress expression of *tetA*, which encodes a protein that exports the antibiotic tetracycline out of the cell and thereby confers tetracycline-resistance on the bacteria (34). The TetR exerts its inhibitory effect by binding to a specific DNA sequence that lies downstream of the promoter for *tetA* and, thus, inhibiting transcription initiation. This sequence, called the *tet* operator, is also present upstream of the *tetR* gene. When tetracycline is present, TetR binds the antibiotic and undergoes a conformational change that prevents it from binding the *tet* operator. As a result, transcription is initiated from the *tetA and tetR*. The *T. brucei* inducible expression system takes advantage of the tightly-regulated system in bacteria. The constructs that are generated for inducible expression contain an EP promoter (in procyclic form parasites) or an EP promoter and a T7 promoter (in bloodstream for parasites) that are under regulation by the *tet* operator, as well as 5' and 3' flanking regions targeting silent regions of the genome (usually rRNA) and a selectable marker (32). The constructs are then transfected into a transgenic *T. brucei*

line that constitutively expresses the TetR and bacteriophage T7 RNA polymerase (35). Addition of the tetracycline to the culture media will induce expression of the target gene.

Inhibition of gene expression by RNAi has become the method of choice to study gene function in *T. brucei* (36). Transient RNAi was first achieved in 1998 by electroporation of *in vitro* synthesized dsRNA (37) and was followed, two years later, by the first stably maintained RNAi construct, which expressed a stem-loop transcript (36). Later that year, a vector (pZJM) was developed for *in vivo* tetracycline-inducible synthesis of dsRNA in stably-transformed procyclic *T. brucei* (38) and, just a few months later, its use was extended to bloodstream form parasites (39). The pZJM vector allows PCR generated fragments of any target gene to be inserted between opposing tetracycline-T7 promoters. The vector takes advantage of many of the elements described above for tetracycline-inducible expression, including the T7 promoters, Tet operators, homology region, phleomycin selectable marker, and integration into a non-transcribed region of the genome of parasites that express the TetR and T7. As discussed above, conventional gene knockouts are time-consuming, especially when the gene of interest is present in a multi-copy tandem repeat. In contrast, RNAi in *T. brucei* can take a little as three weeks from the identification of a gene sequence to the appearance of a phenotype and has the benefit of inhibiting the expression of multiple gene copies at one time. RNAi techniques in *T. brucei* were also developed several years before the completion of the parasite genome (17), and thus had a particular advantage in that only a few hundred base pairs of a gene sequence is needed for targeting. Forward genetics strategies are possible using RNAi, and chromosome-wide analysis of gene function by RNAi has been carried out (18). It should not be long until all of the *T. brucei*

chromosomes have been targeted by RNAi (40), an achievement that will no doubt facilitate the identification of new drug targets for the treatment of HAT.

PROTEASES AS PARASITIC DRUG TARGETS

Proteases of Protozoan Parasites

Proteases are critical to the life-cycle and pathogenicity of parasitic organisms and protease inhibitors have been validated as drug targets in number of organisms, and most importantly humans (41,42). It is no surprise, then, that proteases are attractive targets for drug development to treat HAT, as well as other parasitic diseases. Parasite proteases are sufficiently divergent from homologous host enzymes such that small molecule chemical inhibitors can be designed to selectively inhibit the parasite enzyme and not result in deleterious inhibition of the host's enzyme(s) (16). Several families of parasitic proteases have been targeted, including cysteine proteases, aspartylproteases, serine proteases, and metalloproteases (16,43).

Cysteine Proteases of Primitive Protozoa: An Evolutionary Perspective

Cysteine proteases have emerged as a particularly important class of enzymes in parasitic protozoa, both in terms of their biological functions and potential as exploitable drug targets. In particular, Clan CA (papain-like) cysteine proteases carry out many of the functions of Clan SA (trypsin-like) serine proteases in higher eukaryotes. It has been shown that papain-like cysteine proteases and Clan SA (trypsin-like) serine proteases underwent an evolutionary inversion, which resulted in the more abundant cysteine proteases of primitive eukaryotes giving way to serine proteases with the evolution of arthropods (http://merops.sanger.ac.uk/) (44). Further, parasitic cysteine proteases and

aspartylproteases are known to carry out functions that, in vertebrates, are the responsibility of proteases from other classes (43).

Genomic data indicate that there was an explosion of gene diversity in the clan CA cysteine proteases coincident with the evolution of the first eukaryotic cell. Biochemical analyses of several protozoa, which exist today in large part because of their successful adaptation to parasitism, suggest that many Clan CA cysteine proteases can function in a broader range of chemical environments than homologous host enzymes. The broad pH profile for these proteases is consistent with numerous extra-lysosomal functions that have been proposed in recent years, including host protein degradation, tissue and cell invasion, excystment/encystment, protein processing and activation, and immunoevasion (43). The biological functions of this enzyme family are, thus, diverse and, in many cases essential, making them attractive drug targets. Along with aiding drug discovery, an understanding of the specific functions of parasitic Clan CA cysteine proteases is worthwhile in that it will contribute to our understanding of what makes this enzyme family so common and so useful to primitive cells.

Proof of Concept: Cruzain and K11777

Proof of concept for the use of cysteine protease inhibitors to treat tropical parasitic diseases was first demonstrated in mouse models of malarial and *Trypanosoma cruzi* infections (45-47). *T. cruzi* is the causative agent of Chagas' disease, a chronic disease that is prevalent in South America and fatal if untreated. *T. cruzi* belongs to the same order as *T. brucei*, although the geographical distribution, parasite life-cycle, and pathology in its insect and mammalian hosts differ significantly. A class of cysteine protease inhibitors derived from a fluoromethyl ketone scaffold was first used in the

malaria and *T. cruzi* studies. Importantly, the inhibitors not only arrested the parasitic infections, but they also selectively targeted the parasite cysteine proteases. With initial proof of concept firmly established, work on cysteine protease inhibitors to treat *T. cruzi* infection shifted from the more toxic fluoromethyl ketone derivatives to the less toxic vinyl sulfone-derivatised pseudopeptides. The vinyl sulfone derivatives were shown to cure a mouse model of *T. cruzi* infection (48) and to specifically target cruzain, a cathepsin L-like cysteine protease in *T. cruzi* (49). The most effective inhibitor in these studies was N-methyl-Pip-F-hF-VS-phenyl, also known as K11777 (49). Work on K11777 has progressed to late stage of pre-clinical development for *T. cruzi*, with the compound passing toxicity tests in rodents, dogs, and primates and demonstrating good pharmacokinetic properties (43,50,51). The effectiveness of the vinyl sulfone scaffold for treatment of parasitic diseases is evident in the diversity of parasites that have now been targeted, including trypanosomes and schistosomes (52) (16), and the fact the scaffold is the now most widely studied cysteine proteases inhibitor scaffold (16,52). Thus, the work with K11777 to treat Chagas' disease clearly demonstrates that cysteine protease inhibitors can be viable drug candidates (43).

CYSTEINE PROTEASES IN *TRYPANOSOMA BRUCEI*

Cysteine Proteases and *T. brucei*: Review of Literature Prior to 2003

Evidence for cysteine protease activity in *T. brucei* dates back to at least the early 1980's (53). In these initial studies, protease activities were identified by their ability to cleave fluorescent peptide substrates, by their appearance on polyacrylamide gels containing protein substrates, and by the protease inhibitors that reduce their activity (54).

Cysteine proteases were distinguished from other protease classes (serine proteases, for example) by the inhibitors that reduced their activity. In particular, sensitivity to E-64 (a Clan CA cysteine protease inhibitor) suggested the presence of one or more cysteine proteases in parasite lysates and conditioned medium (54). On their own, though, these inhibition data revealed little about the identity and function of specific cysteine proteases in *T. brucei*. Inhibition studies have remained an important tool for characterization, although the emphasis of this work has moved towards the identification of drug leads. The following highlights the key discoveries that shaped our understanding of cysteine proteases and their function in *T. brucei* through the end of 2002, when this dissertation project began.

An important observation was made in 1986, when researchers compared the thiol-dependent protease activities of four African trypanosomes: *T. brucei* (*T. brucei brucei* and *T. brucei gambiense*), *T. evansi*, *T. congolense*, and *T. vivax*. Lonsdale-Eccles *et al.* identified thiol-dependent protease activity in the trypanosomes that resembled mammalian cathepsins B and L (55) in peptide and substrate specificities, and had a pH profile between 5 and 6. Interestingly, they found that cysteine protease activity was maximal in bloodstream *T. brucei*, as compared to procyclic parasites (55). In follow-up studies, the group localized a cathepsin L-like activity to lysosomes in bloodstream form *T. brucei brucei* (56). The first clue to identity of this cysteine protease came in 1989 when Mottram *et al.* cloned and sequenced a *T. brucei* cDNA that showed considerable homology with mammalian cathepsin L (57). This homology included the pre-, pro- and central regions of the *T. brucei* protease, but did not include a proline-rich C-terminal extension, which the researchers concluded was unique to trypanosomes (57). Mottram

et al. also discovered that the parasite's genome contains more than 20 copies of the cysteine protease gene, which are arranged in a tandem array (57). Working at approximately the same time, Eakin *et al*. identified a genomic DNA fragment from *T. brucei* that shared homology with chicken cathepsin L (58). Less than a year later, Pamer *et al.* reported cloning and sequencing a cathepsin L-like cysteine protease from *T. brucei rhodesiense* (59). To clone the protease, Pamer *et al.* used the genomic fragment identified by Eakin *et al.* (58) to screen a *T. brucei rhodesiense* cDNA library (59). Sequencing revealed that the cysteine protease was nearly identical to that obtained by Mottram *et al.* (57).

It is worth noting out here that different names are used today to describe homologous cathepsin L-like cysteine proteases in *T. brucei* subspecies. Initially, all cysteine proteases from African trypanosomes were referred to as trypanopains (hence, trypanopain-Tb from *T. brucei* (60) and trypanopain-Tc from *Trypanosoma congolense* (61)). Later, researchers wanted to distinguish the cathepsin L-like proteases from *T. brucei rhodesiense* and *T. brucei brucei* and, thus, termed them rhodesain and brucipain, respectively. Rhodesain and brucipain are nearly identical in sequence and it is assumed that they play the same functional role in both subspecies of *T. brucei*.

Very little was known about the biochemical properties of the *T. brucei* cathepsin L-like protease until recombinant rhodesain was expressed in *Pichia partoris*, purified, and biochemically characterized (62). Earlier expression of the enzyme in *Escherichia coli* indicated that the C-terminal extension was not required for proteolytic activity (63). In 1996, Troeberg *et al.* used a combined purification scheme to isolate trypanopain-Tb and an important serine protease, oligopeptidase-Tb, from *T. brucei brucei* lysates (64). They

showed that trypanopain-Tb and oligopeptidase-Tb have distinct pH optima (acidic and alkaline, respectively) and substrate specificities (consistent with cysteine and serine proteases, respectively) (64). Interestingly, they also evaluated the effectiveness of host proteases inhibitors on the purified enzymes and found that trypanopain-Tb was effectively inhibited by kininogens and various cystatins, even when these inhibitors are present in concentration that are 10 times lower than their physiological K_i (64). In 2001, Caffrey *et al.* sought to express reagent quantities of rhodesain for use in structure-based inhibitor design and inhibitor screening with the goal of identifying new drug leads. The group expressed rhodesain in *P. pastoris* and obtained active, mature protease. They then used a relatively simple scheme (lyophilization, incubation at acidic pH, and buffer exchanges) to purify the enzyme. Subsequently, the group produced antibodies to purified rhodesain and used them to confirm the enzyme's lysosomal localization (56) and differential expression – that is, that rhodesain activity is higher in short stumpy bloodstream form *T. brucei rhodesiense* than in procyclic and long slender bloodstream form parasites (65,66). Caffrey *et al.* also reported the pH profile and P2 substrate specificity of recombinant rhodesain, with a maximal activity against the Z-Phe-Arg-NMec substrate between 5.0 and 5.5 and preference for bulky hydrophobic amino acids at P2 (62). Importantly, the group also confirmed that rhodesain is the major cysteine protease in *T. brucei* by using an active site label that is specific to cysteine proteases to probe *T. brucei rhodesiense* and *T. brucei brucei* extracts (62). Both the label and the antibody produced against recombinant rhodesain recognized a 40 kDa protein (62) and labeling could be inhibited using cysteine protease inhibitors. Caffrey *et al.* pointed out that active site label produced fainter labeling of proteins with molecular weights of 33

and 29 kDa, and hypothesized that they may represent differentially glycosylated forms of rhodesain lacking the C-terminal domain. Thus, by the end of 2002, only one Clan CA cysteine protease, rhodesain/brucipain, had been identified and studied in *T. brucei*.

In the process of identifying and characterizing cysteine protease activity in *T. brucei*, researchers obtained some clues as to the function of these enzymes. The first indication of a function for *T. brucei* cysteine proteases in parasite protein degradation came from the observation that a cathepsin L-like protease localized to the lysosome (55). Cysteine proteases were further implicated as playing a role in host protein degradation when transferrin, which is the sole source of iron for *T. brucei*, was found to co-localize with a lysosomal cysteine protease (67,68). The localization of FITC-transferrin to the lysosome was dependent on treatment with cysteine protease inhibitors[4], further implicating cysteine proteases as being responsible for degrading host transferrin upon arrival to the lysosome (68). Cysteine proteases were also implicated in the processing of a lysosomal membrane glycoprotein, p67 (69). The p67 protein co-localizes with transferrin and rhodesain and its cleavage is inhibited by leupeptin (a thiol protease inhibitor) (69,70).

T. brucei cysteine proteases were believed to play a role in parasite differentiation and development. Prior to the identification of cysteine protease cDNA by Mottram *et al.* (57) in 1989, Pamer *et al.* reported the presence of a developmentally regulated cysteine protease in *T. brucei* (65). The protease had the same molecular weight as the cysteine protease identified by Lonsdale-Eccles et al. in 1986 (55) and was found to be more prevalent in morphologically short stumpy bloodstream forms than in long slender bloodstream or procyclic forms (65). Pamer *et al.* later compared the cathepsin L-like cysteine protease from *T. brucei rhodesiense* (59) with this developmentally regulated

[4] Under normal conditions, FITC-transferrin is degraded rapidly and cannot be visualized in the lysosome.

(but unidentified) cysteine protease and showed that they were the same protease (63). More recently, Mutomba *et al.* discovered that cultured *T. brucei* fail to multiply following treatment with a selective cysteine protease inhibitor (71). The treated parasites retained both VSG and gPGK, a glycolytic enzyme that is normally down-regulated during differentiation, and expressed high levels of procyclin (71). Thus, these results suggested that one or more cysteine proteases may be involved in releasing VSG and regulating the expression procyclin during differentiation.

An additional role for cysteine proteases in pathogenesis was suggested by the presence of protease activity in the plasma of mice infected with *T. brucei brucei* (72,73). This activity, it was hypothesized, could contribute to pathogenesis by degrading host mediators (proteins). It was later reported that *T. brucei* release distinct proteases after incubation in cold (4 °C) phosphate-saline-glucose buffers of acidic and neutral pH (73-75). One of these proteases had substrate and inhibitor specificities consistent with a cysteine protease (75). Further characterization of the proteases, revealed both serine and cysteine protease activities (76) and showed that lysosomotropic drugs could inhibit the release of these enzymes (76,77). One of the extracellularly released proteases was purified to homogeneity and found to be a putative cathepsin B-like cysteine protease (78). Importantly, this 63kDa protease was released by viable, actively motile, and highly infective trypanosomes (characteristics that the authors argued ruled out the possibility that the released proteases were the product of cell lysis) (78). While these results suggest that cysteine proteases could be important in pathogenesis because they are released from parasites, the authors did not identify a specific function or functions for the protease. An argument against any role for extracellular *T. brucei* proteases is

supported by the fact that purified trypanopain-Tb is effectively inhibited by endogenous host protease inhibitors (64). Host kininogens and cystatins effectively inhibited trypanopain-Tb, while oligopeptidase-Tb was not inhibited by mammalian protein inhibitors (64). Lonsdale *et al.* (1995) reported that a kininogen-like molecule from rat serum enhances the activity of trypanopain (79). Thus, reports leading up the end of 2002 suggested a possible, but not validated, role for extracellular *T. brucei* cysteine proteases in mediating pathogenesis.

Before 2003, *T. brucei* cysteine proteases were implicated in at least two other functions. The enzymes were thought to be important in trypanosome lytic factor (TLF) mediated lysis, since both leupeptin and E-64 inhibit killing by TLF (80)('94 (5). Leupeptin was also found to inhibit the metabolism of lipids carried by low density lipoprotein (LDL), suggesting that a serine or cysteine protease is involved in this process (81).

Although cysteine protease inhibitors have been used to help identify functional roles for *T. brucei* cysteine proteases, a primary purpose for inhibition studies prior to 2003 was to identify inhibitors that are trypanocidal, or capable of inhibiting parasite growth. A number of cysteine protease inhibitors (peptidyl diazomethanes, for example (82)) were shown to be trypanocidal in early studies, although the first rigorous demonstration that these compounds could serve as drug leads came in 1999 when Scory *et al.* showed that a diazomethyl ketone, Z-Phe-Ala-CHN_2, is toxic to bloodstream *T. brucei in vitro* and *in vivo* (30). This compound inhibited proteinolysis in lysosomes (*i.e.* transferrin lysosomal degradation) *in vitro* and almost completely abolished cysteine protease activity *in vivo (30)*. The Z-Phe-Ala-CHN_2 inhibitor was known to be selective for Clan

CA cysteine proteases (83) and it was previously reported that oligopeptidase-Tb is insensitive to the inhibitor (84). Since rhodesain/brucipain is the major cysteine protease activity in *T. brucei*, the authors concluded that the cathepsin L-like cysteine protease was the critical target of Z-Phe-Ala-CHN_2 (30). However, in retrospect, their results did not rule out the possibility that other, unidentified, or relatively minor cysteine proteases may be critical targets. At the same time that Caffrey *et al.* published their work with Z-Phe-Ala-CHN_2 (85), Troeberg *et al.* reported the results of inhibition studies with various cysteine protease inhibitors, including vinyl sulfones, peptidyl chloromethylketones, diazomethylketones, and fluoromethylketones, on brucipain (60,64). This group evaluated the effect of the inhibitors on *in vitro*-cultured *T. brucei brucei* and on brucipain that was purified from *T. brucei brucei* (64). They showed that micromolar concentrations of methylketone and vinyl sulfone inhibitors were trypanocidal for the cultured parasites and suggested that brucipain was their most likely target (60). Together, Scory and Troeberg demonstrated that Clan CA cysteine protease activity is required for *T. brucei* viability *in culture* and added strength to the hypothesis that rhodesain/brucipain is a potential target for antitrypanosomal drugs (30,60,86).

Three additional classes of cysteine proteases inhibitors were shown to trypanocidal in studies carried out prior to 2003. Aryl urea compounds were shown to inhibit recombinant rhodesain and kill *T. brucei* in culture (87). Chalcone, acyl hydrazides, and related amides were likewise trypanocidal (29). Troeberg *et al.* showed that the compounds could protect mice from an otherwise lethal *T. brucei* infection and that many of them also inhibited purified brucipain (29). The potential of acyl hydrazides as antitrypanosomal chemotherapeutic agents was further investigated by screening a library

of 500 non-peptidyl acyl hydrazide compounds for inhibition of cysteine protease activity in *T. brucei* extracts and the most effective inhibitors were tested for efficacy against cultured *T. brucei* (88). Despite some cytotoxicity towards human HL-60 cells, several of the acyl hyrdazide compounds demonstrated trypanocidal activity comparable to the commercially available HAT drug, suramin (88). The results of all of these investigations validated the potential for cysteine proteases as drug targets and, along with equivalent studies in other protozoan parasites, provided a basis for subsequent studies in this area (85).

Although most of the research on cysteine proteases in *T. brucei* through 2002 was focused on members of the Clan CA cysteine proteases, a few reports were published on other classes of cysteine proteases. In 2001, Hertz-Fowler *et al.* discovered a cytoskeleton-associated protein in *T. brucei* and showed, using bioinformatics techniques, found that it belongs to a family of novel calpain-type proteases (89). The first *T. brucei* metacaspases were also reported during this period. Szallies *et al.* subsequently cloned five metacaspses from *T. brucei* (*TbMCA1-5*) in 1992 (90).

Summary of the Proposed Role of Cysteine Proteases in *T. brucei* Prior to 2003

Early studies of cysteine proteases in *T. brucei* indicated that the most abundant protease of this class is the cathepsin L-like cysteine protease known as rhodesain (from *T. brucei rhodesiense*) or brucipain (from *T. brucei brucei*). The protease localizes to lysosomes and may be released extracellularly (although, an intracellular function for the enzyme is more likely). In studies through the end of 2002, Clan CA cysteine proteases were shown to be critical for *T. brucei* survival in culture and in mouse models of infection, as well as valid targets for potential new chemotherapies to treat HAT. While

several of the most trypanocidal cysteine protease inhibitors studied were shown to effectively inhibit purified or recombinant rhodesain/brucipain, the cathepsin L-like protease could not be confirmed as the critical target. Other cysteine proteases may play a role in the various functions that were proposed for *T. brucei* cysteine proteases, including lysosomal protein degradation, trypanosome differentiation and development, and pathogenesis.

SPECIFIC AIMS DESIGNED TO INVESTIGATE THE FUNCTION OF CYSTEINE PROTEASES IN *TRYPANOSOMA BRUCEI*

As discussed above, Clan CA cysteine proteases are critical for the survival and pathogenicity of many parasitic organisms, including *Trypanosoma brucei*. Incubation of *T. brucei* with Clan CA cysteine protease inhibitors showed that CACP activity is essential for parasite viability in culture (30) and infection in mice (29). However, the identity and biological function of the essential protease or proteases targeted by these inhibitors was not known. The work presented in the following chapters was designed to address these issues by using established or modified biochemical, molecular biology, and proteomics techniques to investigate cysteine protease function in *T. brucei.* Two specific research aims were proposed. First, I sought to determine the Clan CA cysteine protease repertoire in *T. brucei* and identify the key protease targets of the inhibitors used in previous studies. Preliminary data suggested that a cathepsin B-like cysteine protease, tbcatB, was a likely target of the inhibitors used and critical for parasite viability in culture. Therefore, my second aim was to define the biological function of tbcatB.

Determine the Cysteine Protease Repertoire in *T. brucei* and Identify Potential Targets of Inhibition

As previously stated, the Clan CA cysteine protease inhibitors used in previous studies were not selective, and further analysis was needed to identify the target(s) whose inhibition led to parasite death. I sought to identify all possible targets of inhibition using a genomics approach and then evaluate their contribution to parasite viability using RNAi techniques. Novel Clan CA cysteine proteases can be identified by their sequence similarity to known homologous cysteine proteases, such as papain or human cathepsins B and L. Most notably, these proteases have conserved active site residues: Cys^{25} (papain numbering), His^{159}, Gln^{19}, and Asn^{175}. The conserved amino acid sequences flanking these residues provide the necessary information to identify homologous genes. Comprehensive genome screens for these and other characteristic residues and motifs have been successful in identifying the Clan CA cysteine protease repertoire in humans, as well as parasites (58,91). I proposed to use a similar approach to identify the Clan CA cysteine protease repertoire in *T. brucei*.

It could be assumed from the results of the aforementioned inhibitor studies that one or more of the target(s) of inhibition are essential for parasite survival—that is, they carry out a critical function in *T. brucei*. In order to identify potential targets of inhibition, I proposed to target each of the proteases identified in the genome search for knock-down by RNAi. The phenotypes observed upon induction of RNAi were to be compared to those observed with the non-specific diazomethane cysteine protease inhibitor used in previous studies. A similar phenotype was expected if the protease that was targeted by RNAi was also targeted by the inhibitor. The motivation for establishing an inducible

RNAi system for *T. brucei* cysteine proteases extended beyond determining which protease or proteases were targets of the inhibitor. For example, changes in the localization of a protease (or substrate) upon induction could provide information about the biological function of the protease.

Define the Biological Role of TbcatB

Initial analysis of the *T. brucei* genome revealed two potential targets, a cathepsin L-like protease, rhodesain and, a cathepsin B-like protease, tbcatB. I hypothesized that these gene products have distinct functions. Preliminary results from RNAi studies suggested that TbcatB was critical for parasite viability in culture and a likely target of the Clan CA cysteine protease inhibitors used in previous studies. However, further study was required to determine the specific role that this protease plays in *T. brucei*. I proposed to define the biological function of tbcatB by determining its localization and identifying its natural substrates.

Clues to the function of a protease can be obtained by determining its localization. The intracellular site of a protease suggests what cellular process(es) the protease may contribute to and what substrates are available for cleavage. In the case of rhodesain, localization to the lysosome suggested that rhodesain is involved in parasite and/or host protein degradation (62). Given its localization, candidate substrates for rhodesain are proteins that are processed or degraded in the lysosome. I proposed to use immunofluorescence and immunoelectron microscopy labeling and co-localization of GFP-tagged proteins with molecular markers, both established protein localization techniques in *T. brucei* (62,92,93), to localize tbcatB.

Since the function of a protease is directly related to the role that substrate cleavage plays in an organism's biology, valuable information regarding the function of a protease can be obtained by identifying the enzyme's natural substrates. I proposed to use two complementary approaches, substrate specificity and two-dimensional gel analyses, to identify candidate substrates for tbcatB. Substrate specificity information obtained from screening positional-scanning synthetic combinatorial libraries (PS-SCLs) has facilitated substrate identification for *Schistosoma mansoni* cercarial elastase (94) and granzyme B (95), and I proposed to use a similar approach for tbcatB. I proposed to express, purify, and biochemically characterize tbcatB, and use the recombinant protease to screen a PS-SCL library made available by the laboratory of Charles Craik (96,97). Preferred substrate motifs would then be used to screen a database of host serum and *T. brucei* proteins for candidate substrates. Candidate substrates would be chosen from the list of proteins identified in the database screen based on prior knowledge about the substrates and supporting experimental evidence. Taking a different approach, I also proposed to identify candidate substrates by comparing the protein content of cell lysates from wild-type and tbcatB RNAi knockdown parasites using 2D gel analysis. The identity of candidate substrates (or products) that accumulate (or disappear) in the RNAi knock-down parasites would be determined using mass spectrometry. I proposed to test the ability of tbcatB to cleave candidate substrates *in vitro* using recombinant protease.

Summary of Proposed Research

I proposed to study the function of cysteine proteases in *T. brucei* by a cross-disciplinary approach utilizing biochemical, molecular biology, and proteomics techniques. My results would provide the basis for understanding essential cysteine

protease function(s) in *T. brucei*, and also contribute to a broader understanding of Clan CA cysteine protease function in other single-cell organisms. I also sought to validate tbcatB as a potential drug target, thereby contributing to the identification a cysteine protease inhibitor that will serve a lead for new chemotherapy for HAT.

CHAPTER 1

A CATHEPSIN B-LIKE PROTEASE IS REQUIRED FOR HOST PROTEIN DEGRADATION IN *TRYPANOSOMA BRUCEI*

ABSTRACT

Identification and analysis of Clan CA (papain) cysteine proteases in primitive protozoa and metazoa has suggested that this enzyme family is more diverse and biologically important than originally thought. The protozoan parasite *Trypanosoma brucei* is the etiological agent of African sleeping sickness. The cysteine protease activity of this organism is a validated drug target as first recognized by the killing of the parasite with the diazomethane inhibitor Z-Phe-Ala-CN_2H. While the presumed target of this inhibitor was "rhodesain" (aka brucipain and trypanopain) the major cathepsin L-like cysteine protease of *T. brucei,* genomic analysis has now identified tbcatB, a cathepsin B-like cysteine protease as a possible inhibitor target. The mRNA of tbcatB is more abundantly expressed in the bloodstream versus the procyclic form of the parasite. Induction of RNAi against rhodesain did not result in an abnormal phenotype in cultured *T. brucei*. However, induction of RNAi against tbcatB led to enlargement of the endosome, accumulation of FITC- conjugated transferrin, mitotic arrest and death of cultured parasites. Therefore tbcatB but not rhodesain is essential for *T. brucei* survival in culture and is the most likely target of the diazomethane protease inhibitor Z-Phe-Ala-CN_2H in *T .brucei*.

CHAPTER 1

INTRODUCTION

The Clan CA cysteine proteases include the papain-related proteases of plants, and the lysosomal "cathepsins" of mammalian cells. Recent genomic and biochemical studies of protozoa and primitive metazoa suggested that there was an explosion of gene diversity in this family coincident with the evolution of the first eukaryotic cell (98). In contrast to higher plants and most mammalian cells, the cysteine proteases of primitive protozoa and metazoa function in a variety of chemical environments and cellular compartments (43,99). Therefore the biological importance and distribution of cysteine proteases is much greater than originally proposed for the "cathepsins".

Because primitive protozoa include many of the major parasitic organisms of humans and domestic animals, parallel studies of the pathogenesis of parasitic diseases have underscored the importance of Clan CA proteases as virulence factors. Furthermore, considerable progress has been made in targeting these proteases for the development of new anti-parasitic chemotherapy (43,48,100,101). One notable observation in this regard was that the diazomethane cysteine protease inhibitor, Z-Phe-Ala-CN_2H, was lethal to *Trypanosoma brucei,* the causative agent of African sleeping sickness, *in vitro* and *in vivo* (30,102). The presumptive target for this inhibitor was a cathepsin L-like protease, "rhodesain", isolated from *T. brucei rhosesiense* and the homologue of "brucipain", "trypanopain", or "congopain" in other *Trypanosoma* species (103,104). However, peptide diazomethanes are relatively non-selective irreversible cysteine protease inhibitors, and recent genomic analysis of trypanosomes suggested that a repertoire of Clan CA protease genes may be present.

To identify and validate the target of Z-Phe-Ala-CN_2H in *T. brucei*, as well as clarify its biological function, a genomic scan using papain as a probe was first undertaken. The previously characterized cathepsin L-like cysteine protease, rhodesain (62), was identified as expected but a second cathepsin B-like gene product was also discovered. Subsequent expression, biochemical analysis, and localization studies suggested that the cathepsin B-like protease in *T. brucei* was a plausible target for the diazomethane inhibitor. Therefore to clarify the roles of both the *T. brucei* cathepsin B and cathepsin L homologues, RNA interference (RNAi) was used in conjunction with radio-labeled active site probes.

MATERIALS AND METHODS

Identification of Clan CA Cysteine Proteases in the *T. brucei* genome

The 159 amino acid sequence C19 to N178 representing the active site of papain, EC3.4.22.2, was used to blast search the *T. brucei* genomic databases from the Sanger Center and The Institute for Genomic Research (TIGR) for cysteine protease homologues {http://www.sanger.ac.uk/ #133;http://tigrblast.tigr.org/tgi/ #132}.

Subcloning of TbcatB cDNA into *Escherichia coli*

Reverse Transcription Polymerase Chain Reactions (RT-PCR) were carried out using the One Step with Platinum Taq kit (Invitrogen). Two micrograms of total RNA from *T. brucei* were mixed with the splice leader primer, TbSL 5'-ATTATTAGAACAGTTTCT GTACTATATTG-3', plus the reverse primer, TbCatBXhoIR 5'-GCTAATATCTCAGATACGCCGTGTTGGGTGCA-3' to amplify the full length cDNA of tbcatB. To amplify the open reading frame of tbcatB for recombinant expression, the

primers TbCatBBHIF 5'-GTCTATAGGATCCATGCATCTCATGCGTGCCT-3' and TbGSTHisR 5'-GTCGACGAGATGGAGATGGAGATGCGCCGTGTT-3' were used. All of the amplified products were subcloned into the TOPO TA cloning vector and transformed into competent *E. coli* for propagation (Invitrogen).

Purification of Recombinant TbcatB from *E. coli*

One liter of Terrific Broth (Invitrogen) containing 100 μg/ml ampicillin was inoculated with 5 ml of *E. coli* expressing the pGSTbcatBHis plasmid. The *E. coli* were incubated at 37^{o}C until the A_{600} reached 1.0 then induced with IPTG to a final concentration of 1 mM for 5 hours. Bacteria were centrifuged at 9000 x g for 15 minutes using a Beckman JLA 10.5000 rotor. After centrifugation, the pellet was re-suspended in 50 ml of sonication buffer (150 mM NaCl, 1% NP-40, Tris pH 7.5, 10% glycerol) and sonicated on ice five times for two minute intervals with 3 minute breaks between each interval. The crude lysate was cleared by centrifugation for 15 minutes at 25,000 x g. The cleared supernatant was decanted and the pellet was re-suspended in 50 ml of GuHCl buffer (6M GuHCl, 20 mM Tris. pH 8.0, 100 mM NaH_2PO_4) for 2 hours at room temperature. After 2 hours, the lysate was cleared by centrifugation and 10 ml of equilibrated nickel agarose beads (Qiagen) in 50% slurry were added to the cleared lysate. The beads were incubated with the lysate for 3 hours at room temperature. The mixture was poured into a 10 ml gravity column and washed with GuHCl buffer pH 8.0. The recombinant 6xHis tagged protein was eluted from the beads according to manufacturer's manual (Qiagen). Three microliters from each fraction was mixed with 2μl of SDS loading dye and examined by SDS-PAGE. Peak fractions were pooled and dialyzed 3 times in 1 liter of dialysis buffer

(50 mM Tris. pH 7.5, 50mM NaCl and 3.0 M urea) and 1.5 mg of protein was sent to AnimalPharm Inc. for production of rabbit polyclonal antibodies.

Northern Blot Analysis of *T. brucei* RNA

T. brucei total RNA was purified from 10^8 parasites using Trizol reagent (Invitrogen). Thirty micrograms of total RNA were loaded on a 1.2 % agarose-formaldehyde gel and resolved by electrophoresis at 50 V for 2.5 hours. After electrophoresis, the RNA was transferred to PVDF membrane and cross-linked to the membrane with a Stratalinker (Stratagene). ^{32}P-Labeled cDNA probes were generated using the random primed labeling kit (Amersham). The probes were denatured at 100^{o}C and hybridized to the blot overnight at 42^{o}C in buffer containing (50% formamide, 5X SSC, 4X Denhardt's solution, 0.1% SDS, 0.1% Na-Pyrophosphate).

Culturing of *T. brucei*

Procyclic *T. brucei* strain 427 was incubated at 27^{o}C without CO_2 and maintained in complete Cunningham's media containing 10% Fetal Bovine Serum (FBS) and 1x Penicillin/Streptomycin. The transgenic bloodstream form *T. brucei* clone 90-13 was a gift from the laboratory of George A. M. Cross (35). Bloodstream parasites were incubated in 5% CO_2 at 37^{o}C in HMI-9 medium containing 10% FBS, 10% Serum Plus (Omega Scientific), 1x Penicillin/Streptomycin with 5.0 µg/ml Hygromycin B and 2.5 µg/ml G418.

Introduction of RNAi Transgenes into Bloodstream *T. brucei* by Electroporation

For electroporation, 10^8 parasites were pelleted by centrifugation and washed twice with 10 ml of cytomix (120 mM KCl, 150 µM $CaCl_2$, 10 mM K_2HPO_4/KH_2PO_4, pH 7.6, 25 mM HEPES, pH 7.6, 2 mM EGTA, pH 7.6, 5 mM $MgCl_2$, pH 7.6 adjusted with KOH)

(105). After the second wash, the parasites were re-suspended in 0.5 ml of cytomix. The plasmid pZJM, which allows for stable tetracycline inducible expression of double-stranded RNA in *T. brucei*, was a gift from the laboratory of Paul T. Englund (38). One hundred micrograms of pZJM vector containing the first 597 nucleotides of the rhodesain cDNA (pZJMTbRho) or nucleotides 300 through 1020 of the tbcatB cDNA (pZJMTbCB) was linearized with Not I restriction endonuclease and precipitated with ethanol. The DNA was re-suspended in 100 µl of cytomix buffer and mixed with the 0.5 ml suspension of *T. brucei* in a 4 mm electroporator cuvette. The parasites were pulsed with 1.7kV and 25 µF. After pulsing, the parasites were transferred to 24 ml of complete medium and incubated overnight at 37^{o}C with 5% CO_2. To select for parasites stably expressing the transgenes, phleomycin was added to the parasites at a concentration of 2.5 µg/ml and the parasites were aliquoted in a 24 well plate for 7-12 days. Stably transfected parasites were maintained in complete medium containing 2.5 µg/ml phleomycin. Induction of the dsRNA in bloodstream parasites was carried out by adding tetracycline to a final concentration of 100 ng/ml.

Western Blots of RNAi Clones

T. brucei were either induced for twenty four hours with 100 ng/ml tetracycline or maintained uninduced. The parasites were lysed with Tb lysis buffer (1.0% Tx-100, 10mM Tris pH 7.5, 25mM KCl, 150mM NaCl, 1mM $MgCl_2$, 0.2mM EDTA, 1mM DTT, 20% Glycerol) and 25 µg of crude lysate was resolved by SDS-PAGE and transferred to PVDF membrane. After transferring and blocking, the PVDF membranes were incubated with rabbit anti-tbcatB (1:2,000 dilution) or anti-rhodesain antiserum (1:5,000 dilution) (62) for one hour and washed three times for five minutes with TBST. After the third

wash, HRP-conjugated donkey anti-rabbit IgG (1:1,000 dilution) was added to the blots for 1 hour. The blots were then washed again in the same buffer three times for five minutes and then examined by ECL (Amersham).

FACS Analysis and 4,6 Diamidino-2phenylindole (DAPI) Staining

For FACS analysis, parasites were fixed overnight in 70% methanol and 30% PBS at 4^{o}C. Afterwards, the parasites were washed with cold PBS and re-suspended to 10^6 cells/ml. RNAse A and propidium iodide were added to the cells to a final concentration of 10 µg/ml each and incubated at 37^{o}C for 60 minutes. FACS analysis was performed with a Becton Dickinson FACScalibur using FL2-H. Data analysis was carried out with either FlowJo version 4.52 or CellQuest version 3.3.

Analyzing Degradation of FITC-Conjugated Transferrin in *T. brucei*

FITC-conjugated bovine transferrin (Sigma) was re-suspended at 1 mg/ml in 10 mM HEPES buffer pH 7.4. Parasites were incubated in HMI-9 medium containing 15 µg/ml of FITC-conjugated bovine transferrin at 37^{o}C and 5% CO_2 for 3 hours. The parasites were then washed twice in PBS pH 7.4 and fixed in 0.1M Cacodylate buffer containing 2.5% glutarldehyde and 1.6% paraformaldehyde and applied to poly-L-lysine coated slides. Parasites were visualized using an Axioskop2 microscope (Zeiss).

Identification of Clan CA Cysteine Protease Active Sites with ^{125}I-labeled Inhibitors

Ten million *T. brucei* cultured in 10 ml of complete HMI-9 medium at 37^{o}C and 5% CO_2 were incubated with ^{125}I-JPM565 for 2 hours (106). After 2 hours, the parasites were pelleted by centrifugation at 900 x g for 20 minutes with a Beckman GH 3.8A rotor and lysed in 100 µl of lysis buffer (50 mM sodium acetate, 1 mM EDTA, 1% Triton X-100, pH 5.5) for 1 hour on ice. Alternatively, ten million unlabeled parasites were pelleted and

lysed using identical conditions. Lysates were cleared by centrifugation at 16,000 x g for 15 minutes at 4^{o}C in Eppendorf tubes. The protein concentration of the cleared lysates was determined by Bradford assay and equal amounts of parasite lysates were labeled with ^{125}I-MB-074 for one hour at 25^{o}C (107). Quantification of labeled enzymes was determined by PhosphorImager analysis (Molecular Dynamics).

***T. brucei* Viability Assay**

Uninduced control or tetracycline induced *T. brucei* were grown in T-25 flask under standard conditions for 48 hours. After 48 hours, 100 µl of the cultures were aliquoted into white opaque 96 well palates. To assay for viability, an equal volume of CellTiter-Glo^{TM} (Promega) was added to the corresponding wells. The mixture was placed on an orbital shaker at room temperature for 5 minutes before reading the plates with a SpectraFluor Plus multi-detection plate reader (Tecan). Alternatively, the parasites were counted by hemocytometer 48 hour post tetracycline induction.

RESULTS

Identification of TbcatB, a Cathepsin B-like Homologue in *T. brucei*

Using the highly conserved catalytic region of papain as a probe, we searched *T. brucei* databases for homologues to papain. From this search, a cathepsin L-like and a cathepsin B-like protease sequence were identified. The cDNAs encoding these two gene products were amplified from *T. brucei* RNA by RT-PCR, subcloned and sequenced. The 1.3 kb cDNA encoded a 450 amino acid polypeptide with a predicted MW of 48,431 identical to rhodesain, the previously characterized cathepsin L-like protease identified by biochemical assays in *T. brucei* lysates (59). The 1.0 kb cDNA encoded a cathepsin B-

like protease, tbcatB, having 341 amino acids with a predicted MW of 37,223. The tbcatB open reading frame contained each of the conserved motifs identified in the active site of lysosomal cathepsins including the residues that form the catalytic triad, Cys 42, His 282 and Asn 302 (tbcatB numbering). The tbcatB open reading frame also encodes two conserved motifs identified in cathepsin B family proteases: Gly-Cys-Xxx-Gly-Gly which is identical to human cathepsin B (residues 70-74) and an occluding loop motif that is thought to be responsible for the exopeptidase activity of cathepsin B-like proteases (108) (Fig. 1.1). The tbcatB sequence has been deposited in the NCBI GeneBank Database under accession number AY508515.

TbcatB mRNA Expression is Increased in Bloodstream versus Procyclic *T. brucei*

Rhodesain has been characterized extensively with synthetic peptides demonstrating that it is the major cysteine protease activity in *T. brucei* (56,75,82). Consistent with the high level of its biochemical activity, genomic analysis indicated that there are 20 copies of the rhodesain gene repeated in tandem (57). We examined the mRNA expression of rhodesain and tbcatB to elucidate their relative abundance in the two major developmental stages of *T. brucei*. Northern blot analysis demonstrated that the amount of rhodesain mRNA expressed in either the bloodstream (mammalian host) or the procyclic (insect) forms of the parasite were equivalent (Figure 1.2A). In shorter exposures of the autoradiography, the rhodesain mRNA could be visualized as a doublet in the RNA from both forms of the parasite. These mRNA results were surprising because results from previous protein expression assays showed that this protease was up-regulated in the bloodstream form parasites (62). Therefore it is reasonable to conclude that rhodesain may be translationally regulated in procyclic parasites. We used

gene specific probes to hybridize to tbcatB mRNA for Northern blot analysis. Our results demonstrated that the amount of tbcatB mRNA was less than the amount of rhodesain mRNA in both developmental stages of *T. brucei.* The similar size of the transcripts and the low expression level of tbcatB made it necessary to carry out the blots in parallel rather than use blots that were stripped and re-probed to avoid ambiguous results. These properties of tbcatB can probably explain why it was not identified earlier in cDNA screens. Northern blot analysis also demonstrated that the message for tbcatB was upregulated in the bloodstream form parasites (Fig. 1.2B). The differential expression of tbcatB between the bloodstream form and procyclic form suggest that in contrast to rhodesain, this protease is regulated at the transcriptional level. Upregulation of tbcatB mRNA in the bloodstream form of the parasite suggests that it may primarily function in the bloodstream parasites.

Silencing of Rhodesain mRNA Expression in *T. brucei*

To identify the role of the two cathepsins in bloodstream form *T. brucei*, the mRNA expression of rhodesain or tbcatB was silenced by RNAi. Tetracycline was used to induce double-strand RNA in transgenic 90-13 strains of *T. brucei* stably expressing either rhodesain; pZJMTbRho, or tbcatB; pZJMTbCB transgenes. The tetracycline induced pZJMTbRho parasites did not exhibit visible phenotypic abnormalities, signs of cell cycle arrest or changes in growth rate compared to the uninduced parasites. Total RNA from induced and control parasites was extracted and analyzed by northern blot analysis twenty four hours post induction. The rhodesain probe hybridized with two distinct messages on the northern blot with about equal intensity. Since the northern blot was carried out on total RNA the two transcripts recognized by the probe may represent

processed mRNA transcripts of rhodesain with either immature and or alternatively processed transcripts. However, both of these bands were reduced to almost undetectable levels in tetracycline induced parasites (Fig. 1.3A). Immunoblot analysis was used to compare the amount of rhodesain in control parasites to the amount in RNAi silenced parasites. Affinity purified rabbit anti-rhodesain antibodies recognized two bands, 45 and 47 kDa, in the western blots of control parasites. These two bands could reflect that rhodesain has become glycosylated, as a cryptic glycosylation site has been identified in rhodesain (62) and these antibodies do not distinguish between glycosylated or nonglycosylated forms of rhodesain. Recently, it has been demonstrated that a species of mammalian cathepsin L is able to initiate translation from a second downstream Met codon and become translocated into the nucleus (109). Rhodesain is a cathepsin L-like protease that contains several downstream Met codons where translation can initiate. Initiation at a downstream Met codon may also account for the second species of rhodesain detected by the antibodies. In either case, these two bands were nearly undetectable by the same antibodies in extracts where rhodesain expression was silenced in parasites by RNAi (Fig. 1.3B).

To confirm the effects of mRNA silencing on protease activity *in vivo,* we used JPM565, a derivative of E-64, the irreversible inhibitor of papain and other cysteine proteases. E-64 and its derivatives form a thioether bond with the sulfhdryl group in the active center of cysteine proteases and are useful for active site titration since one mole of these molecules inhibits one mole of protease (110). JPM565 can be used for active site labeling because of its suitability for iodination and its preference for cathepsin L-like proteases (106,111). When parasites were incubated with ^{125}I-JPM565, the amount of

labeling for both species of rhodesain was reduced in the RNAi induced parasites (Figg 1.3C). Induced parasites showed a 65% reduction in labeling of rhodesain by ^{125}I-JPM565 (Fig. 1.3D). Together, these observations suggested that rhodesain was not essential for parasite replication in culture.

"Knockdown" of TbcatB Leads to Dismorphism and Death of *T. brucei*

When the pZJMTbCB clones were induced with tetracycline, distension of the anterior endosome/lysosome compartment of the parasites was easily visualized within 12 hours post induction. Distension of these RNAi-induced parasites in the region of the endosome reached a maximum by twenty four hours post induction. In addition to anterior swelling, the RNAi-induced parasites displayed multiple flagella similar to parasites undergoing mitosis in the uninduced controls (Fig. 1.4A-Phase Contrast). To examine the nature of the swelling, we used DAPI to stain the nuclei and kinetoplast of control and induced parasites. In uninduced controls, the population was composed of parasites containing one kinetoplast and one nucleus (1K1N), two kineotoplast and one nucleus (2K1N), and two kinetoplast and two nuclei (2K2N). These observations were consistent with the control parasites existing as an asynchronous population (112). When DAPI was used to stain the nuclei of RNAi induced pZJMTbCB clones, the clones demonstrated a dramatic increase in the number of parasites containing two kinetoplast and two nuclei. After forty eight hours of RNAi induction, no parasites containing one kinetoplast and one nucleus (1K1N) were detected. All of the parasites in this population contained multiple nuclei and multiple kinetoplasts (Fig. 1.4A-DAPI). The DNA content of control or induced parasites were then analyzed by flow cytometry to verify the karyotype results observed by microscopy. In the uninduced control population, a similar number of parasites

contained either 2C or 4C DNA. A similar profile was observed in the parental 90-13 and wild-type 221 blood-stream form parasites which suggest that uninduced parasites exist as an asynchronous population (data not shown). After twenty four hours of tetracycline induction, the majority of parasites observed contained 4C DNA or greater amounts of DNA suggesting that the tetracycline induced population of parasites were able to complete several rounds DNA synthesis and mitosis (Fig. 1.4A-FACS). But by 48 hours post-induction, no proliferation in the pZJMTbCB clones was detected by either direct counting with a hemocytomer or by a luciferase based proliferation assay that detects ATP generation (Fig. 1.4B) (113). The tetracycline induced parasites died after 72 hours. These abnormalities were not observed in control parasites where normal proliferation occurred. The effect of RNAi on tbcatB protease in the parasites was confirmed by western blot analysis. A modest but significant decrease in the amount of tbcatB protein was detected in the extracts of the induced parasites versus the control parasites (Fig. 1.4C). We used the cathepsin B specific inhibitor MB-074 to confirm reduction of cathepsin B activity in the tetracycline induced clones. MB-074 is a derivative of CA-074 which binds specifically to the occluding loop found in cathepsin B-like proteases but not other cysteine proteases (114). MB-074 has a tyramine group that allows it to be labeled by ^{125}I. When extracts from control or induced pZJMTbCB clones were incubated with ^{125}I-MB-074, a 34 kDa band consistent with tbcatB was visualized in both (Fig. 1.4E). The amount of the 34 kDa tbcatB was reduced by 32% in the tetracycline-induced parasites versus the control parasites (Fig. 1.4E).

TbcatB but not Rhodesain is Required for Degradation of Transferrin

Because they lack cytochromes, the bloodstream form of *T. brucei* acquires iron from the host by internalizing transferrin through receptor mediated endocytosis. The host transferrin is then rapidly degraded in the "lysosome/endosome" located between the nucleus and kinetoplast of the parasite. FITC-conjugated transferrin was used to analyze the phenotypes associated with silencing rhodesain or tbcatB in cultured parasites. No accumulation of FITC-conjugated transferrin was detected in control pZJMTbRho parasites or in tetracycline induced pZJMTbRho clones indicating that transferrin was being rapidly turned over in these parasites (data not shown). In pZJMTbCB clones the nucleus and kinetoplast was visualized by DAPI staining (Fig. 1.5A). No accumulation of FITC-conjugated transferrin was detected in pZJMTbCB uninduced control clones. However when these clones were induced with tetracycline, FITC-conjugated transferrin began to accumulate throughout the parasite and within the lysosome/endosome (Fig. 1.5B). Similar accumulation of FITC-conjugated transferrin was observed when *T. brucei* were treated with the cysteine protease inhibitor Z-Phe-Ala-CN_2H (30).

DISCUSSION

Scory et al. showed that a peptide diazomethane inhibitor was ultimately lethal to *T. brucei* in culture and first produced swelling of the endosome/lysosome compartment of *T. brucei* (30). The presumptive target of this inhibitor was "rhodesain", the major proteolytic activity and cathepsin L-like protease of the parasite. We have identified a cathepsin B-like homologue, tbcatB, in the *T. brucei* genome which confirms that the clan CA cysteine protease repertoire of *T. brucei* is more complex than previously

thought. TbcatB message and activity is relatively low compared to rhodesain activity in the parasites. This may explain why tbcatB was not identified in previous studies where synthetic peptides were used to characterize the different proteolytic activities in *T. brucei*.

Whereas rhodesain mRNA was expressed at equivalent levels in both digenic stages of the parasite, the mRNA of tbcatB was differentially up-regulated in the bloodstream form. Previous studies that examined the cathepsin B and L-like mRNAs in the related kinetoplastid *Trypanosoma cruzi,* revealed that these two proteases were both differentially expressed among this parasite's three developmental stages (115,116). However as shown here for *T. brucei*, the cathepsin L-like protease represented the major cysteine protease activity.

Because both proteases are expressed in the bloodstream form, it is conceivable that they represent a redundant system of host-protein degradation. However, the differential regulation of tbcatB suggested that they may have distinct biological roles. To address this issue we utilized RNA interference to selectively "knockdown" rhodesain or tbcatB in *T. brucei*. In cultured bloodstream trypanosomes, no observable phenotype was found following nearly complete knockdown of rhodesain message, protein, and proteolytic activity. In contrast, induction of RNAi in the pZJMTbCB clones produced a modest 32% reduction in protein and protease activity but led to a distinctive dismorphic phenotype. Dilation of the anterior end of these organisms produced a "tadpole-like" morphology with an enlarged lysosome/endosome compartment. The observation that *T. brucei* bloodstream forms degrade host proteins in an unusual endosome/lysosome compartment differs from the intracellular protein degradation classically attributed to the

Clan CA family I mammalian and plant cells. However, there have been recently elucidated parallels to this phenomenon in mammalian syxtems, where extracellular proteins are degraded by cathepsins- either exocytosed from lysosomal compartments (Sloan *et al.*) or released through a regulated secretory pathway (Brix *et al.*). Taken together, these results suggest that the Clan CA cysteine protease family evolved very early to carry out a broad array of biologic functions in primitive eukaryotic cells, some of which have been retained by higher eukaryotes. These parasites were able to complete multiple rounds of genomic replication and mitosis as evident by the appearance of multiple kinetoplast and nuclei, but were not able to complete cytokinesis. Since these phenotypes are nearly identical to what has been reported for alpha-tubulin depleted parasites, it is possible that tbcatB could also be involved in a microtubule related event (37). Alternatively, lack of cytokinesis may be an indirect consequence of iron depletion due to inability of the parasite to degrade transferrin. The fact that a dismorphic and later lethal phenotype was observed with modest reduction in the total protease suggests that this enzyme may be slowly replenished or at a critical steady-state concentration in the parasites. Finally, the lethal RNAi effect associated with inhibition of fluorescein-labeled transferrin degradation recapitulated the phenotype seen with parasites exposed to a peptide diazomethane cysteine protease inhibitor. This suggests that tbcatB was in fact the major target of this inhibitor and plays a major role in host serum protein degradation by the parasite.

T. brucei is the causative agent of African sleeping sickness, a major health problem in Sub-Saharan Africa, and one of the “great neglected diseases”. Identification of a

specific enzyme target required for the viability of bloodstream trypanosomes represents an exploitable target for the development of new chemotherapy.

ACKNOWLEDGEMENTS

This work was supported by AI35707, the UCSF Liver Center Microscopy and Imaging Core, an UNCF/Merck Scientific Initiative Fellowship and the Sandler Family Supporting Foundation. We also thank C. Caffrey for anti-Rhodesain antibodies, George Cross for the 90-13 *T. brucei* strain and Paul Englund for the pZJM Vector and Matt Bogyo for active site probes.

FIGURES FOR CHAPTER 1

Figure 1.1. ClustalW alignment of tbcatB with other cathepsin B-like proteases. TbcatB contains each of the conserved amino acids that form the catalytic triad of the active site in clan CA cysteine proteases including Cys 42 (C) blue triangle, His 282 (H) blue triangle and Asp 302 (N) blue triangle. TbcatB also contains the occluding loop (black bar) identified in cathepsin B-like proteases from other species. *Trypanosoma brucei* (Tb), *Trypanosoma cruzi* (Tc), *Leishmania donovini* (Ld), *Schistosoma mansoni* (Sm), *Homo sapiens* (Hs), *Toxoplasma gondii* (Tg).

Figure 1.2. Northern blot analysis of bloodstream and procyclic forms of *T. brucei*. Total RNA from bloodstream (BF) or procyclic (PF) forms of *T. brucei* was crosslinked to PVDF membrane and then hybridized with rhodesain (A) or tbcatB (B) specific probes. Ribosomal RNA loading controls are shown beneath each blot. Note that while

message for tbcatB is less abundant that rhodesain, it is differentially upregulated in the mammalian bloodstream form.

Figure 1.3. Detection of rhodesain mRNA and protease after RNAi induction. Bloodstream form pZJMTbRho clones were either uninduced (-) or induced with 100 ng/ml of tetracycline for 24 hours to produce double-stranded RNA (+). Total RNA was prepared from the parasites and thirty micrograms of total RNA was used in northern blot analyses. A rhodesain specific probe was used to examine the mRNA expression in control or induced parasites. Ribosomal RNA loading controls are shown beneath the blots (A). Control or tetracycline induced pZJMTbRho clones were labeled *in vivo* with ^{125}I-JPM565 for 3 hours then lysed. Equal amounts of the labeled extracts were resolved by 12.5% SDS-PAGE and first visualized by western blot analysis (B). The amount of rhodesain labeled *in vivo* by the active site tag was visualized by autoradiography (C) or quantified by PhosphorImager (D). The values represent the average of 3 independent tests.

Figure 1.4. Morphology and Karyotype analysis of pZJMTbCB clones after induction. Morphology of control (-Tet) or induced (+Tet) *T. brucei* clones was compared by several methods. Note the swelling of RNAi-induced parasites with often marked anterior end distention but thin flagella (Phase Contrast Microscopy). The same clones were stained to visualize their nucleic acid content (DAPI). Comparison of DNA content was carried out in control or induced pZJMTbCB clones (FACS). Note the shift of the induced parasites from 2C to 4C DNA content 24 hours post induction (A). Survival of the pZJMTbCB clones was measured by luciferase based assay for ATP detection at zero and 48 hours post induction note almost complete lethality 48 hours post

induction (B). Values observed are the mean of luciferase assays done in triplicates. Equal amounts of extracts made from control (-) or tetracycline induced (+) pZJMTbCB clones were resolved by SDS-PAGE for western blot analysis (C) or active site labeling by ^{125}I-MB-074 (D). Quantitative analysis was carried out by PhosphorImage analysis (E).

Figure 1.5. Accumulation of FITC-conjugated transferrin in *T. brucei.* Clones of pZJMTBCB were induced with tetracycline or maintained untreated for 24 hours. Parasites were then incubated with FITC-conjugated transferrin. Merging of phase contrast and DAPI stain of uninduced control (-Tet) or tetracycline induced (+Tet) pZJMTbCB clones depicted in column (A). DAPI staining shows nuclei and extra nuclear staining of kinetoplast DNA in parasites. Accumulation of FITC-conjugated transferrin in induced but not uninduced parasites that shows only dim background fluorescence. Note also distention of anterior end of tbcatB RNAi induced parasites due to enlarged lysosome/endosome (arrow) containing transferrin column (B).

Figure 1.1.

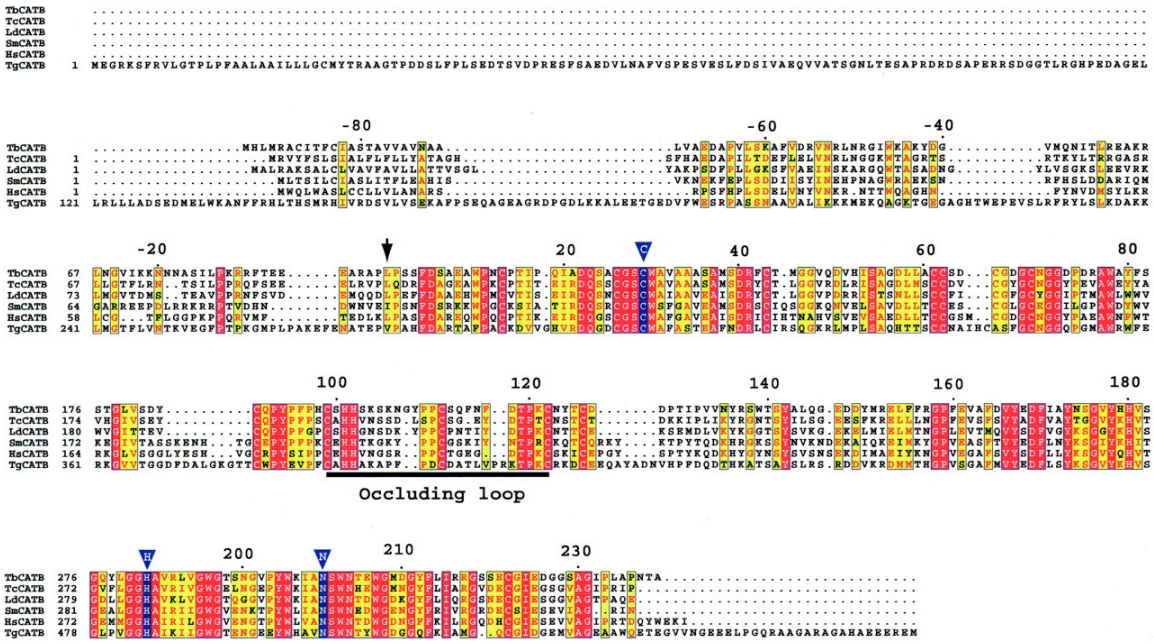
TbCATB
TcCATB
LdCATB
SmCATB
HsCATB
TgCATB
-80
-60
-40
-20
20
40
60
80
100
120
140
160
180
200
210
230
Occluding loop

Figure 1.2.

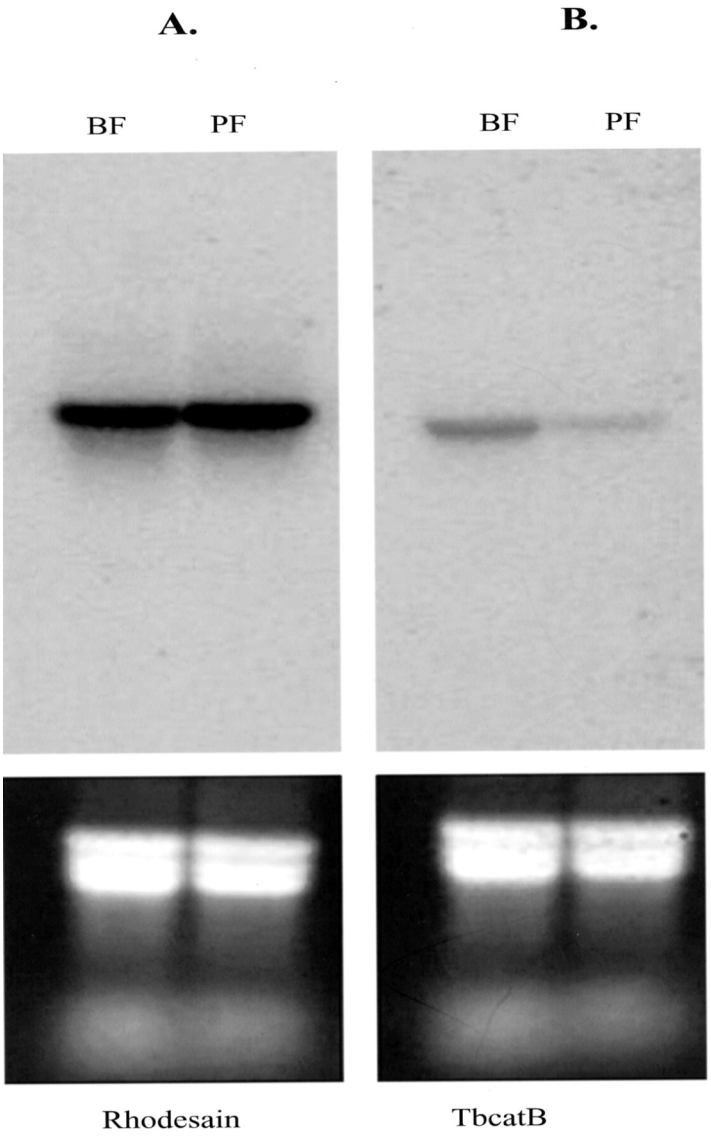

Figure 1.3.

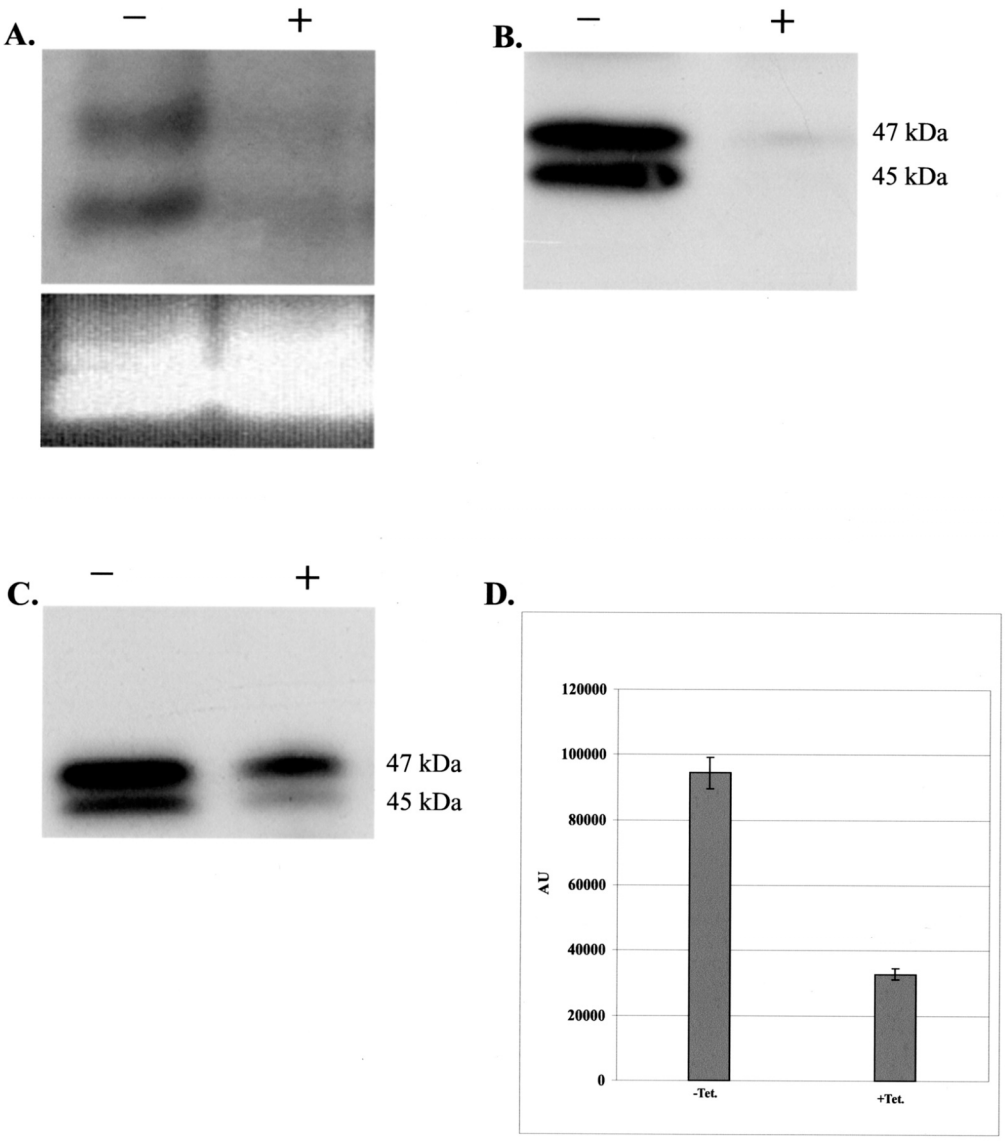
A.
−
+
B.
−
+
47 kDa
45 kDa
C.
−
+
47 kDa
45 kDa
D.
120000
100000
80000
60000
40000
20000
0
AU
-Tet.
+Tet.

Figure 1.4.

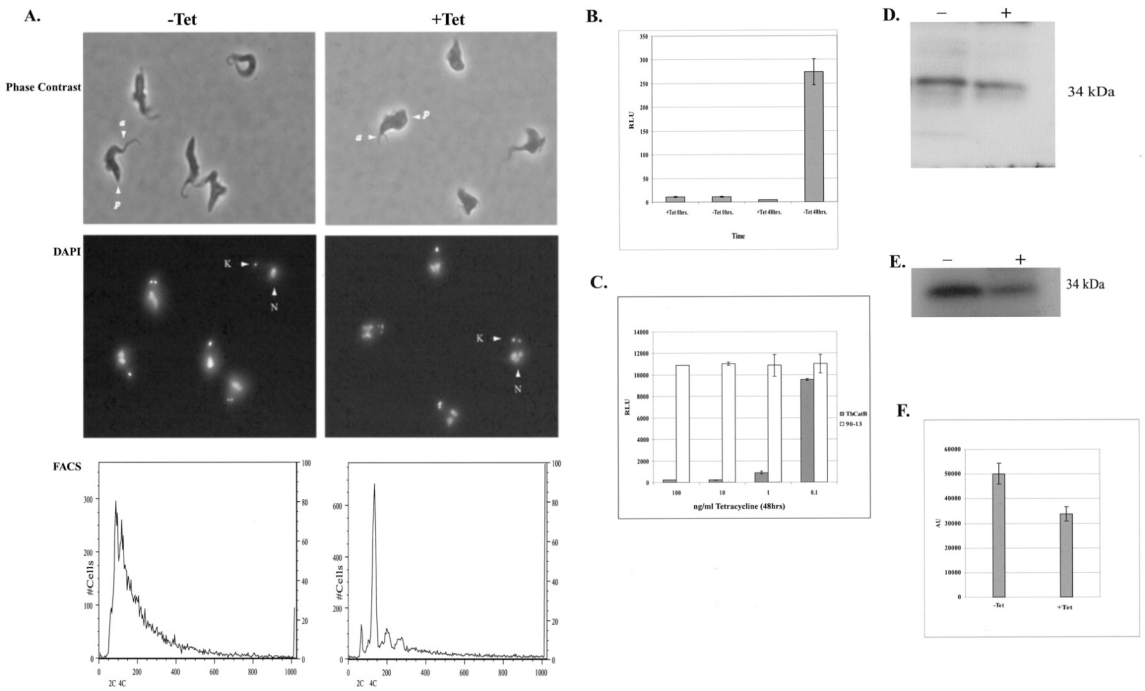
A.
-Tet
+Tet
Phase Contrast
DAPI
FACS
K
N
#Cells
2C 4C
B.
RLU
Time
C.
RLU
ng/ml Tetracycline (48hrs)
D.
34 kDa
E.
34 kDa
F.

Figure 1.5.

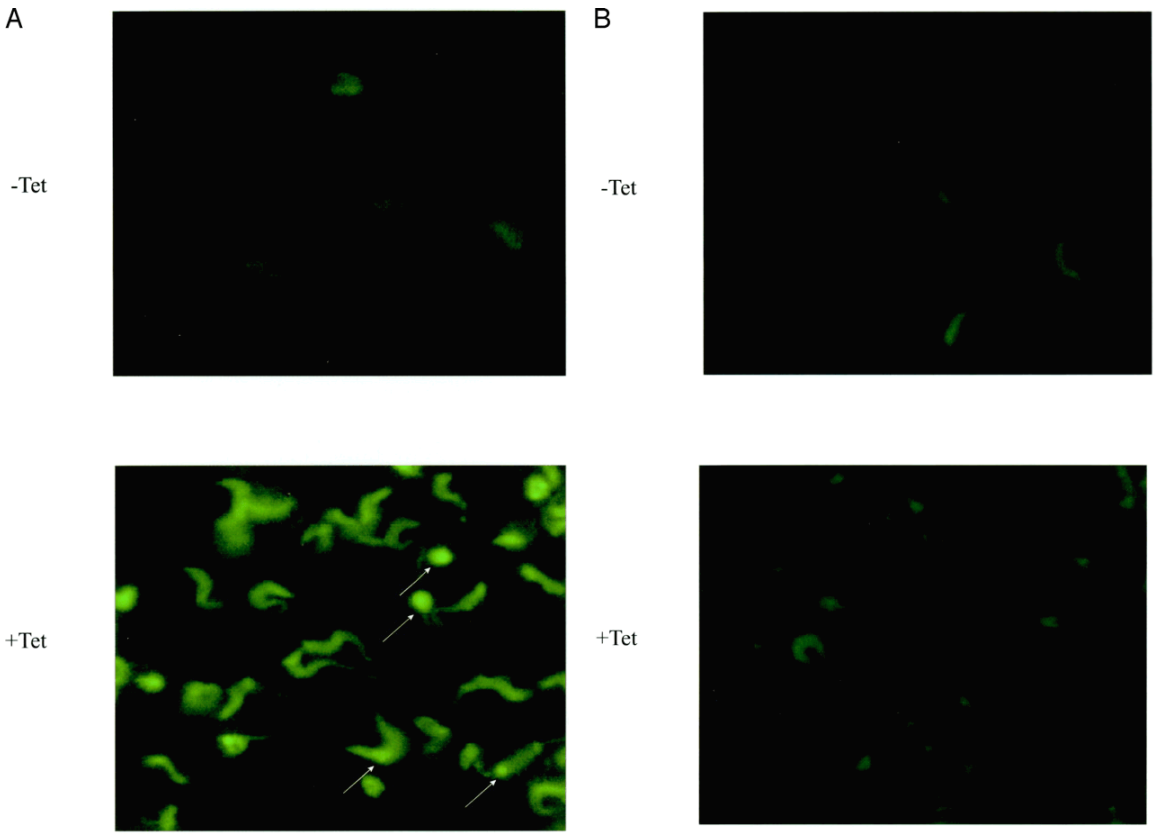

CHAPTER 2

RNAi OF *TRYPANOSOMA BRUCEI* CYSTEINE PROTEASES *IN VIVO* CLARIFIES THEIR CONTRIBUTION TO DISEASE PROGRESSION

INTRODUCTION

Subspecies of *Trypanosoma brucei* are causative agents of human African trypanosomiasis. Studies utilizing both small molecule cysteine protease inhibitors and RNAi have implicated the Clan CA (papain) family of cysteine proteases as critical to the successful lifecycle of *Trypanosoma brucei in vitro* (30,117). *In vivo* studies demonstrated that cysteine protease inhibitors prolonged the lives of mice infected with lethal inocula of trypanosomes (30,60). There are two distinct Clan CA cysteine proteases identified in the *T. brucei* genome. Rhodesain (aka trypanopain-Tb, brucipain) is a cathepsin L-like protease responsible for the bulk of protease activity in the organism (117). *Trypanosoma brucei* cathepsin B (tbcatB) is a more recently characterized protease that is upregulated in the bloodstream stage of the parasite (117). RNA interference (RNAi) of tbcatB *in vitro* produced swelling of the endosome compartment analogous to that seen with class-specific cysteine protease inhibitors (30,117). This led to arrest of trypanosome replication and death. In contrast, RNAi of rhodesain *in vitro* produced no detectable phenotype. TbcatB has been implicated in the degradation of host transferrin within the endosome compartment or flagellar pocket of *T. brucei* (30). While no phenotype was observed for RNAi of rhodesain *in vitro*, it has been hypothesized that

this enzyme might play a role in the degradation of mistargeted glycosylphosphatidylinisotol (GPI) anchored proteins, VSG turnover, disruption of the blood-brain barrier, or degradation of host immunoglobulin (118). To test whether transcriptional silencing of either of these two proteases alters the course of *T. brucei* infection *in vivo*, we utilized RNAi in a mouse model of infection (119).

MATERIALS AND METHODS

Generation of *T. b. brucei* RNAi Strains

Bloodstream *T. b. brucei* strain 90-13 (a gift of George A. M. Cross) was electroporated with plasmids containing either rhodesain (TbRho), or tbcatB (TbCB), or GFP transgenes (117). The plasmid used, pZJM (a gift of Paul T. Englund), allows transfected organisms to be induced to produce RNAi in the presence of tetracycline. The TbRho and TbCB transgenes have been described previously. To generate the GFP transgene, the gene encoding GFP (714 nucleotides) was amplified from the pHD-HX-GFP vector (93). Methods for electroporation and selection of stable transformants have been described (117).

Trypanosome Culture and Infection of Mice

Bloodstream form (BF) 90-13 cells expressing T7 RNA polymerase and tetracycline repressor protein were maintained in HMI-9 medium (35). BALB/c mice (6-8 weeks old) were infected by intraperitoneal injection with 600 parasites carrying pZJMTbRho, pZJMTbCB, or pZJMGFP plasmids or with control 90-13 parasites. Mice were monitored every other day for weight loss, general appearance, and behavior.

Experiments were carried out in accordance with protocols approved by the Institutional Animal Care and Use Committee (IACUC) at UCSF. Infected mice included the following categories: Two groups of mice were infected with the parental *T. b. brucei* strain 90-13. One of these groups was given doxycycline-containing food (200-mg/Kg, Bioserv Corporation, San Diego, CA) and water containing 1 mg/ml doxycycline hyclate (Sigma-Aldrich). These two groups served as controls for any direct effects of doxycycline on the course of trypanosome infection in mice. Six other groups of mice were infected with either *T. b. brucei* containing an RNAi-producing plasmid for rhodesain (pZJMTbRho), *Trypansoma brucei* Cathepsin B (pZJMTbCB), or GFP (pZJMGFP). These in turn were given standard food and water, or food and water containing doxycycline. The two groups infected with pZJMGFP served as a control for a gene that is not found in the trypanosome.

Real-time Reverse Transcription-PCR

Gene transcripts for rhodesain were quantified in freshly isolated *T. b. brucei* from mice infected with pZJMTbRho at 5 days post infection. Blood was separated by DEAE-sepherose column as described previously (120). Total RNA was extracted from *T. b. brucei* using the TRIzol reagent (Invitrogen, Carlsbad, CA). RT-PCR was then performed using the one-step RT-PCR kit (Invitrogen, Carlsbad, CA) and gene-specific primer pair. The relative amount of gene transcripts was calculated using methods described previously (121).

Preparation of Trypanosome Lysates

Parasites were purified from mice infected with 90-13 and pZJMTbRho. As reported previously in (120), *T. b. brucei* from infected mice were harvested by centrifugation,

washed once in PBS-containing 1% glycose, and resuspended in lysis buffer (1.0% Triton X-100, 10 mM Tris pH 7.5, 25 mM KCl, 150 mM NaCl, 1 mM MgCl2, 0.2 mM EDTA, 1 mM dithiothreitol, 20% glycerol). The lysates were incubated on ice for 20 minutes and cleared by centrifugation at 16,000 g for 15 minutes at +4 °C. Protein concentration of was determined by Bradford assay (Bio-Rad).

Western Blots of Trypansome Lysates Following RNAi Induction

A total of 10 μg of trypanosome lysate was resolved by 15% SDS-PAGE and transferred to polyvinylidene difluoride (PVDF) membrane. After transferring and blocking, the PVDF membranes were incubated with rabbit anti-rhodesain antiserum (1:2500 dilution) (Caffrey 2001) for 1 h and washed three times for 5 min with TBST (10 mM Tris, pH 7.4, 150 mM NaCl, 0.4% Tween 20). After the third wash, horseradish peroxidase-conjugated donkey anti-rabbit IgG (1:1,000 dilution) was added to the blots for 1 h. The blots were then washed again in the same buffer three times for 5 min and then examined by ECL (Amersham Biosciences).

Radiolabeling of Cysteine Protease Active Sites with ^{125}I-labeled Inhibitors

Equal amounts of trypanosome lysate (10μg) were labeled with ^{125}I-DCG-04 (107) in the presence of ~2 mM dithiothreitol for 45 minutes at room temperature and subjected to SDS-PAGE. Quantification of labeled enzymes was determined by Phosphoimager analysis (Molecular Dynamics).

RESULTS AND DISCUSSION

Doxycycline itself produced no significant alteration (+/- 1 day) in the course of *T. b. brucei* 90-13 infections (Fig. 2.1A). Equivalent levels of parasitemia and splenomegaly were observed in both groups of mice whether or not they were maintained on a doxycycline containing diet (not shown). The *in vivo* induction of RNAi against rhodesain in *T. b. brucei* did not cure infection, but extended the survival of five out of ten mice beyond 60 days (Fig. 2.1C). However, in all mice infected with trypanosomes having rhodesain transcript knockdown, parasitemia and splenomegaly equivalent to control infections were observed at the time of their sacrifice (not shown). Analysis of mRNA levels in infected mice confirmed rhodesain transcript knockdown (Fig. 2.2A). A greater than 80% reduction in rhodesain protein level was found in pZJMTbRho parasites induced with doxycycline *in vivo* versus uninduced control (Fig. 2.3A). Active site labeling of rhodesian from purified trypansomes showed 60% inhibition in rhodesian protease activity (Fig. 2.3B). A control cell line with an insert of GFP was generated to investigate the role of RNAi construct itself on the parasites *in vivo*. No difference was seen in mouse pathology or in rhodesain or tbcatB levels with GFP-induced parasites. The irrelevant RNAi construct had no influence on parasitemia or disease progression.

The mice infected with pZJMTbCB RNAi trypanosomes died by day 11-post infection in the absence of RNAi induction by doxycycline. In contrast, *in vivo* induction of pZJMTbCB RNAi resulted in survival of all five mice for up to two months post infection after which time the experiment was terminated (Fig. 2.1B). No trypanosomes were detected in the blood of mice infected with pZJMTbCB trypanosomes after

induction of RNAi with doxycycline. These mice also had normal spleen weights compared to un-induced controls (Fig. 2.2B). The last day on which untreated mice died from the trypanosome infection may vary depending on exact parasite inoculum absorbed and other host defense and host metabolic factors (Fig. 2.1A vs 2.1B).

In conclusion, induction of RNAi targeting tbcatB transcripts *in vivo* mimics the results observed in previous *in vitro* RNAi experiments (30,117). In the mouse model of infection, RNAi of tbcatB rescued mice from a lethal *T. b. brucei* infection, resulting in no splenomegaly and no detectable parasites in blood. While induction of RNAi against rhodesain did not cure mice of their infection, it did significantly prolong the survival of five out of ten mice. Since RNAi led to a 60% reduction of rhodesain activity (Fig. 2.3B), it is still possible that a 100% knockdown might uncover a more direct role for rhodesain in parasite viability. However, even the modest knockdown achieved for tbcatB (quantified in (117)) produced a profound effect on parasite viability both *in vitro* (122) and *in vivo*.

These results suggest that tbcatB and rhodesain have different biological roles. TbcatB appears essential to parasite viability and represents a more rational target for protease inhibitors as chemotherapy against human African trypanosomiasis (16). Rhodesain may play a role in *Trypanosoma* pathogenesis. Nikolskaia *et al.* (122) showed that a cysteine protease inhibitor, known to target Rhodesain, blocked the ability of *T. b. brucei gambiense* to cross a model of the blood-brain barrier (122). Such a role in pathogensis would explain why knockdown of rhodesian transcripts and activity had no effect on parasitemia and splenomegally but did prolong survival of 50% of the mice in two independent experiments.

ACKNOLEDGEMENTS

This work was supported by the Drugs for Neglected Diseases Initiative (DNDi), The Sandler Family Supporting Foundation and TDRU grant AI35707 from the NIAID.

FIGURES FOR CHAPTER 2

Figure 2.1. Survival curves for mice infected with *T. brucei* under control and RNAi induction conditions. *A-C.* Survival curves for mice infected with non-transfected *T. b. brucei* but given an inducing dose of doxycycline (red) versus standard food and water (blue) (n=5 in each group) (A). Infection with trypanosomes containing RNAi plasmid for rhodesian plus or minus induction by doxycycline rescued 5 out of ten mice *p=0.003* (B). Infection with RNAi plasmid for tbcatB plus or minus induction by doxycycline. Note that all 5 mice with RNAi induction survived until experiment was terminated (C).

Figure 2.2. Rhodesain expression and splenomegally after RNAi induction.

A. Evidence that RNAi reduces expression of Rhodesain mRNA in parasites isolated from mice infected with rhodesain RNAi containing plasmid induced with doxcycycline versus un-induced controls. *B.* Splenomegally is absent in trypansome-infected mice if RNAi of tbcatB is induced. The hatched line represents the baseline for age-matched uninfected mice.

Figure 2.3. Detection of rhodesain protein and protease activity after RNAi induction. *A.* Rhodesain protein level and activity is decreased after RNAi induction in pZJMTbRho parasites recovered from infected mice. Control or doxycycline-induced

pZJMTbRho parasites were purified from mice. Equal amounts of protein were resolved by 15% SDS-PAGE and stained with anti-rhodesain antibody and visualized by Western blot. *B.* The level of rhodesain activity in pZJMTbRho parasite purified from mice was determined with the active site tag ^{125}I-DCG-04, visualized by autoradiography, and quantified by PhosphorImager. *C.* The level of rhodesain and tbcatB activity in parasites purified from mice infected with the 90-13 strain was determined with the active site tag ^{125}I-DCG-04 and visualized by autoradiography.

Figure 2.1.

A.

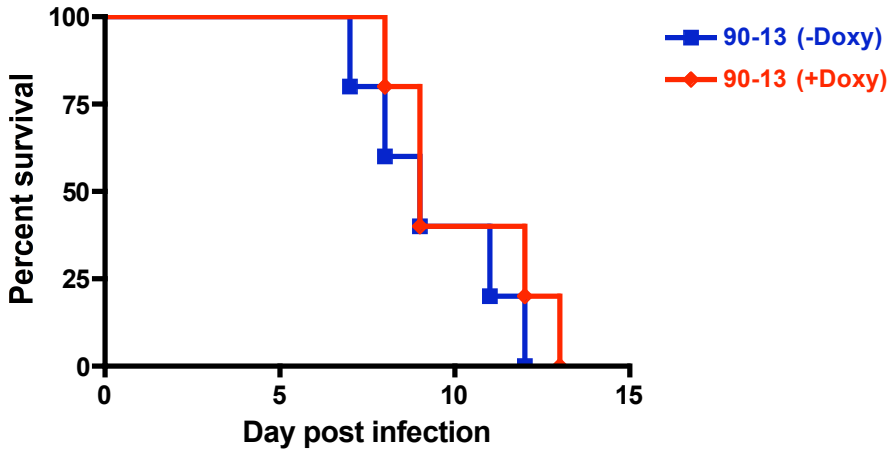

B.

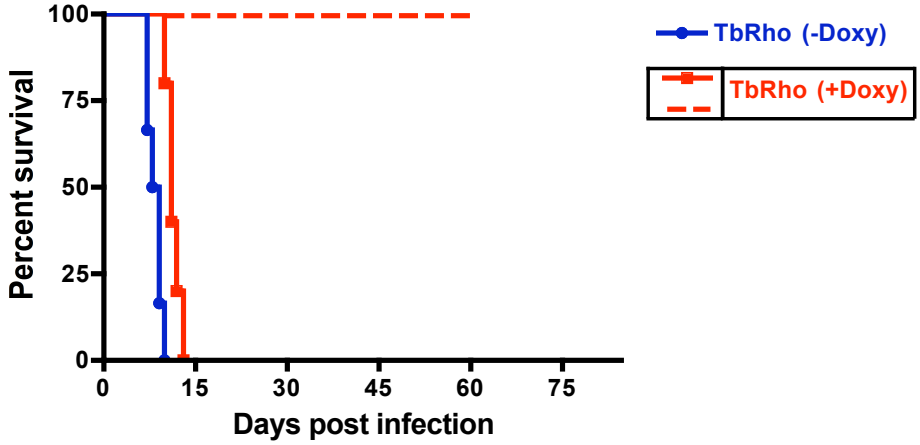

C.

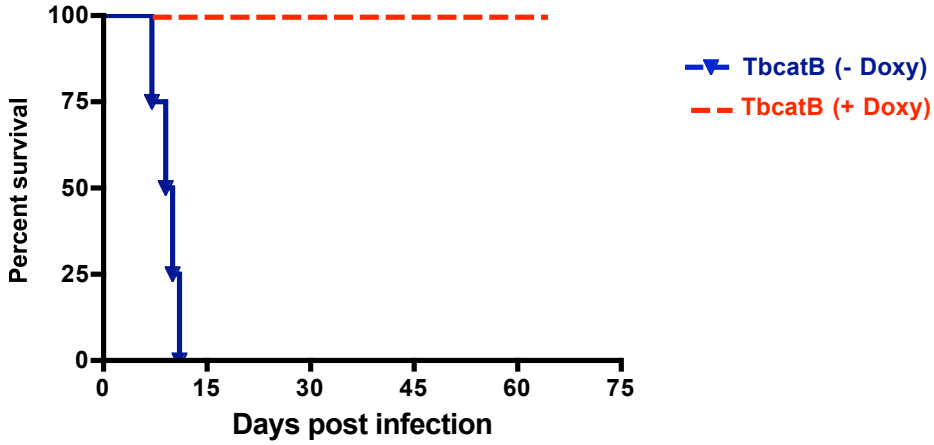

Figure 2.2.

A.

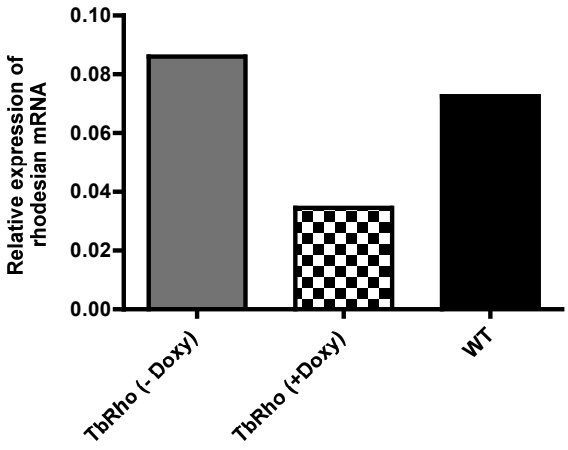
Relative expression of rhodesian mRNA
0.10
0.08
0.06
0.04
0.02
0.00
TbRho (- Doxy)
TbRho (+Doxy)
WT

B.

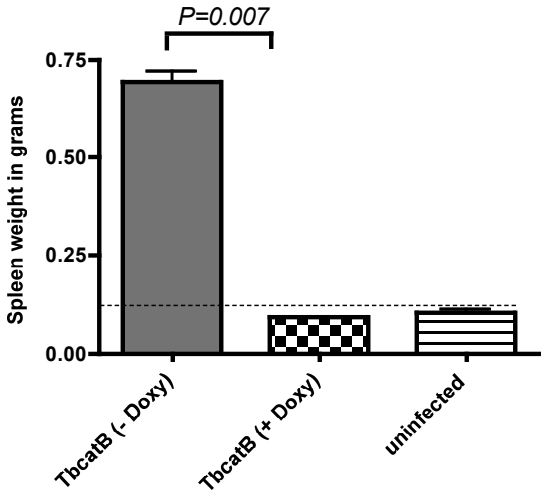
P=0.007
Spleen weight in grams
0.75
0.50
0.25
0.00
TbcatB (- Doxy)
TbcatB (+ Doxy)
uninfected

Figure 2.3.

A.

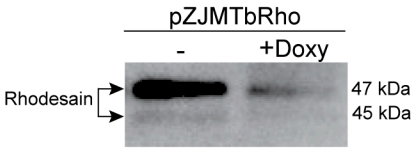

B.

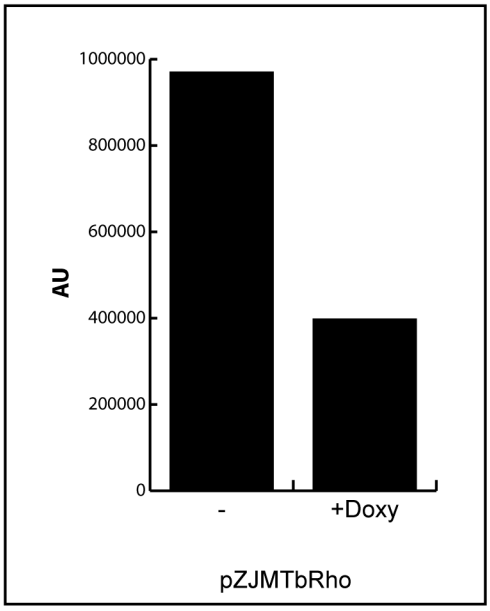

C.

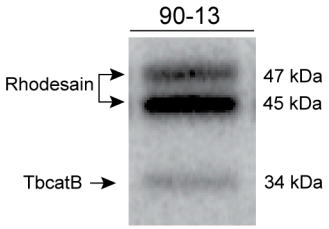

CHAPTER 3

A PARASITE CYSTEINE PROTEASE IS KEY TO HOST PROTEIN DEGRADATION AND IRON ACQUISITION

ABSTRACT

Cysteine proteases of the Clan CA (papain) family are the predominant protease group in primitive invertebrates and promising targets for chemotherapy of protozoan parasite infections. Cysteine protease inhibitors arrest infection by the protozoan parasite, *Trypanosoma brucei*, in a mouse model. While two *T. brucei* Clan CA cysteine proteases, one cathepsin L- and the other cathepsin B-like, are potential inhibitor targets, RNAi studies identified the cathepsin B-like protease, tbcatB, as the key target. Utilizing parasites in which one of the two alleles of the *TBCATB* gene has been deleted, the role of this protease in degradation of endocytosed host proteins is delineated. TbcatB deficiency results in a decreased parasite growth rate and dysmorphism of the flagellar pocket and the subjacent endocytic compartment. Western blot and microscopic analysis indicate that deficiency in tbcatB results in accumulation of both host and parasite proteins, including the parasite lysosomal marker p67. A critical function for parasitism is the degradation of host transferrin which is necessary for iron acquisition. Substrate specificity analysis of recombinant tbcatB identified the optimal peptide substrate cleavage sequence and an informatics search using this sequence identified host transferrin as a likely substrate. This hypothesis was confirmed by both biochemical assay and proteomic analysis of tbcatB-deficient parasites. Because even a modest

deficiency in tbcatB is lethal for the parasite, tbcatB is a logical target for the development of new anti-trypanosomal chemotherapy.

INTRODUCTION

Proteases are ubiquitous enzymes that function in virtually all biological phenomena. Two of the major groups of proteases, Clan CA (papain-like) cysteine proteases and Clan SA (trypsin-like) serine proteases, underwent an evolutionary inversion whereby the more abundant cysteine proteases of primitive eukaryotes gave way to serine proteases with the evolution of arthropods (123) (http://merops.sanger.ac.uk/). Therefore, an analysis of the role of cysteine proteases in protozoa can provide insights into the molecular evolution and diverse functions of this protease class.

Trypanosoma brucei is a protozoan parasite and the causative agent of Human African Trypanosomiasis (HAT), a frequently fatal disease that is transmitted by the bite of the tsetse fly. Cases of HAT have been reported in 36 countries in sub-Saharan Africa (2). Difficulties in disease diagnosis coupled with limited treatment options contribute heavily to the disease burden of HAT. Only four drugs are available to treat HAT: two for the first stage of the disease when parasites proliferate in the blood (pentamidine and suramin) and two for the second stage when parasites have established infection in the cerebral spinal fluid (melarsoprol and eflornithine). These drugs cause serious side effects and are expensive to manufacture and administer. There is an obvious and urgent need to develop new chemotherapies to treat HAT.

T. brucei is also a model system for studying parasite biochemistry and cellular function in protists. *T. brucei* can be grown axenically and is well characterized

ultrastructurally. Trypanosome cellular structure shares much in common with other eukaryotes. For example, all of the major organelles (nucleus, mitochondria, endoplasmic reticulum, and Golgi apparatus), as well a complex endocytic system with coated vesicle transport, are present. *T. brucei* also evolved unique cellular structures, such as the kinetoplast, flagellum, and flagellar pocket. The flagellar pocket is the site of all endocytosis and exocytosis for this polarized cell.

Two Clan CA cysteine proteases have been identified in *T. brucei*: rhodesain, which is cathepsin L-like and is most abundant (62), and tbcatB, a cathepsin B-like enzyme that is less abundant but, by RNAi studies, a key factor for parasite survival (117). Treatment of parasites in culture with the pan-cysteine protease inhibitor, Z-Phe-Ala-diazomethyl ketone (Z-Phe-Ala-CHN_2) is lethal to cultured parasites at 10 μM (30). Parasites treated with this inhibitor exhibit altered cell morphology, are unable to undergo cytokinesis, and are defective in host protein degradation (30), (124). Knockdown of tbcatB expression by RNA interference is also lethal in *T. brucei*, causing phenotypic defects similar to those seen with the inhibitor (117). These results led to the hypothesis that while tbcatB is less abundant, it is nonetheless essential to *T. brucei* survival in culture and is a key target of the inhibitor. Furthermore, when tbcatB is knocked down in a mouse model of *T. brucei* infection, mice are cured of their infection (Abdulla, personal communication).

One clue to the function of tbcatB comes from the observation that a host iron-transporting protein, transferrin, accumulates in Z-Phe-Ala-CHN_2-treated and tbcatB RNAi knockdown parasites (30,117). Transferrin serves as the sole source of iron for *T. brucei* and is rapidly degraded in an endosomal or lysosomal compartment in the parasite

(125). Thus, accumulation of transferrin implicates tbcatB in the process of iron acquisition and suggests that transferrin may be a natural substrate of the protease.

The RNAi studies showed only modest knockdown of tbcatB RNA and protein, yet the phenotype was dramatic (117). Therefore, to validate the previous RNAi data and further our understanding of the functional role of tbcatB, we generated a single allele deletion strain of *T. brucei* and, together with the inducible-RNAi strain, analyzed the effects of tbcatB-deficiency on cell morphology, protease localization, and the iron acquisition pathway. We also expressed recombinant tbcatB and analyzed its substrate specificity profile for clues as to the identity of natural substrates and as a means to determine subsite characterization that will aid future inhibitor design.

MATERIALS AND METHODS

Culturing of *T. brucei*

All bloodstream form strains of *T.brucei* were incubated in 5% CO_2 at 37 °C in HMI-9 medium containing 10% heat-inactivated fetal bovine serum (Omega Scientific), 10% Serum Plus (JRH Biosciences), 1x penicillin/streptomycin. The pZJMTbCB clones were cultured in media containing, 5.0 μg/ml hygromycin B and 2.5 μg/ml G418, as well as 2.5 μg/ml phleomycin. Induction of RNAi was carried out by adding tetracycline to a final concentration of 100 ng/ml.

Generation of TBCATB Single-allele Knock-out Clones ($TBCATB^{+/-}$)

To generate the targeting vector, a cassette containing the phleomycin resistance marker was flanked by the 5' and the 3' flanking regions (FR) of the *TBCATB* gene was constructed. 5'FR forward primer: 5'-gcggccgccagaagctccactgcctcgcattg-3'. 5'FR

reverse primer: 5'-gatatccatgtgtcaccggatttggggtctgca-3'. 3'FR forward primer: 5'-tctagataggttgcacatcgttaa acctagag-3'. 3'FR reverse primer: 5'-gggcccacatccttatcccttccccgagggcg-3'. The cassette was cloned into the pCR2.1 vector (Invitrogen) at NotI and ApaI restriction endonuclease sites. For electroporation, 10^8 strain trypanosomes were pelleted by centrifugation, washed twice with 10 mL of cytomix (105), and finally resuspended in 0.5 ml of cytomix. One hundred micrograms of the targeting vector was linearized with *Not*I restriction endonuclease, precipitated with ethanol, and resuspended in 100 μl of cytomix. The parasites and DNA suspensions were mixed in a 4-mm electroporator cuvette and pulsed with 1.7kV and 25 microfarads. After pulsing, the parasites were transferred to 24 ml of complete medium and incubated overnight at 37 °C with 5% CO_2. Phleomycin was added to the medium to select for clones having the targeting vector integrated into the genome. Proper integration into the *TBCATB* locus was verified by PCR.

Radiolabeling of *T. brucei* Lysates with ^{125}I-labeled Cysteine Protease Inhibitors

Equal amounts of trypanosome lysate (10μg) were labeled with ^{125}I-DCG-04 (107) in the presence of ~2 mM dithiothreitol for 45 minutes at room temperature and subjected to SDS-PAGE. Quantification of labeled enzymes was determined by Phosphoimager analysis (Molecular Dynamics).

***T. brucei* Growth Assay**

Trypanosomes were cultured at a density of $1x10^4$ cells/ml and counted using a hemocytometer after 24, 48, and 72 hours.

Immunofluorescence Microscopy

T. brucei were harvested by centrifugation at 4 °C, washed in cold Dulbecco's phosphate buffered saline (D-PBS), and fixed in 4% paraformaldehyde/D-PBS for 1 hour at 4 °C. All subsequent washes were carried out with excess D-PBS. Fixed cells were washed and applied to 25 mm round cover slips that had been coated with poly-lysine (0.1% w/v in water, Sigma Aldrich) and allowed to settle for 20 minutes at room temperature. The cells were then permeabilized in D-PBS containing 0.1% Triton X-100 (Sigma-Aldrich) for 10 minutes, washed, and blocked for one hour with 1% bovine serum albumin (BSA) prepared in D-PBS. After blocking, the cells were incubated in mouse anti-p67 antiserum (a gift from J. D. Bangs) (126) (diluted 1:400 in 1% BSA/D-PBS) for 1 hour, washed, incubated in Texas Red goat anti-rabbit IgG (Molecular Probes) (diluted 1:400 in 1% BSA/D-PBS) for 1 hour, washed, and finally mounted on slides with Prolong Gold Antifade Reagent with DAPI (Invitogen). The cells were visualized on an AxioImager M1 microscope (Zeiss), equipped with an X-Cite 120 fluorescence illumination system (EXFP Life Sciences).

Transmission Electron Microscopy

Approximately 40 million *T. brucei* were harvested by centrifugation at 4 °C. Pelleted parasites were resuspended in 1 ml of media for high pressure freezing using either a Bal-Tec HPM 010 or Wohlwend HPF Compact 01 high pressure freezer (University of California, Berkeley Electron Microscopy Laboratory). The parasites were processed for conventional EM by freeze-substitution in 1% OsO_4/0.1% uranyl acetate in acetone using a Leica AFS2 and embedded in Eponate 12 resin. Sections were cut with a Leica Ultracut E ultramicrotome using a diamond knife and picked up on Pioloform films on

slot grids. Sections were stained with uranyl acetate and Sato's lead, and photographed using a Gatan 4k x 4k camera on an FEI Spirit TEM operated at 120 kV.

Immuno-electron Microscopy

T. brucei samples for immuno-electron microscopy were prepared by high pressure freezing as indicated above, except freeze-substitution was conducted in 0.2% glutaraldehyde/0.1% uranyl acetate in acetone. Following substitution, the samples were infiltrated in LR White resin at 4° C, and UV-polymerized at -20° C using benzoin methyl ether as the UV catalyst in the LR White. Sections were picked up on carbon-coated Pioloform films on nickel grids. Sections were incubated with primary antibodies (rabbit anti-tbcatB (117) and rabbit anti-transferrin receptor (a gift of P. Borst) (127), both diluted 1:400) and 10 nm gold secondary antibodies (complete antibodies absorbed to gold) (British BioCell International, distributed by Ted Pella) diluted in 1% BSA/0.1% Tween-20 in PBS. After labeling, the sections were fixed 5 minutes with 1% glutaraldehyde in PBS, rinsed with distilled water and stained with uranyl acetate followed by Sato's lead as indicated above. Control sections were immuno-stained using this protocol but with omission of the primary antibody. Sections were photographed as indicated above.

Cloning and Expression of TbcatB in *Pichia pastoris*

Methods for cloning and expression of tbcatB in *P. pastoris* have been described previously (Mallari, manuscript in press). Briefly, the sequence encoding the tbcatB zymogen (pro and mature regions of the protease) was amplified from a cDNA vector that contained the entire open reading frame of tbcatB (117). The forward and reverse primers amplified genomic regions 5'-*ga*gtaaacgccgccctcgttgct-3□ and 5'-

cgccgtgttgggtgcaagagg-3', respectively. The amplified DNA was purified and ligated into the expression vector pPICZαB (Invitrogen) and subsequent transfection and expression techniques were modified from those given by the manufacturer as previously described (62).

Purification of Recombinant TbcatB

Following the 48-hour induction, the *P. pastoris* cultures were centrifuged at 3000 g for 10 minutes and the resulting supernatant containing recombinant tbcatB was lyophilized and stored at 4°C until use. The crude lyophilized protein was resuspended in approximately 10% of the original volume in 50 mM sodium citrate buffer, pH 5.5 and desalted using PD10 columns (GE Healthcare Lifesciences/Amersham Biosciences) by equilibrating in the same buffer. The solution was loaded onto a Mono Q 5/50 anion exchange column using an Akta Purifier-900 chromatography system (both GE Healthcare Lifesciences/Amersham Biosciences). A 50 mM MES, pH 6.5 buffer was used for column equilibration, sample loading, and protein elution, with a flow rate of 1ml/minute. Protein was eluted with a linear gradient of 0 to 1 M NaCl concentration over 20 minutes. Fractions of 0.5 ml were collected and subsequently checked for purity by SDS-PAGE and activity by hydrolysis of Z-Phe-Arg-AMC (Z-FR-AMC) substrate (see enzyme activity assay below).

Radiolabeling of Cysteine Protease Active Sites with ^{125}I-labeled Inhibitors

Ten microliters of MonoQ fractions containing recombinant tbcatB were labeled with the cathepsin B-specific active site label ^{125}I-MB-074 (107) for 1 hour at room temperature in buffer containing 5 mM dithiothreitol (DTT). Samples were then subjected to SDS-PAGE. Once the gels were dried, labeling was visualized by autoradiography.

Deglycosylation of Recombinant TbcatB

Two 10 μl samples of MonoQ-purified recombinant tbcatB were labeled with ^{125}I-MB-074 (107), as described above. A New England Biolabs PNGase F kit was used for deglycosylation. Methods were followed as described in the instruction manual, with the exception that one of the samples did not receive PNGase (maintained as control). The samples were subjected to SDS-PAGE and the dried gel was visualized by autoradiography.

Protease Activity Assay

Protease activity was measured using the fluorogenic peptide substrate Z-FR-AMC (Peptides International, Inc.), which is cleaved by the protease to release free 7-amino-4-methyl coumarin (AMC) fluorogenic leaving group. Enzyme samples (in 10 μl volume) were pre-incubated for 10 minutes with 90 μl sodium citrate buffer (50 mM, pH 5.5) containing 4 mM DTT, giving a total volume of 100 μl. The substrate was diluted from a 20 mM stock solution in DMSO in the same buffer and total volume to give a final concentration of 10 μM Z-FR-AMC and final volume of 200 μl. Hydrolysis was measured at 25 °C using an automated microtiter plate spectrofluorimeter (Molecular Devices Flex Station). Excitation and emission wavelengths were 355 and 460 nm, respectively. One unit of activity was defined as that releasing 1 □mol of AMC per minute. To determine the Michaelis constant, K_m, a range of substrate concentrations from 0.14 to 300 μM was used and the value estimated using graphics software (Prism4, GraphPad).

pH Activity Profiling of Recombinant TbcatB

Purified tbcatB were assayed for protease activity with Z-FR-AMC (62), using 50 mM sodium citrate buffers that ranged in pH from 3 to 8, with 0.5 pH unit increments. Protease activity was assayed as described above.

Protease Inhibitor Profiling

Purified tbcatB was assayed for protease activity with Z-FR-AMC in the presence of various protease-class selective inhibitors. The inhibitors used were K11777 (*N*-methylpiperazine-Phe-homoPhe-vinylsulfone-phenyl) (48), CA074 (N-(L-3-trans-propylcarbamoyloxirane-2-carbonyl)-L-isoleucyl-L-pro line) (128), PMSF (phenylmethanesulphonylfluoride), and E64 (*N*-[*N*-(l-3-*trans*-carboxyoxirane-2-carbonyl)-l-leucyl]-agmatine). Enzyme samples (in 10 μl volume) were pre-incubated with inhibitor for 5 minutes in 90 μl sodium citrate buffer (50 mM, pH 5.5) containing 4 mM dithiothreitol (DTT) to give a total volume of 100 μl. The inhibitor concentration range used was 0.01 to 10 μM. Following incubation, the substrate was added in the same buffer to give a final concentration of 10 μM and final volume of 200 μl. Protease activity was assayed as described above.

Substrate Specificity Profiling and Substrate Screen

P1-P4 substrate specificity profile for tbcatB was determined using a completely diverse positional scanning combinatorial synthetic combinatorial library (PS-SCL) (97). The library contained substrates that are N-terminally acetylated with 7-amino-4-carbamoylmethylcoumarin (ACC) as the fluorogenic leaving group. The procedures used to screen the library were modified from those previously described (97). Briefly, crude lyophilized tbcatB was resuspended in 50 mM sodium citrate buffer, pH 5.5 (final

concentration of ~2 μM□, containing Brj-35 (final assay concentration of 0.01%) and DTT (final assay concentration of 10 mM), and incubated at 25 °C for 5 minutes to activate the enzyme. One microliter aliquots from each of the 20 sub-libraries of the P1, P2, P3, and P4 libraries were added to the wells of a 96-well Microfluor-1 U-bottom plate. The activated enzyme was added to each well to give a final assay volume of 99 μl and concentration of 31.25 nM for each of the 8,000 compounds/well and 1% DMSO (from the substrates). Hydrolysis was measured as in the protease activity assay described above with excitation and emission wavelengths of 380 nm and 460 nm, respectively.

To test the predictive capability of the substrate specificity profile obtained, authentic AMC peptide substrates that were either "good" or "poor" matches to the profile were selected for screening in the protease activity assay described above. The range of substrate concentrations used was 3.5 to 300 μM. The substrates were: Z-FR-AMC (Peptides International, Inc.), Z-Arg-Arg-MCA (Z-RR-AMC) (Peptides International, Inc.), Z-Arg-Glu-Lys-Arg-AMC (Z-REKR-AMC) (Bachem), Ac-Ile-Glu-Pro-Asp-AMC (Ac-IEPD-AMC) (Bachem), Ac-Ala-Ser-Thr-Asp-AMC (Ac-ASTD-AMC) (Bachem), Z-Leu-Arg-Gly-Gly-AMC (Z-LRGG-AMC) (Bachem), H-Arg-Gln-Arg-Arg-AMC (H-RQRR-AMC) (Bachem), Ac-Lys-Gln-Lys-Leu-Arg-AMC (Ac-KQKLR-AMC) (AnaSpec, Inc.) and Z-Arg-Arg-Leu-Arg-AMC (Z-RRLR-AMC), which was custom synthesized by SynPep. Michelis constants were estimated for each substrate as described above.

Human Serum and *T. brucei* Protein Database Search

A database of host serum proteins was created by first searching the Protein Data Bank (PDB) (http://www.pdb.org/) (129), using the keyword "serum" and limiting the search to *"homo sapiens*" proteins. The results of the search were downloaded in FASTA format. The database of serum proteins was then screened using the EMBOSS fuzzpro protein pattern program (130) for the amino acid motif: P4: R/K, P3: R/K, P2: X, P1: R/K.

*T. bruc*ei proteins were also screened to see if any contained tbcatB's optimal substrate specificity motif. The virtual screen was carried out using the "Search Using Quick Matrix Method" Database Search option on Scansite's website (http://scansite.mit.edu) (131). Once the amino acid motif (P4: R/K, P3: R/K, P2: X, P1: R/K) was entered, the following parameters were selected: Organism Class: Invertebrates, Database: SWISS-PROT, and Single species: brucei. No limits were set for other parameters.

Lysate preparation for 2-D PAGE

T. brucei strain 221 and TBCATB$^{+/-}$ were harvested by centrifugation, washed once in D-PBS, and resuspended at ~1x10^{8} cells/ml in lysis buffer (50 mM sodium acetate, pH 5.5, 1 mM EDTA, 1% TritonX-100, 5 mM DTT, and 5 µl/ml Protease Inhibitor Cocktail Set II (CalBiochem, stock solution contains 20 mM AEBSF, Hydrochloride, 1.7 mM Bestatin, 200 µM E-64 Protease Inhibitor, 85 mM EDTA, Disodium, and 2 mM Pepstatin)) that had been supplemented with 0.1 units/µl DNase (RNase-free, Roche), 45 µM RNase A (Roche), and 30 mM $MgCl_2$. The lysates were incubated on ice for 20 minutes and then cleared by centrifugation at 16,000 g for 50 minutes at 4 °C. The protein concentration of the cleared lysates was determined by Bradford assay (132). If not used immediately, lysates were stored at -80 °C. Equal amounts of each lysate (200

μg) were prepared for isoelectric focusing (IEF) and 2-D gel electrophoresis using the ReadyPrep 2-D Cleanup Kit (Bio-Rad). The subsequent procedures used for IEF and 2-D gel electrophoresis were carried out as described in the ReadyPrep 2-D Starter Kit (Bio-Rad) instruction manual. Bio-Rad ReadyStrip IPG strips, pH 4-7 were used for IEF and 8-16% Criterion Ready Gels (Bio-Rad) were used for SDS-PAGE. Following SDS-PAGE, the gels were immediately transferred to polyvinylidene difluoride (PVDF) membrane (Millipore), using procedures described below.

Western Blots of 2-D PAGE Gels

2-D gels were transferred to PVDF membranes and blocked for 1 hour (10 mM Tris, pH 7.4, 5% w/v dry milk, and 0.1% w/v BSA). After blocking, membranes were incubated with rabbit anti-transferrin antiserum (1:2500 dilution) (transferrin H-65 antibody, Santa Cruz Biotechnology, Inc.) for 1 hour and washed 3 times for 10 minutes with TBST (10 mM Tris, pH 7.4, 150 mM NaCl, 0.4% Tween 20). After washing, membranes were incubated with horseradish peroxidase-conjugated donkey anti-rabbit IgG (1:5000 dilution) (GE Healthcare Lifesciences/Amersham Biosciences) for 1 hour. The blots were washed three times for 10 minutes with TBST and twice for 10 minutes with TBS (TBST without 0.4% Tween 20). Finally, the blots were visualized using ECL reagents (GE Healthcare Life Sciences/Amersham Biosciences).

Transferrin Starvation

Trypanosomes were incubated at a density of $5x10^4$ cells/ml for 36 hours in appropriate media (see methods for culturing *T. brucei* above), containing 10% fetal bovine serum or dog serum (Innovative Research). After the incubation period, equal numbers of parasites ($1x10^7$) were resuspended in lysis buffer (50 mM sodium acetate, 1 mM EDTA, 1%

Triton X-100, pH 5.5, 5 mM DTT). The lysates were incubated on ice for 20 min and cleared by centrifugation at 16,000 g for 15 minutes at +4 °C. The extracts were resolved by SDS-PAGE and subjected to Western blot analysis, using procedures described above and rabbit anti-transferrin receptor antiserum (127) (diluted 1:250) as primary antibody. Labeling was quantified by densitometry using Image J software (National Institute of Health).

RESULTS

Single-allele Deletion of the *T. brucei* Cathepsin B Gene Leads to Decreased Parasite Replication

Silencing of tbcatB by RNAi produced a marked phenotype (117). Parasites exhibited endosomal or lysosomal swelling, decreased growth rate, arrest in cytokinesis, and eventual death. However, this dramatic phenotype was associated with only a modest decrease in tbcatB protein, RNA, and protease activity (117). Therefore, to validate and extend the RNAi results, a tbcatB heterozygous knock-out clone ($TBCATB^{+/-}$) was produced by homologous recombination using a *TBCATB* targeting vector. The rate of replication of the $TBCATB^{+/-}$ clones was approximately 40% less than the control 90-13 strain after 72 hours (Fig. 3.1). TbcatB activity, as measured using the clan CA cysteine protease active site label, ^{125}I-DCG-04 (133), was reduced by approximately 60% in $TBCATB^{+/-}$ clones versus strain 221 control parasites (Fig. 3.9, Supplemental).

Abnormal Lysosomal and Flagellar Pocket Morphology in TbcatB-deficient Parasites

Treatment of wild-type *T. brucei* with the diazomethyl ketone cysteine protease inhibitor Z-Phe-Ala-CHN_2 lead to enlargement of the lysosome and an increase in total protein content, presumably as a result of decreased protein degradation (124). RNAi knockdown of tbcatB lead to a similar endosomal or lysosomal swelling (117). To compare the tbcatB-deficient phenotype with the phenotype of inhibitor-treated parasites, we first examined the lysosomal compartment by the localization of p67, a lysosomal type I membrane glycoprotein (70). In control parsasites, p67 staining was limited to a discrete organelle focus between the kinetoplast and nucleus (Fig. 3.2A & 2B). In contrast, both induced RNAi clones (Fig. 3.2E & 2F) and $TBCATB^{+/-}$ clones (Fig. 3.2C & 2D) showed enhanced p67 labeling in large distorted organelles.

Electron microscopy was used to further delineate the phenotype of induced RNAi clones and $TBCATB^{+/-}$ parasites. In contrast to controls (Fig. 3.3A & 3B), both the heterozygous knockout (Fig. 3.3C) and RNAi knockdown (Fig. 3.3D) parasites had swollen flagellar pockets and swollen endosomal compartments. The flagellar pockets of both tbcatB-deficient parasites were approximately 5 times larger in diameter than the flagellar pocket of the controls.

TbcatB Localizes to the Lysosome

Rhodesain, the most abundant cysteine protease activity in *T. brucei*, is localized in lysosomal compartments (62). Immunoelectron microscopy revealed that tbcatB, while less abundant, also localizes to lysosomes (Fig. 3.4A). When tbcatB expression is

disrupted by RNAi, tbcatB protein fails to enter lysosomes but instead accumulates in adjacent tubular/vesicular structures (Fig. 3.4B).

Expression, Purification, and Biochemical Properties of Recombinant TbcatB from *Pichia pastoris*

Expression of the tbcatB zymogen lead to secretion of both zymogen and mature forms of tbcatB (42 and 31 kDa, respectively) from *P. Pastoris.* Both protein species were identified by the cathepsin B active site label ^{125}I-MB-074 (107), indicating that the recombinant protease is active (Fig. 3.5A). Purification of active tbcatB was carried out by lyophilization, desalting, and MonoQ anion exchange chromatography. Protease activity was monitored using the fluorogenic peptide substrate Z-FR-AMC and a K_m value of 63 μM was measured for the purified enzyme. When the purified enzyme was subjected to deglycoslyation with PNGase F, a decrease in the molecular weights of both the zymogen and mature forms of the enzyme was observed: the zymogen lost ~8 kDa whereas the mature enzyme lost ~4 kDa, consistent with two glycosylation sites in the pro region (at amino acids Asn^{58}-Ile-Thr and Asn^{76}-Ala-Ser) and one in the mature region of tbcatB (Asn^{216}-Tyr-Thr). The optimal pH range for recombinant tbcatB with Z-FR-AMC was measured between pH 5.0 and 5.5 (Fig. 3.5B), consistent with the localization of the enzyme in an acidic organelle. TbcatB activity was inhibited by the Clan CA cysteine protease inhibitors E-64 and K11777, but not by the serine protease inhibitor PMSF. The cathepsin B cysteine protease inhibitor, CA074, inhibited tbcatB better or equivalent to the generic clan CA cysteine protease inhibitors (E64 and K11777), confirming the cathepsin B-like activity of the recombinant enzyme.

Substrate Specificity Profiling of Recombinant TbcatB Identifies an Optimal Substrate Motif

Substrate specificity profiling using positional scanning synthetic combinatorial libraries (PS-SCL's) has been used to determine the P1-P4 sequence preference of a protease for peptide substrates (134). These libraries contain a series of peptide substrates with fluorogenic leaving groups in which one position (P1, for example) is a fixed amino acid and all other positions are varied (in an isokinetic mixture). Substrate specificity data obtained from screening PS-SCL's has facilitated natural substrate identification for Sc*histosoma mansoni* legumain (96) and granzyme B (95).

A complete diverse PS-SCL was used, containing 160,000 tetrapeptide substrates. This library completely randomizes each of the P1, P2, P3, and P4 positions with 20 amino acids (97). The PS-SCL library demonstrated that tbcatB has a strong preference for arginine or lysine at P1 and for amino acids with large hydrophobic side chains at P2 (Fig. 3.6A). TbcatB was also more selective at P3 and P4 than its orthologs (97) (Fig. 3.6B) and P3 specificity differs significantly from that of human cathepsin B (Fig. 3.6B). The optimal substrate motif for tbcatB, as predicted by substrate specificity profiling, was: P4: R/K, P3: R/K, P2: X, P1: R/K.

The substrate specificity profile for tbcatB was verified by screening authentic fluorogenic peptide substrates that were predicted to be "good" or "poor" substrates for tbcatB. Only those substrates that most closely resembled the predicted optimal substrate motif for tbcatB were efficiently cleaved by the recombinant protease (Table 3.1).

A database of human serum proteins was created and searched for proteins that contain a site that matched the predicted optimal substrate motif for tbcatB. The search

identified fourteen such proteins, of which nine contained a matching site that was solvent accessible (Table 3.2, Supplemental). Those proteins with solvent accessible potential cleavage sites include transferrin, which has an RKDK sequence located at amino acid positions 612-615, and serum response proteins that are elevated as part of the innate immune response. Notably, the site in transferrin is conserved in both mouse (RKEK) and bovine (RKDK) and is adjacent to an iron binding site at His^{604}. A similar search was also carried out with *T. brucei* proteins. Of note, a site matching tbcatB's predicted optimal substrate motif is located in the pro-peptide of the rhodesain zymogen (KRLR, at amino acids 113-116), at the junction between the pro-petide and mature domains.

Undegraded Transferrin Accumulates in $TBCATB^{+/-}$ Parasites

Parasites internalize transferrin via receptor mediated endocytosis in coated vesicles (68). These vesicles form at the flagellar pocket (FP), the site of all endocytosis and excocytosis in *T. brucei*, and rapidly transit the endocytic system (reviewed in (135)). Iron release is thought to occur in acidic vesicles, where transferrin is degraded in endosonal/lysosomal compartments and the transferrin receptor (Tf-R) is recycled to the flagellar pocket (125) (136). We examined the accumulation of transferrin in $TBCATB^{+/-}$ and control parasites by 2D gel electrophoresis and Western blot analysis. Antibody to transferrin identified two protein species of ~64 and ~50 kDa by Western Blot analysis in lysate obtained from $TBCATB^{+/-}$ parasites (Fig. 3.7B), while no transferrin species were detected in lysates obtained from wild-type parasites (Fig. 3.7A).

Transferrin Receptor (Tf-R) Accumulation in TbcatB-deficient Parasites

T. brucei respond to low levels of intracellular iron by upregulating the expression of the Tf-R (137). This upregulation can alter the distribution of the receptor such that it accumulates in the flagellar pocket and on the surface of the parasite (127). Additionally, iron-starved parasites can switch transferrin receptors, exchanging the Tf-R expression site to one that expresses a receptor with higher affinity for host transferrin (138) (139). To explore the hypothesis that tbcatB-deficient parasites undergo iron starvation due to lack of transferrin degradation, we examined the expression and localization of the Tf-R in tbcatB heterozygous knockouts and tbcatB RNAi knockdowns, respectively. Upregulation of Tf-R expression was confirmed using an iron-starvation assay in which parasites were cultured in media containing 10% dog serum versus the fetal calf serum that is typically used. The *T. brucei* Tf-R expressed by strain 221 parasites has a very low affinity for dog serum transferrin (139) and iron-starved parasites respond by upregulating Tf-R expression (137). In TBCATB$^{+/-}$ parasites cultured in media containing dog serum, the Tf-R is upregulated by more than 40% above levels in the wild-type strain, suggesting that the tbcatB-deficient parasites experience a severe iron starvation phenotype (Fig. 3.8A & 8B). Tetracycline-induced pZJMTbCB parasites accumulated abundant Tf-R in swollen flagellar pockets (Fig. 3.8C & 8D), whereas controls did not (not shown).

DISCUSSION

Both *in vitro* and *in vivo* studies have shown that cysteine protease activity is required for *T. brucei* survival (30,85,104,124). RNAi studies implicated tbcatB as an essential

protease (117) (Chapter 2). However, only modest loss of tbcatB RNA and protease activity is achieved with RNAi (117). Therefore, to validate these results, we now show that parasites containing only a single copy of the tbcatB gene ($TBCATB^{+/-}$ clones) also exhibit decreased growth rate and morphological abnormalities similar to those observed in studies using cysteine protease inhibitors (30,104,124) or RNAi knockdown of tbcatB (117).

The abnormalities in *T. brucei* organelle morphology produced by cysteine protease inhibitors led to the hypothesis that cysteine proteases are required to degrade host proteins (30,124). Parasites treated with Z-Phe-Ala-CHN_2 had an enlargement of the lysosome (30) (124). Enlargement of an endocytic or lysosomal compartment was also observed with tbcatB RNAi knockdown parasites (117). The same abnormality is seen in $TBCATB^{+/-}$ parasites (Fig. 3.2). Using antibody localization of p67, accumulation of this specific lysosomal protein was confirmed. The compartmental swelling, as visualized ultrastructurally in Figure 3.3 clearly includes the flagellar pocket, but could also involve the endocytic pathway downstream of the flagellar pocket, including the lysosome. Because the bulk of host proteins taken up by trypanosomes first enter the flagellar pocket and are then trafficked to the lysosome, the accumulation of undegraded protein, and its osmotic consequences, would be expected to affect not only the lysosome, but also the upstream vesicular (endocytic) and flagellar pocket compartments (140). This is what was observed in Figure 3.3, and is reminiscent of observations following deletion of a cassette of cysteine protease genes in the related kinetoplastid parasite, *Leishmania mexicana* (141). A similar phenotype was also noted in parasites in which RNAi targeted

Rab5 (142), Rab11 (17), actin (143), or clathrin (144) transcripts, all coding for key proteins required for endocystosis.

Results of cysteine protease inhibitor studies suggested a key role for *T. brucei* cysteine proteases in general host protein degradation (30,104,124). In particular, degradation of the iron-transporter molecule, transferrin, was noted as a possible tbcatB function, since inhibitor-treated parasites accumulated fluorescently-labeled transferrin in an organelle located between the nucleus and kinetoplast (30). Subsequent RNAi studies revealed that knockdown of tbcatB also resulted in an accumulation of transferrin (117). With the generation of tbcatB heterozygous knockout parasites, we have confirmed that transferrin accumulates in parasites as a result of tbcatB deficiency. Accumulation of the transferrin receptor (Tf-R) within the flagellar pocket and upregulation of Tf-R protein levels are associated with iron starvation (137). The observation that both of these abnormalities occur in tbcatB-deficient parasites (Fig. 3.8) supports the hypothesis that tbcatB is required for proper acquisition of iron.

Although iron starvation appears to be an important physiologic defect of tbcatB deficiency, other host and parasite proteins are likely substrates for this enzyme in the endosome/lysosome of the parasite. The lysosomal protein, p67, is a potential substrate. This is consistent with the previous observation that a broad-spectrum cysteine protease inhibitor, leupeptin, inhibited p67 processing (69,145). Two other parasite proteins were also identified as enriched (undegraded) in 2D gel electrophoresis of parasite lysates following RNAi treatment, or in $TBCATB^{+/-}$ parasite lysates (data not shown). These were the zymogen of the cathepsin L-like protease, rhodesain, and the major surface glycoprotein, VSG. However, accumulation of both of these proteins was only seen in

parasites where lysates were made in the absence of SDS. These control (wild-type) parasite lysates might still contain active proteases, so processing of the two parasite proteins may have occurred following the preparation of the lysates rather than *in situ*. Nevertheless, these results suggest that if tbcatB encounters either of these proteins during the lifecycle of *T. brucei*, they are potential substrates. Indeed, rhodesain has been localized to the lysosome (62) and some VSG may be turned over in that compartment (118). Furthermore, the identification of a cleavage motif for tbcatB adjacent to the activation site of pro-rhodesain, raises the intriguing possibility that tbcatB may be responsible for activation of the abundant rhodesain protease in the lysosome or in a pre-lysosome compartment.

In summary, *T. brucei* cathepsin B-like protease is a key enzyme in host protein turnover and iron acquisition in *T. brucei* parasites. Even a modest reduction of this enzyme by RNAi induction leads to organelle dysmorphism and parasite death (117). The present study utilizing parasites in which a single allele of the tbcatB gene is deleted validates these RNAi studies, suggesting that the physiologic concentration of tbcatB is at a critical level, where even modest reduction can have a profound effect on the parasite. The drugability of parasite Clan CA cysteine protease inhibitors is well established (48) (51) (16) and the present report suggests that *T. brucei* cathepsin B is a logical target for the development of new anti-trypanosomal chemotherapy.

ACKNOWLEDGEMENTS

We thank George A. M. Cross (The Rockefeller University, New York, NY, USA) for the *T. brucei* 90-13 strain, Paul T. Englund (Johns Hopkins Medical School, Baltimore,

MD, USA) for the pZJM and pLew111 vectors, Matt Bogyo for the ^{125}I-MB074 active site probe (Stanford University, Stanford, CA, USA), James D. Bangs (University of Wisconsin School of Medicine and Public Health, Madison, Wisconsin, USA) for the anti-p67 antiserum, Piet Borst (The Netherlands Cancer Institute, Amsterdam, The Netherlands) for the anti-tranferrin receptor antiserum, and Kent McDonald at the UC Berkeley Electron Microscopy Lab for access to the high pressure freezing devices. We would like to thank Elizabeth Hansell, Christopher Franklin, Juan Engel, and Susan Jean Johns for their technical assistance and Mohammed Sajid for his editorial comments. This work was supported by a National Science Foundation Graduate Research Fellowship (to T. C. O.), National Institute of Allergy and Infectious Diseases Tropical Disease Research Unit Grant AI35707, and the Sandler Family Supporting Foundation.

TABLES AND FIGURES FOR CHAPTER 3

Fig. 3.1. Growth rate (replication) of 90-13 versus TBCATB$^{+/-}$ *T. brucei*. One hundred thousand parasites were cultured at a density of 1x10^4 cells/ml and counted using a hemocytometer after 24, 48, and 72 hours (n = 3). Open squares, strain 90-13 (wild-type); diamonds, TBCATB$^{+/-}$.

Fig. 3.2. Fluorescence localization of the lysosomal membrane glycoprotein p67 in pZJMTbCB and TBCATB$^{+/-}$ clones. *A, B, E, & F.* Clones of pZJMTbCB were maintained as controls (A & B) or induced with tetracycline for 24h (E & F), fixed, and premeabilized as described. Cells were stained with rabbit anti-p67 antiserum and TexasRed goat anti-rabbit secondary antibody (red channel). Mount containing DAPI was used to visualize DNA in the nucleus and kinetoplast by fluorescence microscopy

(blue channel). *B & C.* TBCATB$^{+/-}$ clones (B & C) were prepared in an identical manner. Increased p67-labeling was observed in TBCATB$^{+/-}$ clones (D) and parasites subjected to RNAi against tbcatB mRNA (F).

Fig. 3.3. Transition electron microscopy of abnormal flagellar pocket and associated endocytic compartment morphology in pZJMTbCB and TBCATB$^{+/-}$ clones. Clones of pZJMTbCB were maintained as controls (A & B) or induced with tetracycline for 24h (D). Swollen flagellar pockets were observed in TBCATB$^{+/-}$ clones (C) and pZJMTbCB parasites induced with tetracycline (D). Bar, 0.5 μm. Arrows indicate flagellum. FP indicates the boundaries of the flagellar pocket.

Fig. 3.4. Ultrathin cryosection immunogold labeling of tbcatB in strain 221 and pZJMTbCB parasites after RNA induction. *A & B.* Sections were labeled with anti-tbcatB antiserum and 10 nm gold secondary antibodies. Immunolabeling of tbcatB is observed in lysosomes in 221 parasites (A, short arrows) and outside, but proximal to, lysosomes in parasites subjected to RNAi against tbcatB mRNA (B, long arrows). Bar, 200 nm.

Fig. 3.5. Biochemical characterization and kinetic parameters of recombinant tbcatB. *A.* Recombinant tbcatB was expressed in *P. pastoris*. Crude protein was desalted, concentrated, and purified by anion exchange chromatography. Crude protein (lane 1), column flow-through (lane 2), and fractions (lanes 3, 4, & 5) were resolved by SDS-PAGE and visualized by silver stain (left image). The flow-through and fractions were also labeled with ^{125}I-MB-074 active site probe. Resolved by SDS-PAGE, and visualized by autoradiography (right image). Note both the pro-form at 42 kDa and more abundant mature form at 31 kDa. *B.* pH-dependent activity of recombinant tbcatB.

Protease was pre-incubated in 50 mM sodium citrate buffers (pH 3-8) containing 4 mM DTT. Then the same volume of respective buffer containing Z-Phe-Arg-AMC was added. Activity was determined hydrolysis of the substrate, measured by AMC fluorescence intensity. Assays were prepared in duplicate. Y-axis represents the rate of AMC production expressed as relative fluorescent units per second. X-axis represents the pH of the assay buffer.

Fig. 3.6. Tetrapeptide substrate specificity profiling of tbcatB determined using complete diverse positional scanning synthetic combinatorial library (PS-SCL) and comparison with related enzymes. *A.* The library contained P1, P2, P3, and P4 libraries in which the P position is fixed with one of 20 amino acids (norleucine is used in place of isoleucine) and the other three positions are occupied by the 20 amino acids in an equimolar mix. All of the substrates contained an ACC fluorogenic leaving group. The complete diverse library contains 160,000 unique tetrapeptide substrates. Protease specificity was determined by hydrolysis of substrates, as measured by ACC fluorescence intensity. Assays were performed in triplicate, using sodium citrate assay buffer (50 mM sodium citrate, pH 5.5, 4 mM DTT), and error bars denote the mean ±S.D. Y-axis represents the rate of ACC production expressed as a percentage of the maximum rate observed in each experiment. X-axis indicates the amino acid held constant at position, designated by the one-letter code (with "n" representing norleucine), and amino acids are grouped along the axis to reflect the chemical properties of their side chains (acidic, basic, polar, aromatic, and aliphatic amino acids). *B.* A comparison of preferred substrate motifs for recombinant tbcatB, human cathepsin B (97), rhodesain (97), cruzain (97), human cathepsin L (97), and papain (97) determined using the complete diverse library.

Table 3.1. Kinetic analysis of fluorescent peptide substrates with recombinant tbcatB. To test the predictive power of the substrate specificity profile obtained for tbcatB, di-, tetra-, and pentapeptide substrates that were either "good" or "poor" matches to the profile were selected for screening. All substrates contained an AMC fluorogenic leaving group and assays were carried out in duplicate. *A.* Kinetic parameters are shown for eight commercially obtained substrates: Z-FR, Z-RR, Ac-KQKLR , Z-RRLR, Z-REKR, Ac-ASTD, H-RQRR, Ac-IEPD, Z-LRGG, and Z-RRLR (synthesized bySynpep). Amino acid sequence is indicated using single-letter code. Assays were carried out in duplicate, using sodium citrate assay buffer (50 mM sodium citrate, pH 5.5, 5 mM DTT). Note that K_m and k_{cat} values for Ac-IEPD and Z-LGRR could not be measured (indicated as N.M. in the table), as they demonstrated poor binding and poor turnover. A K_m value could not be measured for Ac-ASTD, although the substrate did have a low k_{cat}.

Fig. 3.7. Transferrin accumulation in stain 221 and TBCATB$^{+/-}$ *T. brucei*. Parasites were harvested, lysed, and protein concentration of the lysates was determined by Bradford assay. Two hundred micrograms of 221 and TCATB$^{+/-}$ lysates was prepared using the ReadyPrep 2-D Cleanup Kit (Biorad), subjected to isoelectric focusing, and resolved by SDS-PAGE. Tranferrin was visualized by Western blot analysis using anti-transferrin antiserum and horseradish peroxidase (HRP)-conjugated donkey anti-rabbit IgG. HRP signal was observed only in the TCATB$^{+/-}$ blot (B, arrows); no signal was observed in the 221 blot (A).

Fig. 3.8. Accumulation of transferrin receptor in pZJMTbCB clones after RNAi induction and in TBCATB$^{+/-}$ parasites. *A & B.* Strain 221 and TBCATB$^{+/-}$ parasites were incubated for 36 hours in media containing either dog serum (Dog) or fetal calf

serum (Calf) at a density of $5x10^4$ cells/ml. Media for TBCATB$^{+/-}$ parasites was supplemented with 2.5 μg/ml phleomycin. After the incubation period, equal numbers of parasites were lysed and the extract resolved by SDS-PAGE for Western blot analysis with transferrin receptor antiserum (A). Labeling was quantified for each lane by densitometry (B). Transferrin receptor antibody-labeling (70 and 52 kDa bands) is greater in dog serum samples when compared to fetal calf serum samples, and greater in TBCATB$^{+/-}$ extracts when compared to 221 extracts. *C & D.* Thin sections from samples of strain 221 parasites and pZJMTbCB clones that had been induced with tetracycline for 24 hours and prepared by high pressure freezing and freeze-substitution. The sections were labeled with anti-transferrin receptor antiserum and 10 nm gold antibodies. Immunolabeling of transferrin receptor was observed in the swollen flagellar pockets of the RNAi-induced parasites (C) but not in controls (D). Bar, 200 nm.

Figure 3.9 (Supplemental). TbcatB activity is reduced in TBCATB$^{+/-}$ parasites. Lysates (10 μg) from strain 221 and TBCATB$^{+/-}$ parasites were labeled with the active site label ^{125}I-DCG-04 (133). TbcatB activity is decreased by approximately 60% in TBCATB$^{+/-}$ parasites versus the control.

Table 3.2 (Supplemental). Results from a screen aimed at identifying proteins with the predicted optimal substrate motif for tbcatB. A database of human serum proteins was created and then screened using the EMBOSS fuzzpro pattern program for the amino acid motif: P4: R/K, P3: R/K, P2: X, P1: R/K.

Figure 3.1.

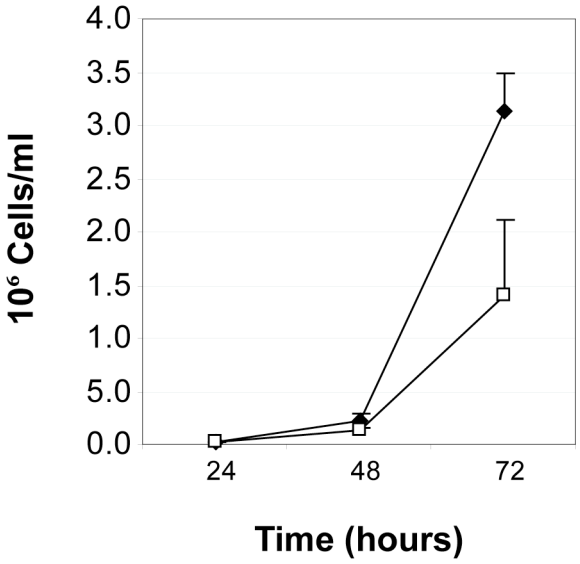

Figure 3.2.

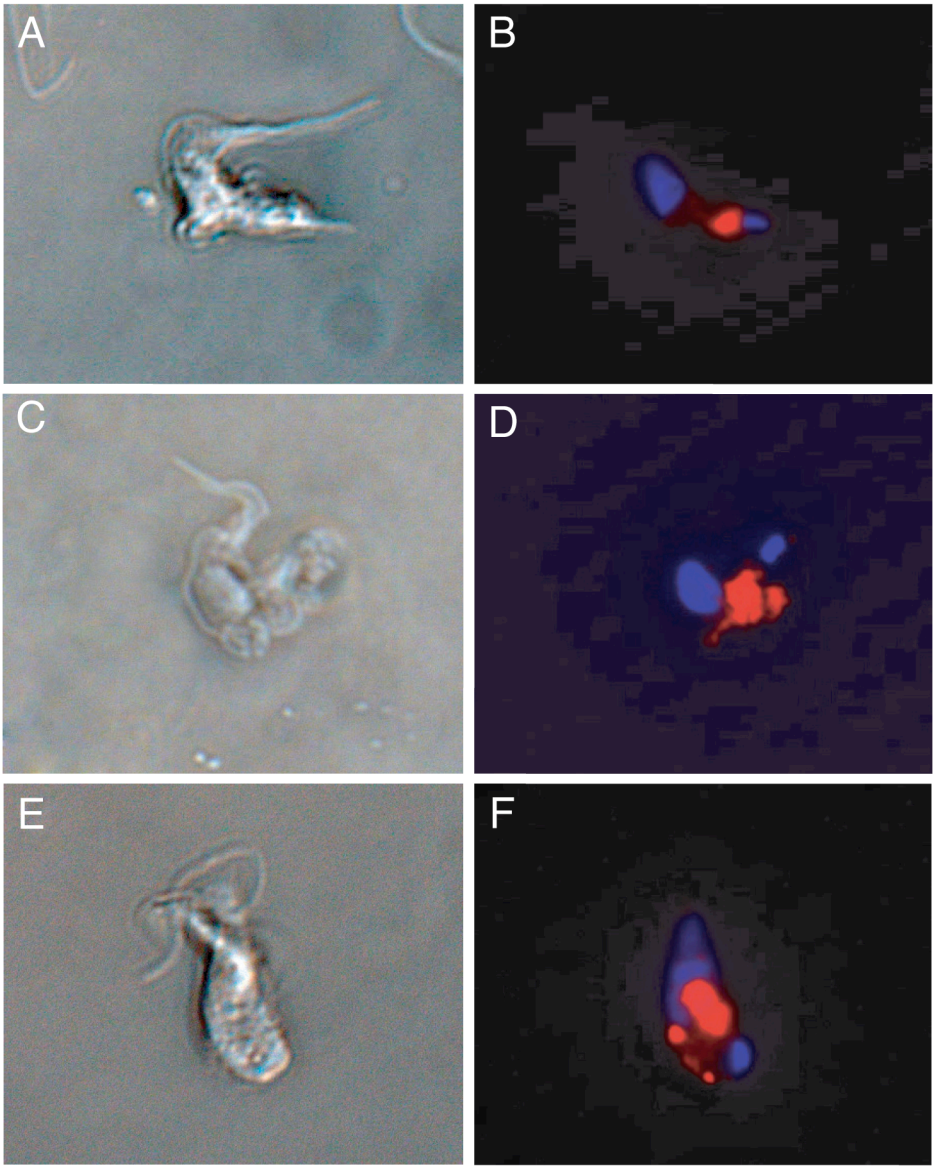

Figure 3.3.

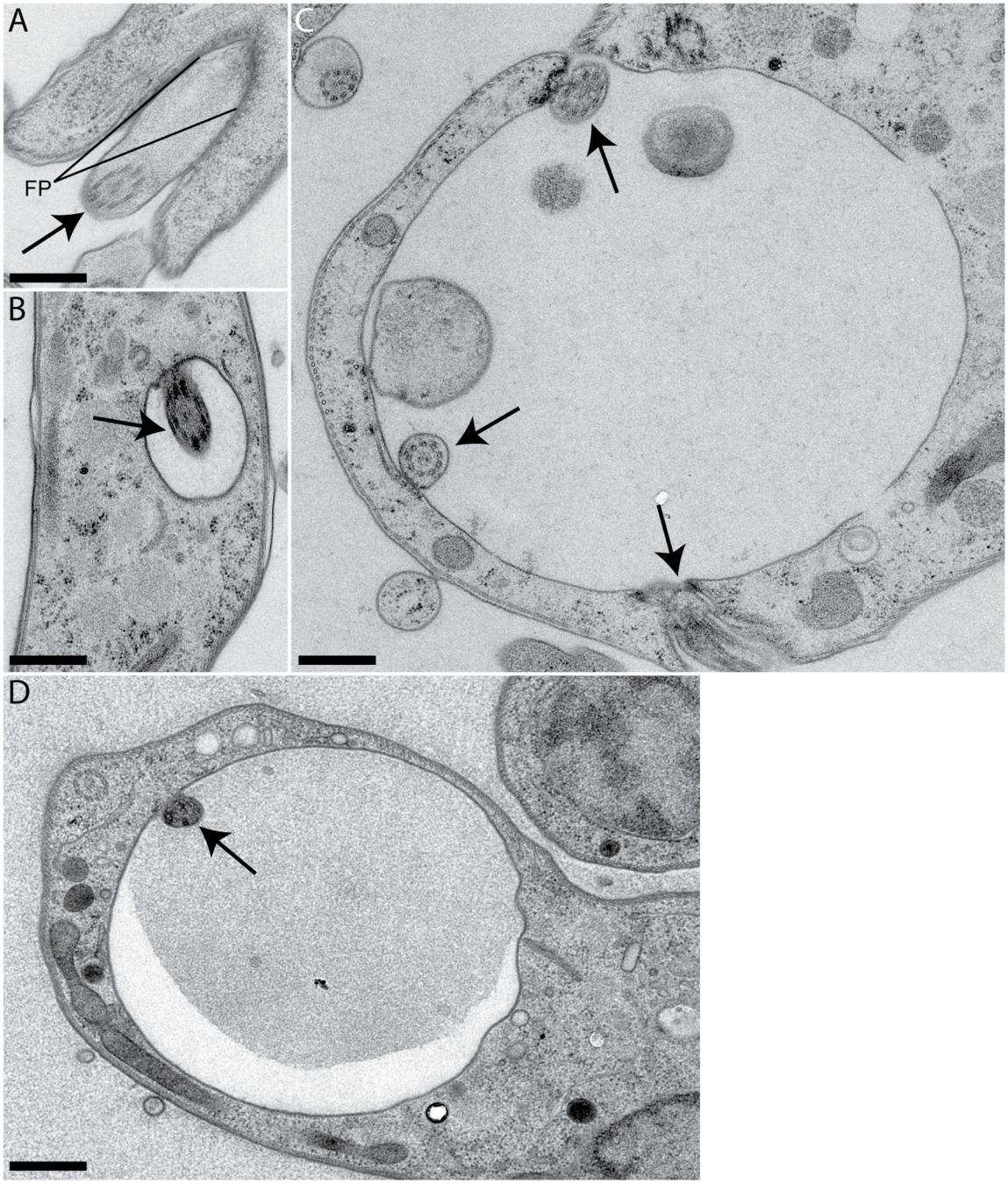

Figure 3.4.

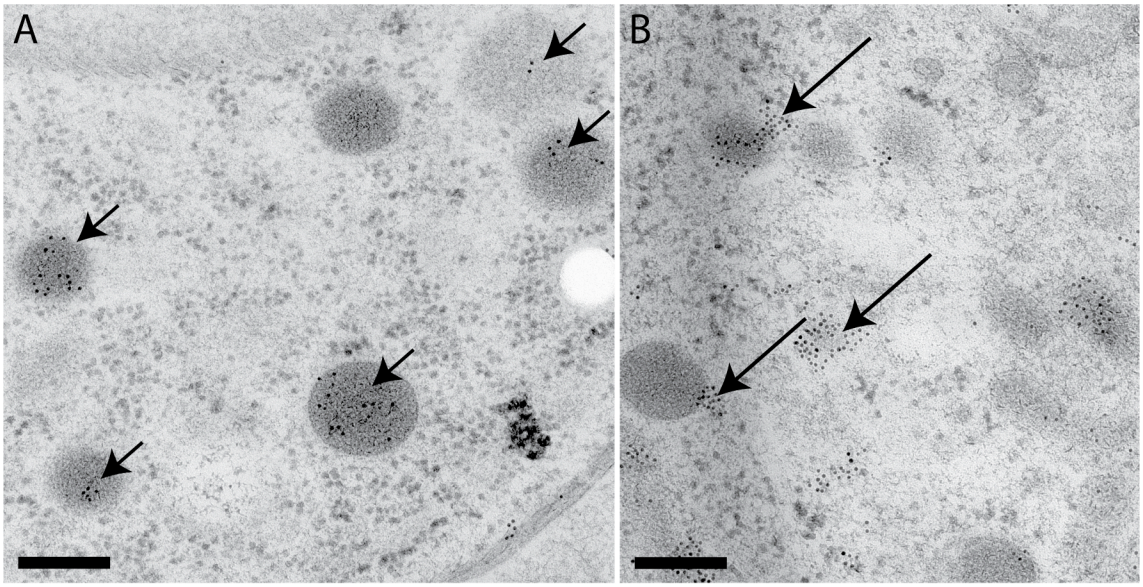

Figure 3.5.

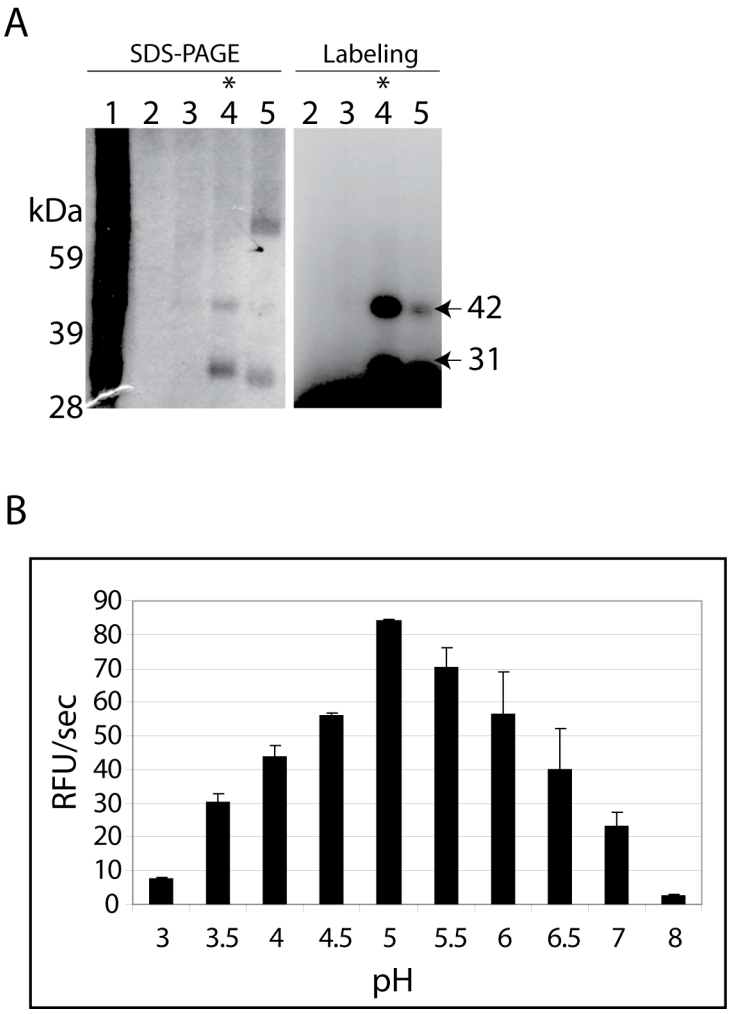
A
SDS-PAGE
Labeling
*
*
1 2 3 4 5 2 3 4 5
kDa
59
39
28
42
31
B
RFU/sec
90
80
70
60
50
40
30
20
10
0
3 3.5 4 4.5 5 5.5 6 6.5 7 8
pH

Figure 3.6.

A

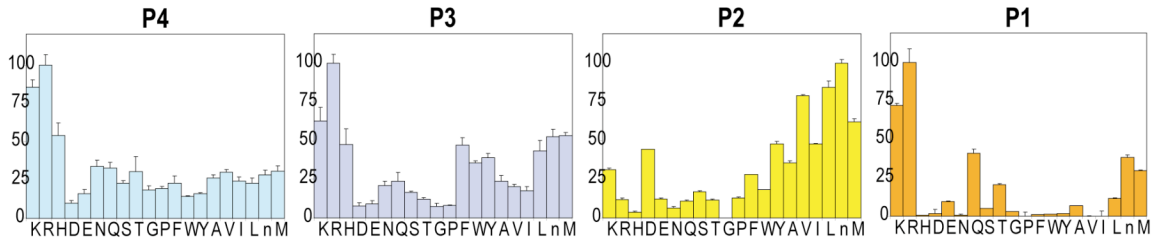

B

Preferred Substrate Motifs for Select Parasitic and Human Cathepsins

	P4	P3	P2	P1
TbcatB	R/K	R/K	X	R/K
Cathepsin B	R/H/X	n/L	V/X	R/K
Rhodesain	H/X	R/P/K	F/W/L/Y	R/K
Cruzain	H/K/X	H/K/X	F/L/Y	R/K/Q
Cathepsin L	H/X	K/R/n	F/W/Y	R/K/Q
Papain	P/X	P/R	V	R/K

Table 3.1.

A

Kinetic analysis of fluorogenic peptide substrates with recombinant tbcatB

AMC Substrate	k_{cat} (s-1) ($x10^{-2}$)	K_m (mM)	k_{cat}/K_m (M^{-1} sec^{-1})	Class
Z-RRLR	10 ± 0.5	15.4 ± 3.0	6.50×10^4	"Good"
Z-FR	4.5 ± 0.5	19.2 ± 8.3	2.34×10^4	"Good"
Ac-KQKLR	10.9 ± 0.2	53.4 ± 3.0	2.05×10^4	"Good"
Z-RR	4.8 ± 0.2	68.7 ± 8.3	0.70×10^4	"Good"
Z-REKR	0.6 ± 0.0	35.6 ± 7.7	0.16×10^4	
H-RQRR	0.2 ± 0.0	19.2 ± 8.7	0.09×10^4	
Ac-ASTD	0.3 ± 0.1	N.M.	N.M.	"Poor"
Ac-IEPD	N.M.	N.M.	N.M.	"Poor"
Z-LRGG	N.M.	N.M.	N.M.	"Poor"

Figure 3.7.

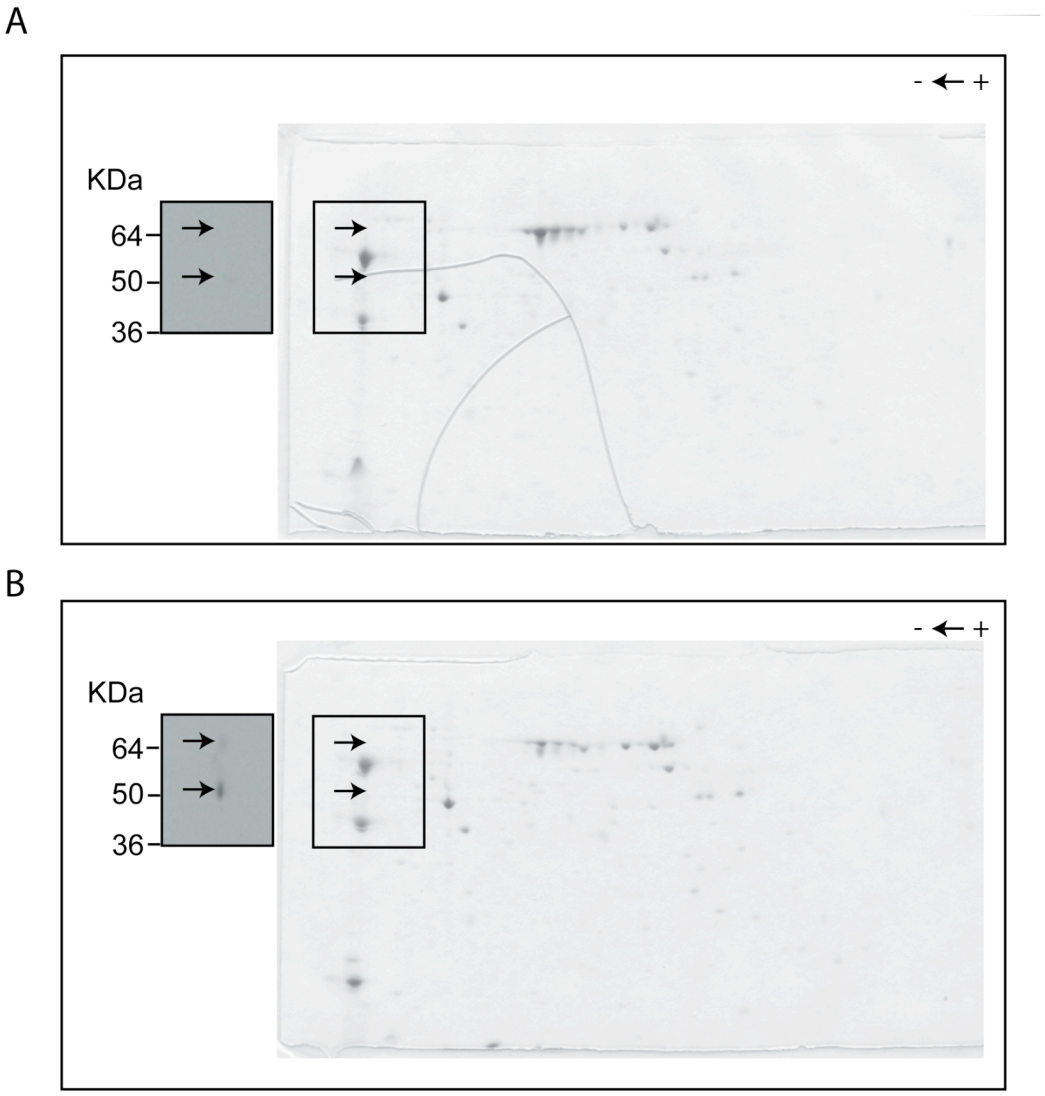

Figure 3.8.

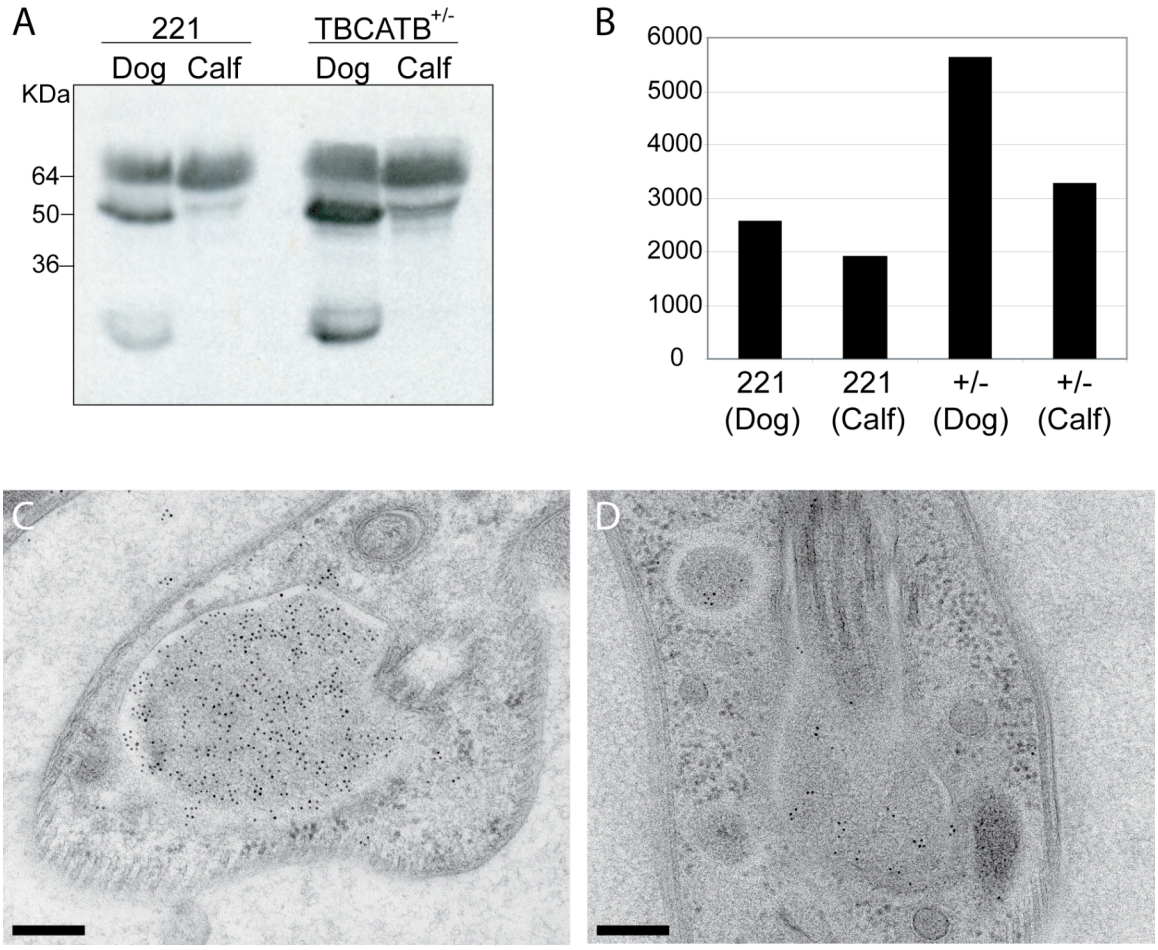
A
221
TBCATB+/-
Dog Calf
Dog Calf
KDa
64
50
36
B
6000
5000
4000
3000
2000
1000
0
221 (Dog)
221 (Calf)
+/- (Dog)
+/- (Calf)
C
D

Figure 3.9. (Supplemental)

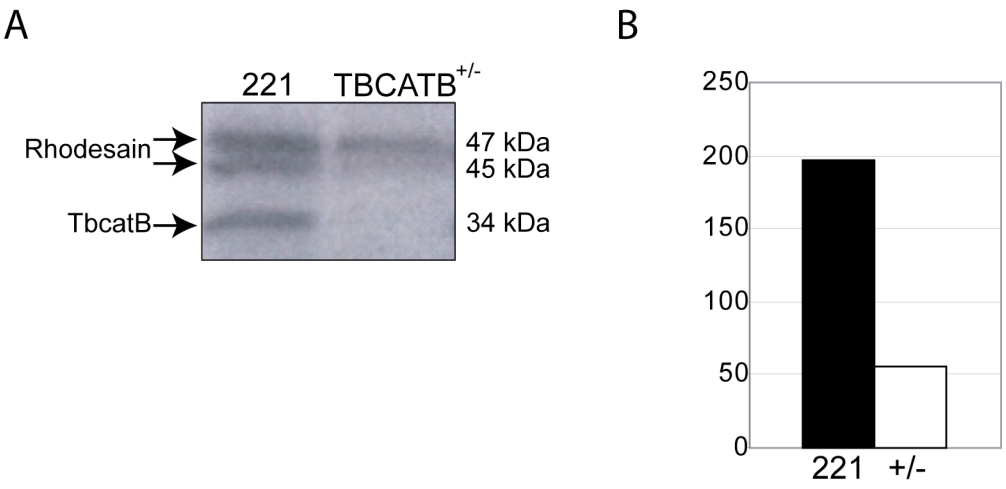

Table 3.2. (Supplemental)

Human Serum Proteins Containing the Predicted Optimal Substrate Motif for TbcatB

	Sequence	Amino acid position	Solvent accessible?
Human serum albumin	KRYK	159 - 162	No
Serum response factor accessory protein 1A (SAP-1)/DNA	RKNK	48 - 51	No
Factor B serine protease domain	KRSR	203 - 206	Yes
	KRQK	224 - 227	Yes
Factor XA inhibitor complex	KRFK	63 - 66	Yes
	RKGK	226 - 229	Yes
Ternary complex of SAP-1 and SRF with specidic SRE DNA	KKTR	138 - 141	Yes
Human ceruloplasmin	RKER	417 - 420	Yes
Vitamin D-binding protein	KKSR	229 - 232	No
Human apolipoprotein-E	RKLR	142 - 145	No
Serum response factor (SRF)	KKTR	138 - 141	Yes
Human zinc-alpha-2-glycoprotein	KKLK	201 - 204	Yes
Human complement component C3	RRTR	37 - 40?	No?
	KKNK	585 - 588	Yes
Apo-human serum transferrin	RKDK	590 - 593	Yes
Human phosphoinositide-dependent protein kinase 1 (PDK1)	RKKR	75 - 78	Yes

CHAPTER 4

UNPUBLISHED DATA

IMMUNOFLUORESCENCE LOCALIZATION OF TBCATB

Rationale

As one approach to determining the function of tbcatB, I identified where the protease is localized in the parasite. Two localization techniques were used: immunofluorescence by fluorescence microscopy and immunoelectron microscopy. Prior to starting these localization studies, it was known that rhodesain localizes to lysosomes (62), suggesting that it is involved in parasite and/or host protein degradation, and that its substrates are those proteins that are processed or degraded in the lysosome. Previous studies with chemical inhibitors indicated that cysteine protease activity was required for lysosomal degradation of the host protein transferrin (30,104), although the identity of the specific protease or proteases responsible for this activity was not known. Other protozoan parasites had been shown to express extra-lysosomal cysteine proteases, or at least exhibit extra-lysosomal function (43). By determining where the tbcatB localizes, we would gain insight into what cellular processes tbcatB might contribute to and what substrates are available for cleavage. I used established techniques and cellular markers for immunofluorescence and immunoelectron microscopy in *T. brucei* (62,92,93). The results obtained by immunoelectron microscopy are discussed in Chapter 3. Below, I discuss the results obtained by fluorescence microscopy and provide a comparison of the results obtained by the two localization techniques in the discussion section. I will also

briefly describe recent efforts to localize cysteine protease activity using fluorescent peptide substrates, an approach that has been used in other parasitic organisms (146) (DuBois and Abodeely, personal communication).

Experimental Approach

T. brucei- Strain 221, pZJMTbCB, and pZJMRho bloodstream form *T. brucei* were used for immunolocalization and related localization experiments described in this chapter. Methods for culturing these parasites have been published (117) and are described in the previous three chapters. Induction of RNAi in pZJMTbCB parasites was carried out by the addition of tetracycline to the media as described in Mackey *et al.* (117) and Chapter 1.

Immunofluorescence microscopy- *T. brucei* were harvested by centrifugation at 4 °C, washed in cold Dulbecco's phosphate buffered saline (D-PBS), and fixed in 4% paraformaldehyde/D-PBS for 1 hour at 4 °C. All subsequent washes were carried out with excess D-PBS. Fixed cells were washed and applied to 25 mm round cover slips that had been coated with poly-lysine (0.1% w/v in water, Sigma Aldrich) and allowed to settle for 20 minutes at room temperature. The cells were then permeabilized in D-PBS containing 0.1% Triton X-100 (Sigma-Aldrich) for 10 minutes, washed, and blocked for one hr with 1% bovine serum albumin (BSA) prepared in D-PBS. After blocking, the cells were incubated with primary antibody diluted 1% BSA/D-PBS for 1 hour, washed, incubated in secondary antibody diluted 1% BSA/D-PBS for 1 hour, washed, and mounted on slides with Prolong Gold Antifade Reagent with DAPI (Invitrogen). Primary antibodies and their dilutions are indicated in the table below. Primary antibodies were

produced in rabbit, mouse, or rat. The respective secondary antibodies used were: TexasRed goat anti-mouse (dilution 1:400) (Invitrogen), TexasRed goat anti-rabbit (dilution 1:200) (Invitrogen), FITC goat anti-mouse (dilution 1:400) (KPL Protein Research Products), and FITC goat anti-rat (diluted 1:250) (Invitrogen). The cells were visualized on an AxioImager M1 microscope (Zeiss), equipped with an X-Cite 120 fluorescence illumination system (EXFP Life Sciences). In cases where double-antibody staining was carried out, cells were incubated with the 1st primary antibody, washed, incubated with the 2nd primary antibody (generated in a different animal than the first 1st antibody), washed, and incubated with two secondary antibodies (recognizing the each of the primary antibodies and having different fluorescent conjugates), before final washing and mounting on slides.

Primary Antibody	**Dilution**	**Source**	**Produced by**	**Ref.**
TbcatB ("34-2")	1:400	Rabbit	J. McKerrow lab.	(117)
p67 (lysosomal)	1:400	Mouse	J. Bangs lab.	(126)
Bip (ER)	1:400	Mouse	J. Bangs lab.	(147)
YL1/2 (basal body)	1:500	Rat	Chemicon/ Millipore	(148) (149)
Rab5A (early/sorting endosomes)	1:400	Rabbit	M.C. Field lab.	(150)
Rab11 (recycling endosomes)	1:400	Rabbit	M. C. Field lab.	(151)
Transferrin (H-16 antibody)	1:200	Rabbit	Santa Cruz Biotechnology, Inc.	
Transferrin receptor	1:400	Rabbit	P. Borst Lab	(127)

□□□

Conconavalin A (Con A) Localization- ConA is a lectin that binds to exposed oligosaccharides in the *T. brucei* flagellar pocket (152). Following binding, ConA is endocytosed and transits the parasite endocytic system, with a terminal destination of the lysosome. This transport can be inhibited at various stages by incubating parasites at different temperatures: at 4 °C, ConA remains bound at the flagellar pocket; at 12 °C, it is

transported to a TbRAB5A positive early endosome; and at 37 °C, it is transported to the lysosome (153) (reviewed in (92,135)). Methods for visualizing ConA binding at the flagellar pocket were adapted from Brickman *et. al*, 1995 (153) and reviewed in Field *et al.*, 2004 (92). Strain 221 and pZJMTbcatB parasites that had been induced with tetracycline to produce RNAi against tbcatB (see the previous three chapters) were harvested by centrifugation, resuspended at ~1x10^7 cells/ml in pre-warmed (37 °C) serum-free HMI-9 media supplemented with 1% BSA, and incubated on ice or in a 4 °C fridge for 30 minutes. Fluorescein Isothiocyanate (FITC) conjugated ConA (Invitrogen) was then added to the cells (final concentration of 5 μg/ml) and the cells were returned to ice/4 °C fridge for 30 minutes. Following incubation, cells were washed once using pre-chilled D-PBS and a centrifuge set at 4 °C, and then fixed, mounted, and visualized, as described above for immunofluorescence.

Transferrin Localization- FITC-conjugated transferrin (FITC-Tf) can be used as an endocytosis/trafficking marker in *T. brucei* (92). Like ConA, FITC-Tf is retained in the flagellar pocket at 4 °C, transported to early endosomes at 12 °C, and appears in the lysosome at 37 °C (92). However, once the molecule reaches the lysosome, it is rapidly degraded. To follow transferrin binding in the flagellar pocket, FITC-transferrin (Sigma) was resuspended at 1mg/ml in 10 mM HEPES buffer, pH 7.4 and strain 221 parasites were incubated in serum-free HMI-9 containing 15 μg/ml FITC-transferrin for 30 minutes at 4 °C. Following this incubation, the cells were washed twice in pre-chilled D-PBS and fixed as described for immunofluorescence above. In some experiments, the fixed cells were not mounted and visualized directly, but were instead used for immunofluorescence with tbcatB antiserum. Similar procedures were used to follow

transferrin trafficking to the lysosome, although pZJMTbCB parasites that had been induced with tetracycline were used instead of strain 221 parasites and the incubation temperature was raised to 37 °C to allow for endocytosis of the marker. The tbcatB RNAi knockdown parasites had been shown previously to accumulate FITC-transferrin in the lysosome.

MNA Substrate Localization- Techniques for localization of the MNA substrates, Z-Phe-Arg-MNA and Z-Arg-Arg-MNA (Peptides International, Inc.) in *T. brucei* were adapted from methods used in *Entamoeba histolytica* (146) and *Giardia lamblia* (DuBois and Abodeely, personal communication). Strain 221 parasites were harvested by centrifugation and washed two times in cacodylate buffer (100 mM, pH 6.8) containing 5% sucrose (CacoS) for Z-Arg-Arg-MNA and in D-PBS for Z–Phe-Arg-MNA. Cells were resuspended to a density of ~1x10^5 cells/ml in culture media containing Z-Arg-Arg-MNA (10-200 μl of 5 μg/μl substrate stock added to 1 ml culture media)[5] or Z-Phe-Arg-MNA (1-25 μl of 10 mM substrate stock added to 1 ml culture media)[5], and incubated at 37° and 5% CO_2 for 35 minutes. After incubation with substrate, coupling reagent (5-nitro-2-salicylaldehyde; 2mM in CacoS buffer) was added in the same or double the volume of substrate used. The cells were again incubated for 35 minutes at 37° and 5% CO_2. Cells were placed on ice following the incubation, and washed three times in D-PBS before being fixed and mounted or visualized immediately (see methods for immunofluorescence microscopy above for details).

[5] Substrate concentration was varied in different experiments.

Results

TbcatB anti-serum localizes to the posterior tip of T. brucei- Rabbit antiserum to recombinant tbcatB expressed in *Escherichia coli* was produced by Mackey *et al*. (117). This anti-serum has been shown by Western blot analysis to recognize native tbcatB in lysates obtained from bloodstream form parasites (117), as well as active, recombinant tbcatB expressed in *Pichia pastoris*. When used for immunofluorescence, the tbcatB antiserum labels a region in the posterior tip of the parasite (Fig. 4.1A). Co-localization experiments, using antibody to the lysosomal membrane glycoprotein p67, showed that the tbcatB antiserum does not does not co-localize with the p67 marker (Fig. 4.1B). Labeling by the tbcatB antiserum was not altered in tbcatB knockdown parasites (Fig. 4.1C), although p67 distribution was altered (Fig. 4.1C & 1D), as previously discussed (Chapter 3).

TbcatB antiserum localizes at or near the flagellar pocket- Localization of tbcatB antiserum to the posterior tip of *T. brucei*, suggested that the cysteine protease might localize to the flagellar pocket. Conconavalin A (ConA) is a lectin that binds to exposed oligosaccharides in the flagellar pocket of *T. brucei* (152). FITC-congugated ConA can be used as a flagellar pocket marker when it is incubated with *T. brucei* at 4 °C, since the cold temperature blocks endocytosis and transport of the fluorescent lectin to the lysosome (92). When strain 221 *T. brucei* were incubated with ConA at 4 °C and subsequently labeled with the tbcatB antiserum, co-localization was not observed (Fig. 4.2.A & 2B). Some co-localization was observed in tbcatB knockdown parasites (Fig. 4.2C). Labeling by ConA in strain 221 parasites was observed in a region close to, but anterior of the kinetoplast (Fig. 4.2A & 2B).

Given that the tbcatB antiserum localizes to a region in the posterior end of the parasite, we investigated whether the antiserum co-localizes with the basal body. The *T. brucei* basal body is a centriole-like structure located at the base of the flagellum (which is also where the flagellar pocket forms). The commercially-available antibody YL1/2 (Chemicon) recognizes tyrosinated alpha-tubulin generally and the basal body specifically in *T. brucei* (148,149,154). Co-localization experiments with YL1/2 and tbcatB antiserum revealed that that the antiserum does not label the basal body (Fig. 4.3). As with labeling by FITC-ConA, the tbcatB antiserum labeled a region that is posterior of the basal body.

In order identify the structure(s) labeled by tbcatB antiserum, additional endocytosis/trafficking markers were used in immunofluorescence experiments. The endoplasmic reticulum (ER) marker, Bip (126), as well as early and recycling endosome markers, TbRAB5A (150) and TbRAB11A (135), localize to vesicles and ER that are anterior of the kinetoplast (Fig. 4.4., A, B, & C). Efforts to co-localize these markers with tbcatB antiserum were hampered by the fact that the source for the RAB markers, rabbit, was the same as for the tbcatB antiserum. Although co-localization data for these markers with antiserum to tbcatB was not obtained, it appeared that the ER, RAB5A, and RAB11A markers do not label the same structure as the tbcatB antiserum.

Discussion

As outlined in the specific aims for this project, both immunofluorescence (IFA) and immunoelectron microscopy (immuno-EM) were proposed as a techniques that would be used in determining the localization of tbcatB. The results of the immuno-EM

experiments, which are detailed in Chapter 3, revealed that tbcatB localizes to lysomomal vesicles. By contrast, IFA experiments by floursecence microscopy indicated that tbcatB localized adjacent to or at the flagellar pocket in the posterior tip of the parasite. There are at least two possible explanations for the incongruence of these data – first, that the tbcatB antiserum does not recognize native tbcatB under the conditions used for IFA, or, second, that tbcatB trafficks through the flagellar pocket in route to the lysosome. This is indeed what is seen for the cysteine protease of *T. cruzi*, cruzain (155), and the leishmania cysteine proteases (140). At present, we cannot distinguish these possibilities.

Engstler *et al*. recently reported that IgG-VSG immune complexes are passively sorted to the posterior tip of *T. brucei* before being encoyctosted and trafficking to the lysosome (156). The authors used IFA techniques to follow VSG antibody clearance and found that clearance was directional, with all IgG-VSG rapidly sorting to the posterior end of the cell prior to uptake in the flagellar pocket (156). They suggest that the rapid redistribution to the posterior pole is due to hydrodynamic drag forces created by the flagellum and the high rate of endocytosis in bloodstream *T. brucei* (156). This report associates a function and localizes a specific structure to the posterior tip of *T. brucei.* TbcatB could be involved in the process of IgG-VSG clearance, given its apparent role in endocytosis (see Chapter 3) and in transferrin degradation (see Chapters 2 and 3). The transferrin receptor has a similar structure as VSG and is rapidly endocystosed at the flagellar pocket (125). TbcatB could (first) encounter transferrin and its receptor at the posterior tip of the parasite.

Follow-up studies are needed to address the localization data obtained by IFA and immuno-EM. Establishing MNA-substrate localization techniques for *T. brucei* would be

worthwhile, both for the determination of tbcatB's localization and for future experiments in which one might want to follow changes in the level and localization of cysteine protease activity under different conditions (with specific inhibitors, for example). Another tool that would aid in tbcatB localization, as well as follow-up experiments, is *T. brucei* that express fluorescently-tagged tbcatB. Constructs for GFP- and orange-tagged (ref) tbcatB have been designed, although cloning procedures were not completed. If generated, parasites expressing fluorescent-tbcatB could be used in co-localization experiments with all of the *T. brucei* cellular markers discussed above. Finally, it would be helpful to have rhodesain antibodies that can be used in IFA (those available in the lab currently, were not amenable to IFA in my hands) or *T. brucei* that express fluorescently-tagged rhodesain, as these would allow for co-localization of the two cysteine proteases.

IN VITRO DEGRADATION OF TRANSFERRIN BY RECOMBINANT TBCATB

Rationale

As discussed previously, early inhibition studies indicated that cysteine protease activity is required for degradation of transferrin (30) (104). More recently, studies of tbcatB-deficient parasites have implicated the cathepsin B-like protease specifically in the degradation of the iron-carrying molecule ((117) and Chapters 2 and 3). Furthermore, substrate specificity data obtained for recombinant tbcatB has been used to predict a cleavage site in bovine transferrin (Chapter 3). Taken together, these data clearly implicate transferrin as a potential substrate for tbcatB. In order to validate transferrin as potential substrate, I proposed to investigate its cleavage *in vitro*, using tbcatB expressed in *P. pastoris*. Following *in vitro* digestion, transferrin cleavage products would be

sequenced and compared with those predicted by the substrate specificity profile for recombinant tbcatB. As discussed in Chapter 3, the tbcatB substrate specificity profile also predicts a cleavage site in rhodesain that could activate this second protease. Since inhibition studies have also implicated rhodesain in transferrin degradation, it is possible that rhodesain is responsible for the bulk of the degradation and that tbcatB is required to activate rhodesain or to carry out an initial processing step required for degradation.

Experimental Approach

Expression of recombinant tbcatB and rhodesain from Pichia pastoris - Methods for expression of recombinant tbcatB and rhodesain from *P. pastoris* have been described in Chapter 3 and Caffrey *et al.* (62), respectively. Following lyophilization, the recombinant enzymes were resuspended at approximately 10% of their original volume in 50 mM sodium citrate buffer, pH 5.5 (tbcatB) or 50 mM sodium acetate buffer, pH 5.5 (rhodesain and tbcatB). TbcatB was used directly, while rhodesain was activated by adjusting the pH of the sodium acetate buffer to 4.5 with 4 M sodium acetate, pH 4.5, and incubating at 37 °C for 5 hours in the presence of 2 mM DTT (62).

In vitro degradation of holo-bovine transferrin by recombinant cysteine protease- *In vitro* transferrin degradation experiments were carried out with a variety of enzyme and substrate concentrations, in order to optimize production of cleavage products. Data is provided from three separate assays:

Assay 1- Holo-bovine transferrin (Sigma) was resuspended in 50 mM sodium citrate buffer, pH 5.5 to give a concentration of 0.4 mg/ml transferrin and placed on ice. Recombinant tbcatB was resuspended in 50 mM sodium citrate buffer, pH 5.5 (as

described above) to give a concentration of ~60 nM and placed on ice. Samples were prepared in microcentrifuge tubes by combining 1400 μl of substrate with 100 μl of 50 mM sodium citrate buffer, pH 5.5 or the recombinant enzyme, and adding DTT to a final concentration of 4 mM. While still on ice, 200 μl was transferred to a new tube and frozen in an ethanol-dry ice bath (zero time point). The samples were then incubated at 37 °C and 200 μl aliquots were taken at 1, 4, and 25 hour time points and frozen in an ethanol-dry ice bath. The digest samples were resolved by SDS-PAGE and subjected to Western blot analysis (methods described in Chapters 1-3), using antibody to transferrin (diluted 1:2500) (H-16, Santa Cruz Biotechnology, Inc.).

Assay 2- Holo-bovine transferrin (Sigma) was resuspended in 50 mM sodium acetate buffer, pH 5.5, containing 4 mM DTT, to give a concentration of 1.0 mg/ml transferrin and placed on ice. Recombinant tbcatB was resuspended in 50 mM sodium acetate buffer, pH 5.5 (as described above) to give a concentration of ~ 55 μM and placed on ice. Recombinant rhodesain was resuspended in 50 mM sodium acetate buffer, pH 5.5 and activated (as described above), giving a final concentration of between 1-100 nM[6]. Samples were prepared in microcentrifuge tubes by combining 35 μl of substrate with 15 μl of 50 mM sodium acetate buffer, pH 5.5 or the recombinant enzyme. Individual samples were prepared for transferrin alone alone, transferrin plus tbcatB, and transferrin plus rhodesain and at each of the following time points: zero, 1, 6, and 12 hours. Samples were incubated at 37 °C until the appropriate time and then frozen in an ethanol-dry ice bath. Following completion of the assay, samples were resolved by SDS-PAGE and

[6] Titration experiments have not been performed for the recombinant rhodesain preparation used in these experiments, so the concentration of active enzyme in the lyophilized and resuspended protein can not be calculated. Based on similar experiments, though, the concentration of active enzyme was estimated.

either visualized with silver stain (Bio-Rad) or transferred to PVDF membrane for N-terminal sequencing (see below).

Assay 3- Substrate and enzyme resuspensions were carried out as described for Assay 2. Samples were prepared in microcentrifuge tubes by combining 54 µl of substrate with 36 µl of 50 mM sodium acetate buffer, pH 5.5 or the recombinant enzyme. Individual samples were prepared for transferrin alone, transferrin plus tbcatB, and transferrin plus rhodesain. Samples were incubated at 37 °C for 5 hours, frozen in an ethanol-dry ice bath, and used for high performance liquid chromatography (HPLC) purification (see below) or resolved by SDS-PAGE.

N-terminal sequencing of transferrin degradation products- As described for the second transferrin degradation assay, digest products were resolved by SDS-PAGE and transferred to PVDF membrane. Methods for transferring proteins to PVDF have been described in Chapters 1-3. Following transfer, membranes were stained briefly with 0.2% Ponceau S (Sigma) and the position of bands representing the major transferrin degradation products were marked with pencil. N-terminal sequencing of these bands was carried out by Dick Winant at the Stanford PAN (Protein and Nucleic Acid) Facility.

HPLC purification of transferrin degradation products- As described for the third transferrin degradation assay, digest products were subjected to HPLC purification. The purification was intended to isolate individual degradation products for N-terminal sequencing or identification by mass spectrometry. Transferrin degradation samples (75 µl) were run on a C_4 column (Vydac) with a 5-95% acetonitrile gradient over 45 minutes using an Agilent HP 1100 Series HPLC with the help of Anthony O'Donoghue. Fractions (1 ml) were collected, concentrated overnight using an EZ-Bio speedvac (GeneVac),

resuspended in 20 μl of 50 mM sodium acetate buffer, pH 5.5. The resuspended fractions (10 μl) were resolved by SDS-PAGE and visualized by silver stain (Bio-Rad).

In vitro degradation of holo-bovine transferrin by T. brucei lysates- Lysates from control and tetracycline-induced pZJMTbCB and pZJMRho parasites were prepared as described in Chapter 1. Holo-bovine transferrin (Sigma) was resuspended in 50 mM sodium acetate buffer, pH 5.5, containing 4 mM DTT, to give a concentration of 1.0 mg/ml transferrin and placed on ice. Samples were prepared with 18 μl of transferrin, 11 μl of buffer (sodium acetate buffer, pH 5.5, with 4 mM DTT), and 1 μl of *T. brucei* lysate (containing approximately 1.5 μg of protein). As a control, buffer was used instead of lysates in one sample. In two other samples, the amount of buffer was decreased from 11 to 10 μl and 1 μl of 10 mM cysteine protease inhibitor (E64 of CA074, both Bachem) was added. All samples were prepared in duplicate, with one sample being frozen immediately and the second incubated at 37 °C for 12 hr before freezing on an ethanol-dry ice bath. Aliquots (10μl) of each sample were resolved by SDS-PAGE and stained with Coomassie (Sigma), as well as subjected to Western blot analysis with transferrin antibody (as described above for transferrin degradation assay 1).

Results

In vitro degradation of transferrin by tbcatB yields cleavage products consistent with those predicted from substrate specificity data- Substrate specificity data obtained for recombinant tbcatB have been discussed in Chapter 3 and are shown in Figure 3.6. These data predict four potential cleavage sites in bovine transferrin, which produce cleavage products of sizes ranging from 2 to 68 kDa (Figure 4.5, cleavage sites and associated

products are indicated in blue). *In vitro* transferrin degradation assays with recombinant tbcatB produced cleavage products with molecular weights close or equal to the weight of predicted cleavage products (Figure 4.6A - 6C). For example, Western blot analysis of tbcatB-derived transferrin degradation products revealed bands at approximately 41 and 36 kDa (Figure 4.6A), which could represent products from cleavage at the sites "HQER" or QNLR" (note that bovine transferrin is present in different glycoslyation states (157), which are not accounted for in the molecular weights of predicted cleavage products given in Figure 4.5). Numerous attempts to determine the N-terminal sequence of the cleavage products failed, suggesting that the products may not be amenable to sequencing by Edman degradation. However, one sequence was obtained using this method (band indicated with a black arrow in Figure 4.6B; sequence in purple in Figure 4.5). The N-terminal sequence and high molecular weight of the product are consistent with the known processing site of the transferrin signal peptide and not a cleavage product.

In order to obtain individual transferrin degradation products that might be more amenable to N-terminal sequencing or, alternatively, to sequencing by mass spectrometry, an HPLC purification scheme was developed. Control and tbcatB-containing 5 hour transferrin degradation samples were used for HPLC purification (Figure 4.6C). However, the amount of protein recovered in the purified fractions was too low for N-terminal sequencing, as proteins could only be visualized by silver stain (data not shown). The success of the HPLC purification scheme in isolating transferrin degradation products, though, suggests that with increased starting materials enough protein could be obtained for both sequencing methods.

In vitro degradation of transferrin by rhodesain yields cleavage products consistent with those predicted from substrate specificity data- Rhodesain is the major cysteine protease in *T. brucei* and may, in combination with tbcatB or activated by tbcatB, degrade host transferrin. *In vitro* transferrin degradation assays with recombinant rhodesain (enzyme preparation described in (62)) produced cleavage products with molecular weights close to those produced by recombinant tbcatB (Figure 4.6B & 6C). As with the tbcatB-derived products, attempts to sequence these products were largely unsuccessful. Importantly, though, a sequence was obtained for one product of approximately 41 kDa (band indicated with a black arrow in Figure 4.6B; sequence in green in Figure 4.5), which matches the predicted cleavage site ("QNLR") in transferrin. Control and rhodesain-containing 5 hour transferrin degradation samples were subjected to HPLC purification, under the same conditions and with similar results as for tbcatB-containing samples (Figure 4.6C).

In vitro degradation of transferrin by T. brucei lysates yields similar cleavage products as with recombinant enzymes- As a means of validating the *in vitro* transferrin degradation data obtained using recombinant tbcatB and rhodesain, degradation assays were performed using lysates from control and tetracycline-induced pZJMTbCB and pZJMRho (RNAi knockdown) parasites. The degradation patterns tetracycline-induced (+T) and control (No T) pZJMTbCB samples and control (No T) pZJMRho sample, were identical, while the pattern for the tetracycline-induced (+T) pZJMRho sample was different, suggesting that the rhodesain-deficient lysate was less efficient at degrading transferrin (Figure 4.6D). Importantly, the cathepsin B-like inhibitor, CA074, and

cathepsin L- and B-like inhibitor, K11777 (abbreviated K77), prevented transferrin degradation by tbcatB and rhodesain RNAi control lysates, respectively (Figure 4.6D).

Discussion

Several experiments have indicated a role for tbcatB in transferrin degradation, most importantly that tbcatB-deficiency leads to an accumulation of partially or undegraded transferrin ((117) and Chapter 3). In addition, the substrate specificity profile determined for recombinant tbcatB can be used to predict four potential tbcatB cleavage sites in transferrin (Chapter 3). Thus, the fact that recombinant tbcatB can cleave transferrin *in vitro* and that the cleavage products are close in molecular weight to what was predicted, adds support to the hypothesis that transferrin is a natural substrate of tbcatB (Figure 4.6A-6C). However, *in vitro* transferrin degradation assays with recombinant rhodesain also yield degradation products that are consistent with the cathepsin L-like protease's substrate specificity profile (97) (Figure 4.6B & 6C). Furthermore, comparison of the degradation patterns for tbcatB- and rhodesain-deficient lysates with controls reveals that the same cleavage products are generated with or without tbcatB (Figure 4.6D). These data can be explained by the abundance of rhodesain relative to tbcatB (117). Since the cathepsin B-like inhibitor prevents degradation of transferrin by tbcatB RNAi control lysates (Figure 4.6D), the activation of pro-rhodesain by tbcatB may be a key tbcatB function.

CHAPTER 4

TWO-DIMENSIONAL GEL ANALYSIS OF CONTROL AND TBCATB-DEFICIENT PARASITES LYSATES

Rationale

The most important functional information that can be obtained for a given protease is the identity of its natural substrates. Clues to the identity of potential substrates can be obtained by a variety of methods, including determining the protease's localization and subsite preferences. A more direct method for identifying potential substrates is to disturb the function of the protease and use a proteomics approach to identify proteins (or protein species) that are over- or under-represented in the protease-deficient condition. Those proteins that are over-represented are potential substrates, while those proteins that are underrepresented are potential cleavage products. This proteomics approach was proposed and carried out for tbcatB, using two scenarios for tbcatB-deficiency: tbcatB knockdown by RNAi and tbcatB heterozygous knockouts.

Experimental Approach

T. brucei- Methods for culturing strain 221, pZJMTbCB, and TBCATB$^{+/-}$ parasites have been reported (221 and pZJMTB, (117)) and/or are described in the previous chapters (221, pZJMTbCB, and TBCATB$^{+/-}$). Induction of RNAi in pZJMTbCB parasites was carried out by the addition of tetracycline to the media as described in Mackey *et al.* (117) and Chapter 1.

Lysate preparation for 2-D PAGE- Lysates from *T. brucei* strain 221, TBCATB$^{+/-}$, and control and tetracycline-induced pZJMTbCB parasites were prepared as described for 2-D PAGE in Chapter 3. The resulting 2-D PAGE gels were used either for proteomics

analysis by mass spectrometry (see procedure below) or for visualization of specific protein species by Western blot analysis (see procedure below). To enhance the separation of protein species for mass spectrometry analysis, 18.3 x 19.3 cm gels (8-16% PROTEAN II Ready Gel, Bio-Rad) were used, while smaller, 13.3 x 8.7 cm gels (8-16% Criterion Ready Gel, Bio-Rad) were used for Western blots. Equal amounts of each lysate, 350 μg (for mass spectrometry) or 200 μg (for Western blotting) were prepared for isoelectric focusing (IEF) and 2-D gel electrophoresis using the ReadyPrep 2-D Cleanup Kit (Bio-Rad). The subsequent procedures used for IEF and 2-D gel electrophoresis were carried out as described in the ReadyPrep 2-D Starter Kit (Bio-Rad) instruction manual. Bio-Rad ReadyStrip IPG strips, pH 4-7 were used for IEF. Following SDS-PAGE, the gels intended for mass spectrometry analysis were stained with colloidal coomassie stain (Bio-Safe Coomassie Stain, Bio-Rad), while gels intended for Western blot analysis were immediately transferred to PVDF membrane (Millipore), using procedures described below.

Mass spectrometry sequencing of protein species separated by 2-D PAGE[7]- Individual gel spots were cut from the gel and in-gel digested with trypsin using procedures that have been previously described (158). The digested samples were then subjected to LC/MS analysis on an Agilent Technologies 1100 nanoHPLC system with the following specifications: reversed phase, C18 column, 75 μm x 150 mm; flow rate ~300 nL/min; solvent A: 0.1% formic acid in water; solvent B: 0.1% formic acid in acetonitrile; 2 μl injected; column is equilibrated @ 2% B; gradient: 2-50% B over 48 min. Data

[7] Sequencing by mass spectrometry was carried out by Ewa Witkowski at the BRC Mass Spec Facility, UCSF, and Kati Medzihradszky and Patricia Castillo at the Mass Spec Facility, UCSF. The methods described here were provided by Kati Medzihradszky.

acquisition was carried out by an LTQ-FT instrument, with mass measurement and 10 Da zoom-in scans in FT; CID of the 3 most abundant multiply charged ions in the ion trap; dynamic exclusion enabled. The Mascot Distiller program was used for peak list generation and ProteinProspector v4.25.3 was used for the database search with the following parameters: digest with trypsin; maximum missed cleavages: 1; database: UniProt.2007.04.19 (4534260/4534260 entries searched); MS/MS parent tolerance: 10 ppm; MS/MS fragment tolerance: 0.8 Da; constant modifications: amidometyl cysteine (same mass as carbamidomethyl Cys); search mode: AcetN (protein N-terminus), Met OX, PyroGlu (from N-terminal Gln); Species: All; acceptance criteria: max expect. value: 0.1; minimal peptide score: 15.

Western blot analysis of 2-D PAGE gels- Western blot analysis was carried out as described in Chapter 3, using antibody to VSG variant 221 (diluted 1:100,000) (a gift of the laboratory of John C. Boothroyd (Stanford, School of Medicine).

Western blot analysis of 1-D PAGE gels- Lysates from *T. brucei* strain 221, TBCATB$^{+/-}$, and control and tetracycline-induced pZJMTbCB parasites were prepared as described for 2-D PAGE in Chapter 3 or, alternatively, parasites were lysed by adding 5xSDS protein buffer and boiling the cells. Equal amounts of protein (33 μg) were resolved by SDS-PAGE. Methods for Western blot analysis were carried out as described in Chapter 3, again using antibody to VSG variant 221 (diluted 1:100,000) (described above).

Results

2-D analysis of control and tbcatB-deficient T. brucei lysates reveals potential cleavage products- 2-D PAGE analysis followed by mass spectrometry sequencing was carried out

on two separate occasions, with the first comparing lysates from tetracycline-induced and control pZJMTbCB parasites and the second comparing these and two additional conditions: strain 221 and TBCATB$^{+/-}$ lysates. Figure 4.7 provides a scheme for this analysis, while Figure 4.8 contains images of 2-D gels from the second set of experiments. A brief comparison of the gels reveals that they are consistent in the placement of major protein species and share a high degree of resolution with minimal streaking. On more careful inspection, a number of proteins can be identified that are present in higher or lower concentration depending on the lysate condition. For example, Spots 1 and 2 in the TBCATB$^{+/-}$ condition are present in a higher concentration than in the control (strain 221) condition (Figure 4.8A & 8B). Likewise, the concentration of protein in Spot 13 is lower in the TBCATB$^{+/-}$ lysates than in lysates from strain 221 parasites (Figure 4.8A & 8B). Since these spots could represent potential undegraded substrates and cleavage products, respectively, they were selected for further analysis.

A total of 20 spots were selected for sequencing by mass spectrometry and the results of this analysis are provided in Table 4.1. In the far right column, data is provided from the earlier 2-D PAGE analysis, where it overlaps with the data obtained from the gels in Figure 4.8. Of note, rhodesain was identified as a protein that accumulates in both tbcatB-deficient conditions (Table 4.1) and was identified in both early and recent analysis. Importantly, though, VSG was identified in the earlier analysis as a protein that disappears in tbcatB RNAi knockdown parasites, but was not identified in the analysis that included SDS in the lysis buffer. Figure 4.9 provides the sequencing data obtained for rhodesain (A) and VSG (B).

Comparison of 1- and 2-D analysis of VSG content does not suggest that VSG is a substrate of tbcatB- To further investigate the hypothesis from earlier 2-D PAGE analysis that VSG may be a substrate for tbcatB, Western blot analysis, using antibody to VSG, was carried out on 2-D gels of lysates from strain 221 and $TBCATB^{+/-}$ parasites (Figure 4.10A). The 2-D gels revealed an overall greater VSG content in the tbcatB-deficient lysates, with no spots disappearing in the tbcatB-deficient condition. Since only a minimal concentration of protease inhibitors were present in the buffer used to lyse the *T. brucei*, we hypothesized that at least some VSG cleavage may occur while the *T. brucei* are incubated in the buffer. To test this hypothesis, we prepared lysates by the standard method or by adding SDS protein buffer to the cells and boiling them directly and compared their VSG protein content by 1-D PAGE (Figure 4.10B). Note that the protein content for the control and induced RNAi conditions were approximately the same, while the protein content for the heterozygous knockout and strain 221 were approximately equal, but higher than both RNAi conditions. No significant difference was observed between the four conditions with either the standard or SDS lysates preparation.

Discussion

Complementing the approaches discussed in previous Chapters, 2-D PAGE and mass spectrometry analysis provided useful information about potential substrates of tbcatB. In particular, the proteomics approach revealed that pro-rhodesain is enriched in tbcatB-deficient parasites (Figure 4.8 & 4.10, Table 4.1). As discussed in Chapter 3, rhodesain contains a sequence in its pro-peptide that matches the predicted optimal substrate

specificity profile for tbcatB, suggesting, that rhodesain may be a natural substrate of tbcatB. Labeling of control and tbcatB-deficient parasite lysates with the Clan CA cysteine protease active site label ^{125}I-DCG04 (107), revealed increased levels of the pro-form of rhodesain in some assays (data not shown). Clearly, follow-up experiments are needed to confirm that rhodesain activation is a function of tbcatB.

2-D PAGE analysis identified two other potential substrates, VSG and transferrin. Western blot analysis of 2-D gels containing strain 221 and TBCATB$^{+/-}$ lysates revealed that both VSG and transferrin protein species accumulate in the tbcatB-deficient condition (Figure 3.7 and 4.10A). In the case of transferrin, this result added to the growing body of data supporting the hypothesis that transferrin is a natural substrate of tbcatB. In contrast, further analysis of VSG protein content in control and TBCATB$^{+/-}$ parasites suggested that undegraded VSG does not accumulate in tbcatB-deficient parasites (Figure 4.10B).

As indicated in Table 4.1, other proteins were identified as over-represented in TBCATB$^{+/-}$ and tbcatb RNAi knockdown parasites and further analysis is required to determine if they represent natural substrates. Rather than being substrates, the stress response proteins, HSP70 and HSP60, could be upregulated in response to the altered growth rate of the tbcatB-deficient parasites. Considering the morphological abnormalities of tbcatB-deficient parasites discussed in Chpter 3, the proteins actin and BiP could also be upregulated to support the growing size of the flagellar pocket (actin) and need for increased protein production (because of mis-trafficking of proteins), at the endoplasmic reticulum (BiP).

TABLES AND FIGURES FOR CHAPTER 4

Fig. 4.1. TbcatB antiserum localizes to the posterior tip of *T. brucei* and not to the lysosome. *A.* Strain 221 parasites were labeled with tbcatB antiserum and TexasRed secondary antibody (red channel). The tbcatB antiserum localized to the posterior tip of the parasite, as indicated in the schematic of *T. brucei* cellular structure (red circle). *B & C.* Tetracycline-induced pZJMRho and pZJMTbCB parasites were labeled with tbcatB antiserum and TexasRed secondary antibody (red channel), and p67 (118) and FITC secondary antibody (green channel). *D.* Tetracycline-induced pZJMRho and pZJMTbCB parasites were labeled with tbcatB antiserum and FITC secondary antibody (green channel), and p67 and TexasRed secondary antibody (red channel).

Fig. 4.2. TbcatB antiserum localizes at or near the flagellar pocket. Strain 221 and tetracycline-induced pZJMTbCB parasites were incubated with FITC-ConA at 4 °C to label the flagellar pocket (green channel) and subsequently labeled with tbcatB antiserum and TexasRed secondary antibody (red channel).

Fig. 4.3. TbcatB antiserum does not co-localize with the basal body. Strain 221 parasites were labeled with antibody to YL1/2 and FITC secondary antibody to visualize the basal body (green channel), and tbcatB antiserum and TexasRed secondary antibody (red channel).

Fig. 4.4. TbcatB antiserum labels a region that is posterior of the ER and of early and recycling endosomes. Strain 221 parasites were labeled with primary antibody to BiP (A), Rab5A (B), and Rab11 (C) to label the ER, early and sorting endosomes, and recycling endosomes, respectively, and TexasRed secondary antibody (red channel).

Labeling of strain 221 parasites with tbcatB antiserum and TexasRed secondary antibody is provided for reference (D).

Fig. 4.5. Potential cleavage sites in bovine transferrin by tbcatB and rhodesain. Potential cleavage sites predicted using substrate specificity data for recombinant tbcatB are indicated in blue. Sequences obtained from N-terminal sequencing of tbcatB- and rhodesain-derived transferrin degradation products are indicated in purple and green, respectively. The molecular weights for predicted and –terminal sequence cleavage products are given.

Fig. 4.6. *In vitro* degradation of bovine transferrin by tbcatB and rhodesain and potential cleavage sites. *A-C. In vitro* tbcatB- and rhodesain-derived transferrin degradation products. Arrows indicate cleavage products for which an N-terminal sequence was obtained (B). Control and tbcatB- and rhodesain-containing samples were subjected to HPLC purification (C). *D.* Transferrin degradation products generated with lysates from control and tetracycline-induced tbcatB and rhodesain parasites.

Fig. 4.7. Scheme for 2D PAGE analysis of control and tbcatB-deficient *T. brucei* lysates. Lysates from stain 221, pZJMTbCB tetracycline induced and uninduded (+Tet and No Tet), and TBCATB$^{+/-}$ parasites were subjected to 2D PAGE and subsequent analyses as indicated. Strain 221 and pZJMTbCB uninduced lysates served as controls.

Fig. 4.8. 2D PAGE gels of lysates from 221, TBCATB$^{+/-}$, and control and tetracycline-induced pZJMTbCB parasites. 2D PAGE gels of lysates from stain 221 (A), pZJMTbCB tetracycline induced (D) and uninduded (C) (*i.e.* +Tet and No Tet), and TBCATB$^{+/-}$ (B) parasites. Strain 221 and pZJMTbCB uninduced lysates served as controls.

Table. 4.1. Mass spectrometry results from 2D PAGE analysis of control and tbcatB-deficient parasite lysates. The identity of 20 protein spots on 2-D PAGE gels of lysates from strain 221, TBCATB$^{+/-}$, and control and RNAi-induced pZJMTbCB parasites are shown (images of the gels are shown in Figure 4.8). Arrows indicate whether the spots are present in higher (upward arrow) or lower (downward arrow) concentration in TBCATB$^{+/-}$ (TbCB$^{+/-}$) or tbcatB RNAi knockdown (TbCB rnai +Tet) parasite lysates, as compared to controls. Data are included from a recent experiment for all four conditions, as well as from an earlier experiment comparing control and tetracycline-induced RNAi parasite lysates (TbCB rnai data '06).

Fig. 4.9. Selected mass spectrometry results for 2D gels of lysates from control and tetracycline-induced pZJMTbCB parasite lysates. 2D PAGE gel images of lysates obtained from pZJMTbCB tetracycline induced (+Tet) parasites are shown. Mass spectrometry sequencing results (shown in red) are given for the spots indicated in red.

Fig. 4.10. Comparison of VSG protein species in control and tbcatB-deficient parasite lysates by 2- and 1-dimensional gel analysis. *A.* Lysates from strain 221 and TBCATB$^{+/-}$ parasites were subjected to 2-D PAGE, followed by Western blot analysis using antibody to VSG. *B.* Control and tbcatB-deficient parasites were lysed using standard lysis buffer (see methods) or by adding SDS and boiling the parasites directly. Lysates were subjected to Western blot analysis using antibody to VSG.

Figure 4.1.

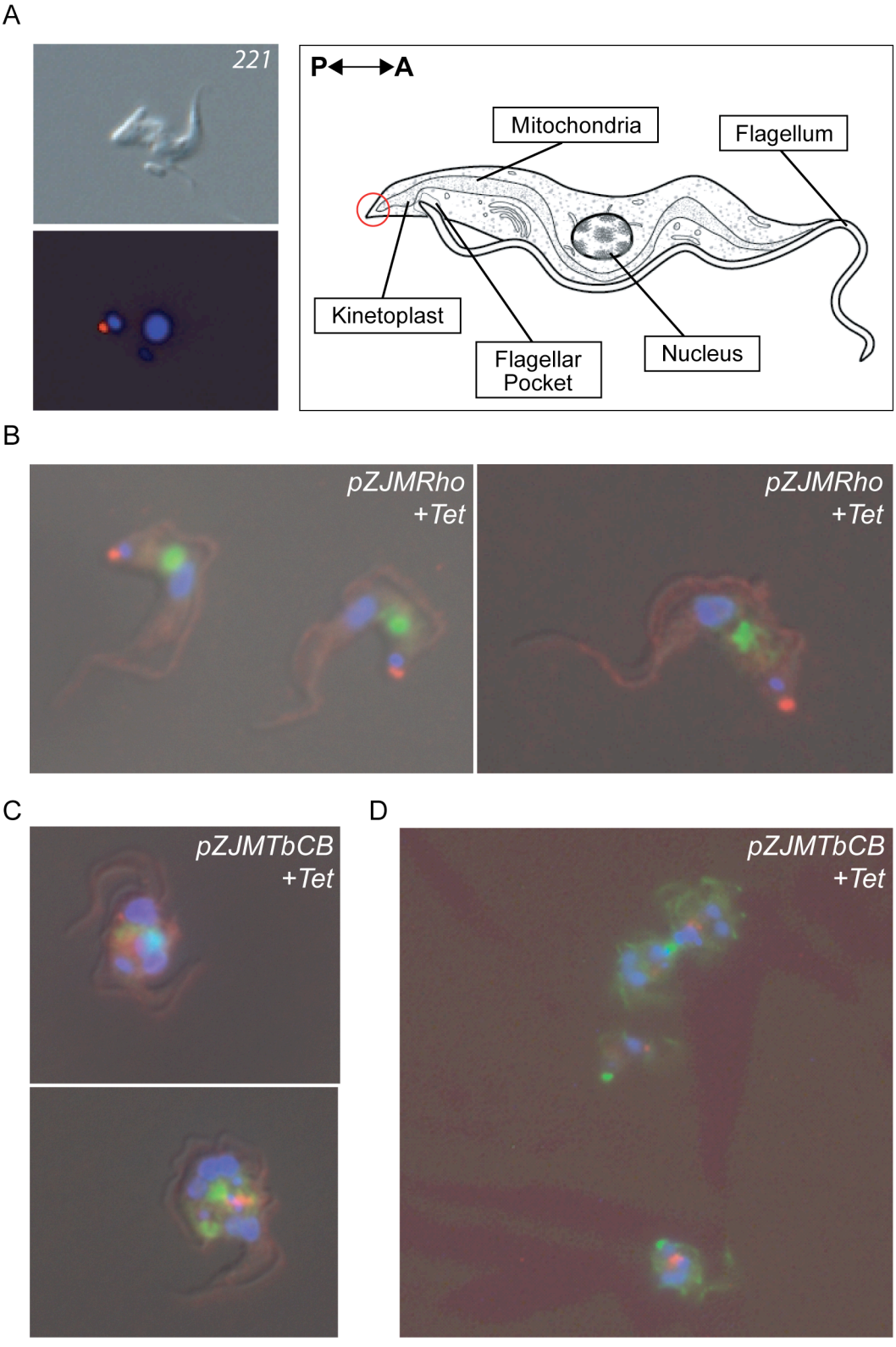
A
221
P
A
Mitochondria
Flagellum
Kinetoplast
Flagellar Pocket
Nucleus
B
pZJMRho +Tet
pZJMRho +Tet
C
pZJMTbCB +Tet
D
pZJMTbCB +Tet

Figure 4.2.

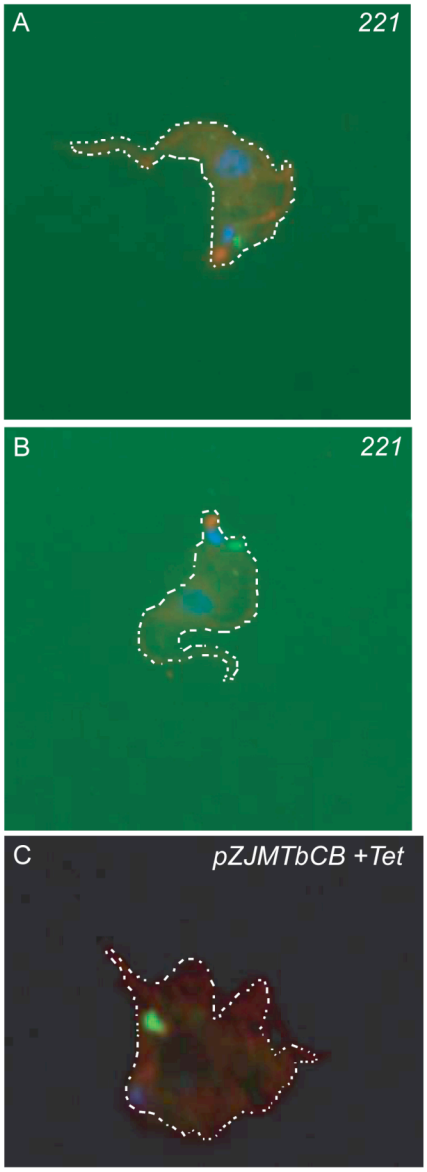

Figure 4.3.

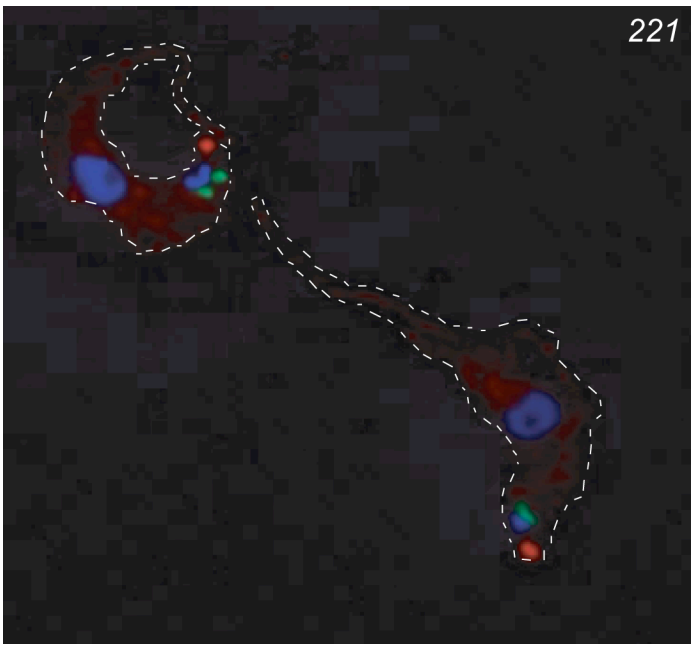

Figure 4.4.

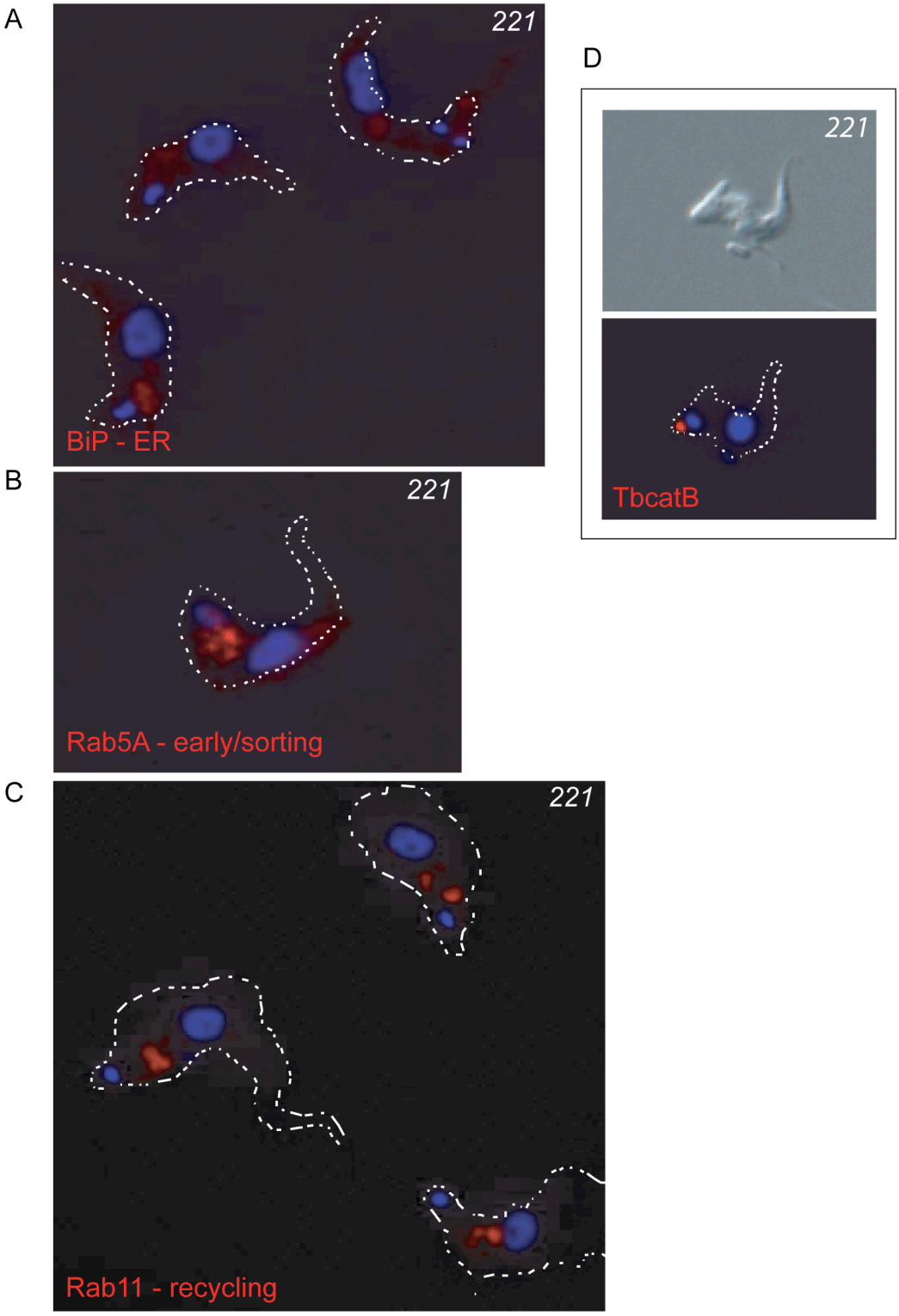
A
221
BiP - ER
B
221
Rab5A - early/sorting
C
221
Rab11 - recycling
D
221
TbcatB

Figure 4.5.

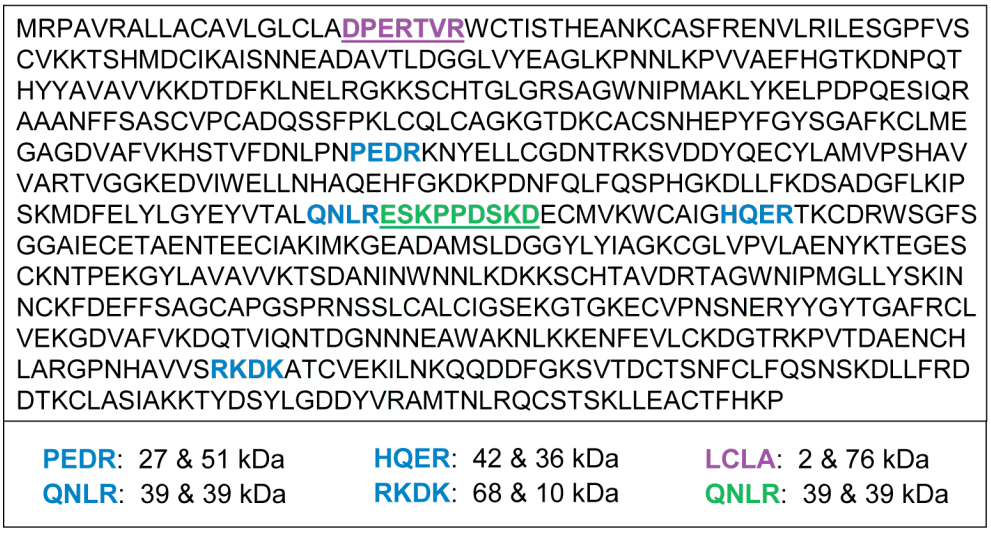
MRPAVRALLACAVLGLCLADPERTVRWCTISTHEANKCASFRENVLRILESGPFVS
CVKKTSHMDCIKAISNNEADAVTLDGGLVYEAGLKPNNLKPVVAEFHGTKDNPQT
HYYAVAVVKKDTDFKLNELRGKKSCHTGLGRSAGWNIPMAKLYKELPDPQESIQR
AAANFFSASCVPCADQSSFPKLCQLCAGKGTDKCACSNHEPYFGYSGAFKCLME
GAGDVAFVKHSTVFDNLPNPEDRKNYELLCGDNTRKSVDDYQECYLAMVPSHAV
VARTVGGKEDVIWELLNHAQEHFGKDKPDNFQLFQSPHGKDLLFKDSADGFLKIP
SKMDFELYLGYEYVTALQNLRESKPPDSKDECMVKWCAIGHQERTKCDRWSGFS
GGAIECETAENTEECIAKIMKGEADAMSLDGGYLYIAGKCGLVPVLAENYKTEGES
CKNTPEKGYLAVAVVKTSDANINWNNLKDKKSCHTAVDRTAGWNIPMGLLYSKIN
NCKFDEFFSAGCAPGSPRNSSLCALCIGSEKGTGKECVPNSNERYYGYTGAFRCL
VEKGDVAFVKDQTVIQNTDGNNNEAWAKNLKKENFEVLCKDGTRKPVTDAENCH
LARGPNHAVVSRKDKATCVEKILNKQQDDFGKSVTDCTSNFCLFQSNSKDLLFRD
DTKCLASIAKKTYDSYLGDDYVRAMTNLRQCSTSKLLEACTFHKP
PEDR: 27 & 51 kDa
QNLR: 39 & 39 kDa
HQER: 42 & 36 kDa
RKDK: 68 & 10 kDa
LCLA: 2 & 76 kDa
QNLR: 39 & 39 kDa

Figure 4.6.

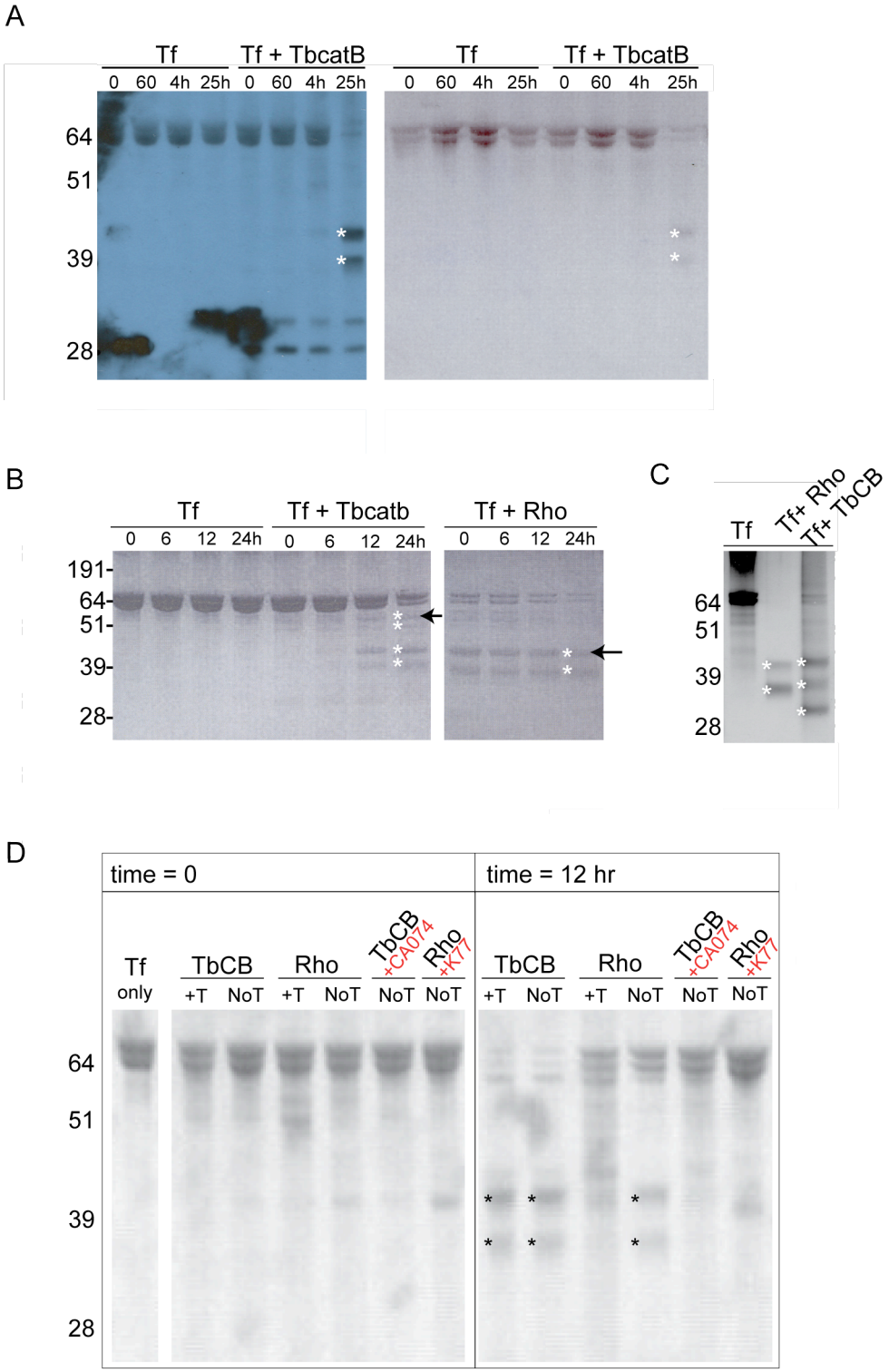
A
Tf
Tf + TbcatB
Tf
Tf + TbcatB
0 60 4h 25h 0 60 4h 25h
0 60 4h 25h 0 60 4h 25h
64
51
39
28
B
Tf
Tf + Tbcatb
Tf + Rho
0 6 12 24h 0 6 12 24h
0 6 12 24h
191-
64-
51-
39-
28-
C
Tf
Tf+ Rho
Tf+ TbCB
64
51
39
28
D
time = 0
time = 12 hr
Tf only
TbCB
Rho
TbCB +CA074
Rho +K77
+T NoT +T NoT NoT NoT
+T NoT +T NoT NoT NoT
64
51
39
28

Figure 4.7.

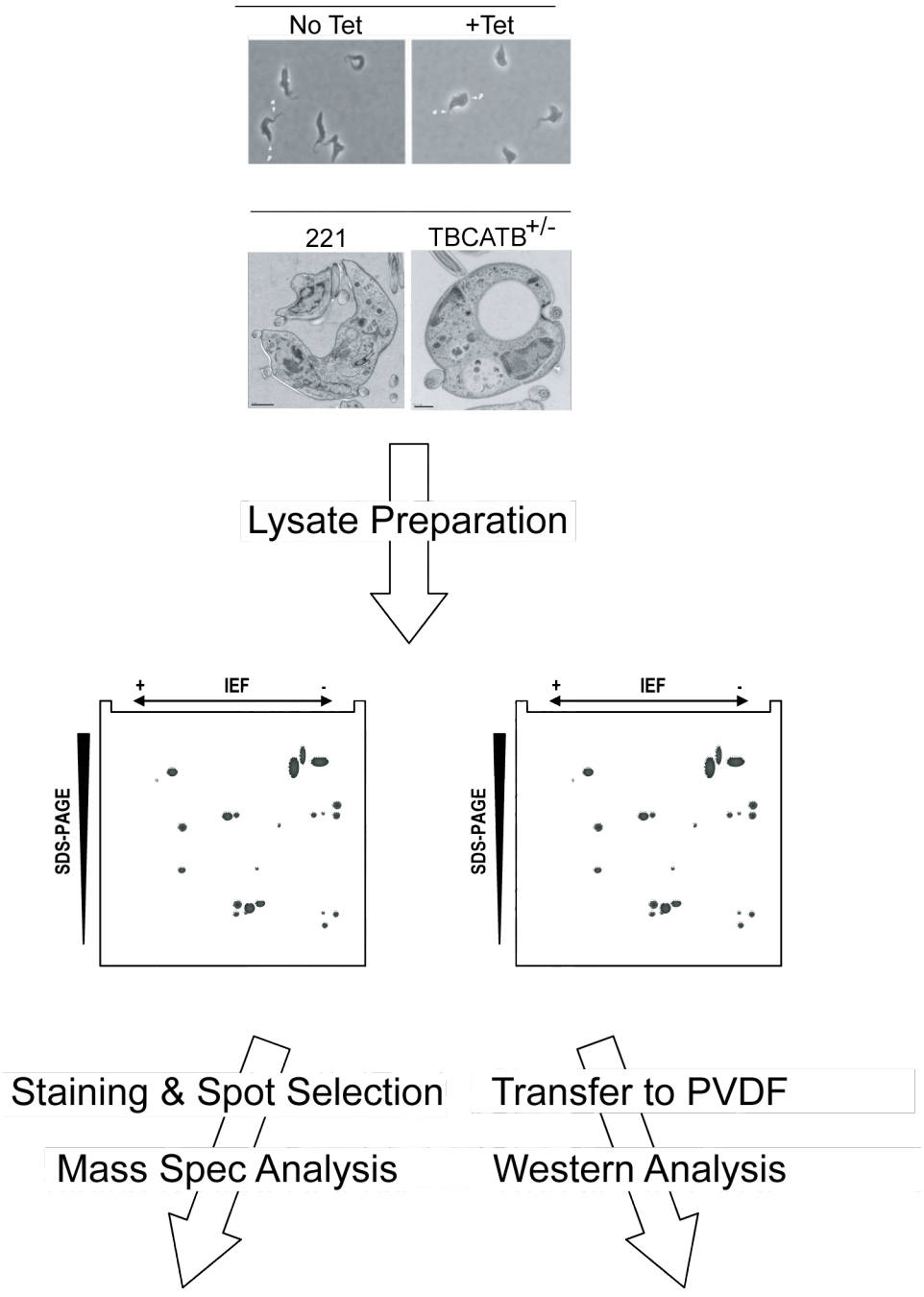
No Tet
+Tet
221
TBCATB+/-
Lysate Preparation
+
IEF
-
SDS-PAGE
+
IEF
-
SDS-PAGE
Staining & Spot Selection
Transfer to PVDF
Mass Spec Analysis
Western Analysis

Figure 4.8.

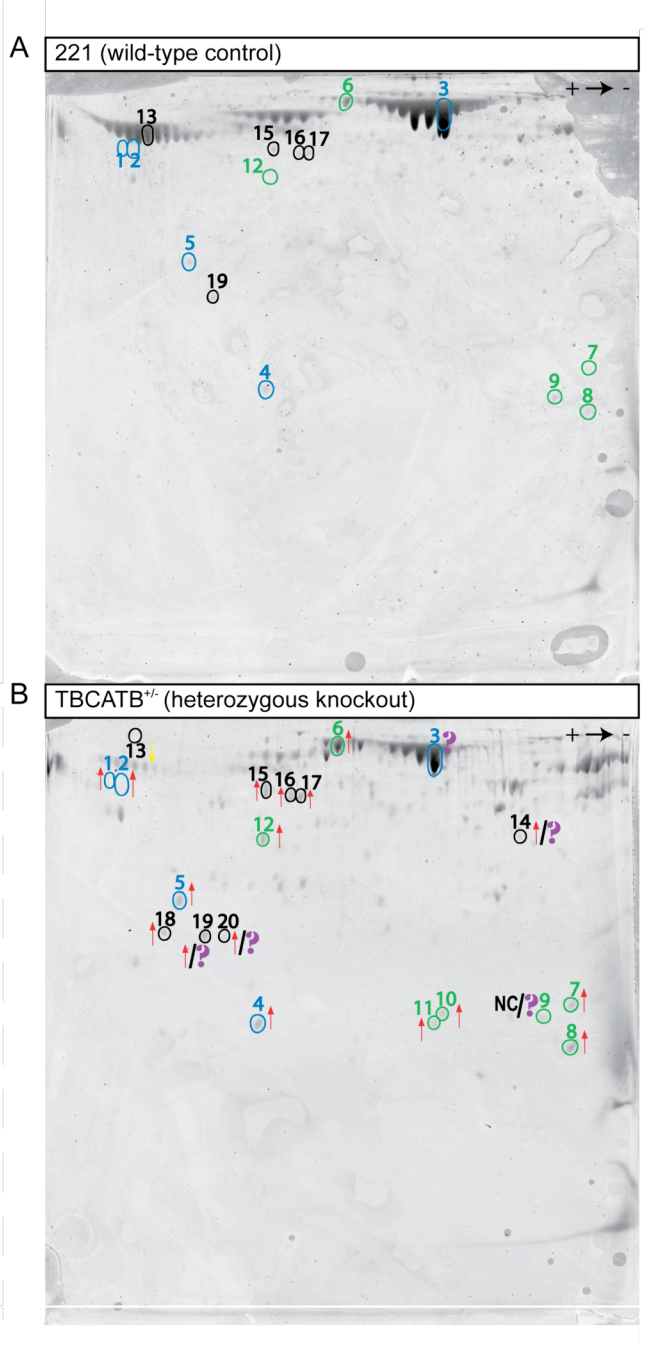

Figure 4.8. (continued)

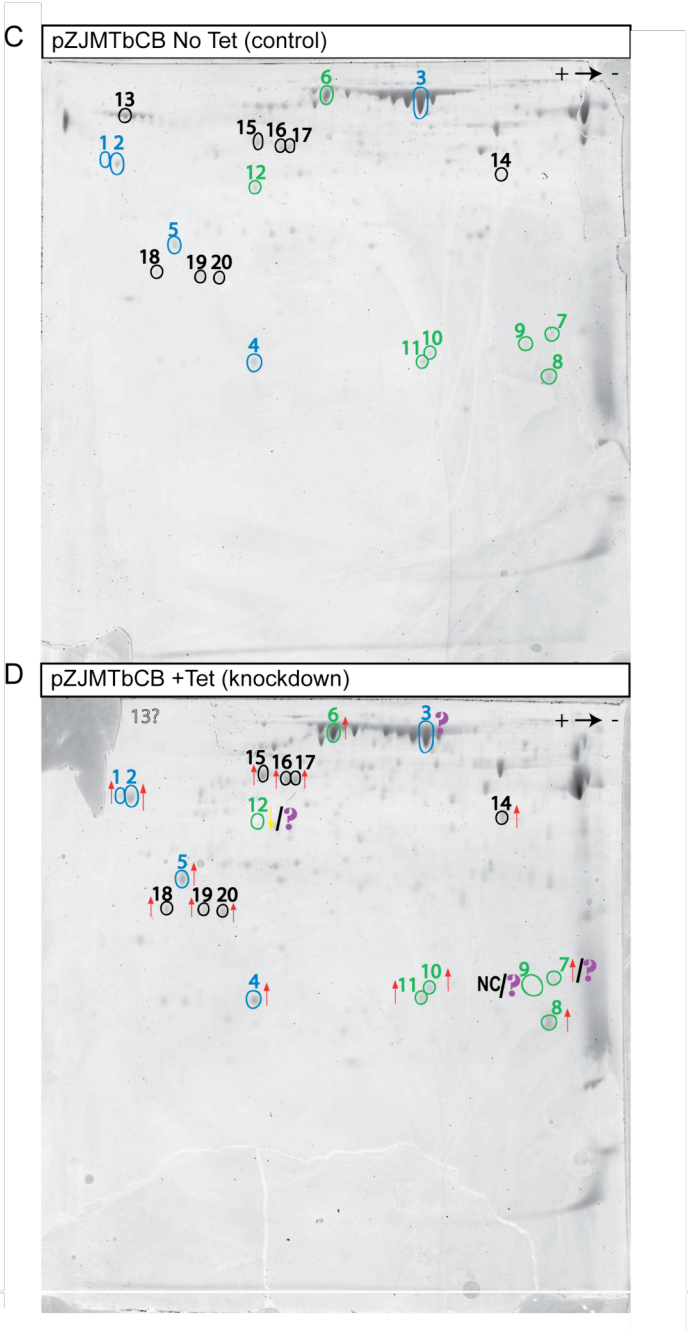

Table 4.1. Proteins Present in Higher or Lower Concentration in TbcatB-deficient Parasite Lysates

spot #		TbCB+/-	TbCB rnai +Tet	TbCB rnai data '06
1	Rhodesain	↑	↑	↑
2	Rhodesain	↑	↑	↑
3	Hypoth protein (Q57YL2), Coronin, HSP 70kDa, Lipophosphoglycan biosysnthetic protein	?	?	
4	Trypareodoxin	↑	↑	↑
5	Hypoth protein (Q57X68)	↑	↑	
6	HSP 70, HSP 60, Bloodstream-specific, BiP/GRP78 precursor	↑	↑	↑
7	Ubiquitin-conjugating, Bloodstream-specific	↑	↑/?	
8	HSP 10, Hypoth protein (Q384D1), Hypoth protein (Q586B2), Eukaryotic initition factor 4a	↑	↑	
9	Ribose 5-phosphate isomerase, Protein disulfide isomerase	NC/?	NC/?	
10	Ubiquitin-conjugating enzyme E2	↑	↑	
11	Cofilin/actin	↑	↑	
12	Hypoth protein (Q38B23), Protein phosphatase 2C, Beta tubulin, HSP HslVU	↑	↑	
13	----------	↓	?	
14	Protein kinase (putative), Elongation factor 2, Proteasome regulartory non-ATPase subunit 11	↑/?	↑	
15	Calrectuculin, Poly(A) binding protein I, Beta tublin, Chaperonin Hsp60, VSGMI-TAT 1.2	↑	↑	
16	Calrecticulin, Hypoth protein (Q585Z8), Hsc70-interacting protein (Hlp)	↑	↑	
17	Calreticulin, Hypoth protein (Q383M5)	↑	↑	
18	IgE-dependent histamine-releasing factor	↑	↑	
19	Eukayotic translation initiation factor 5a	↑/?	↑	
20	Eukaryotic translation initiation factor 5a	↑/?	↑	↑

Figure 4.9.

A

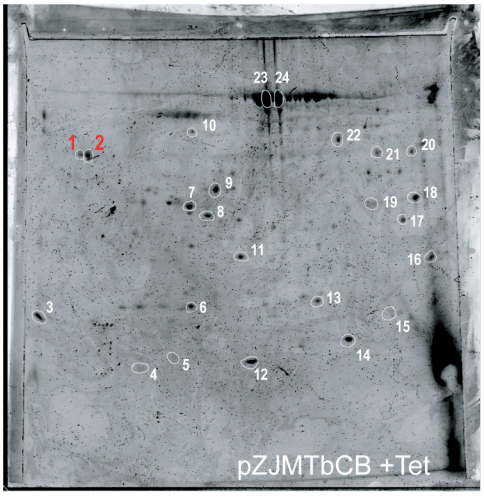

1A: Rhodesain

Match to: **S07051** Score: **245**
cysteine proteinase (EC 3.4.22.-) precursor - Trypanosoma brucei

1 MPRTEMVRFV RLPVVLLAMA ACLASVALGS LHVEESLEMR FAAFKKKYGK
51 VYKDAKEEAF RFRAFEENME QAKIQAAANP YATFGVTPFS DMTREEFRAR
101 YRNGASYFAA AQKRLRKTVN VTTGRAPAAV DWREKGAVTP VKVQGQCGSC
151 WAFSTIGNIE GQWQVAGNPL VSLSEQMLVS CDTIDSGCNG GLMDNAFNWI
201 VNSNGGNVFT EASYPYVSGN GEQPQCQMNG HEIGAAITDH VDLPQDEDAI
251 AAYLAENGPL AIAVDAESFM DYNGGILTSC TSKQLDHGVL LVGYNDNSNP
301 PYWIIKNSWS NMWGEDGYIR IEKGTNQCLM NQAVSSAVVG GPTPPPPPPP
351 PPSATFTQDF CEGKGCTKGC SHATFPTGEC VQTTGVGSVI ATCGASNLTQ
401 IIYPLSRSCS GPSVPITVPL DKCIPILIGS VEYHCSTNPP TKAARLVPHQ
451

2A: Rhodesain

Match to: **S07051** Score: **233**
cysteine proteinase (EC 3.4.22.-) precursor - Trypanosoma brucei

1 MPRTEMVRFV RLPVVLLAMA ACLASVALGS LHVEESLEMR FAAFKKKYGK
51 VYKDAKEEAF RFRAFEENME QAKIQAAANP YATFGVTPFS DMTREEFRAR
101 YRNGASYFAA AQKRLRKTVN VTTGRAPAAV DWREKGAVTP VKVQGQCGSC
151 WAFSTIGNIE GQWQVAGNPL VSLSEQMLVS CDTIDSGCNG GLMDNAFNWI
201 VNSNGGNVFT EASYPYVSGN GEQPQCQMNG HEIGAAITDH VDLPQDEDAI
251 AAYLAENGPL AIAVDAESFM DYNGGILTSC TSKQLDHGVL LVGYNDNSNP
301 PYWIIKNSWS NMWGEDGYIR IEKGTNQCLM NQAVSSAVVG GPTPPPPPPP
351 PPSATFTQDF CEGKGCTKGC SHATFPTGEC VQTTGVGSVI ATCGASNLTQ
401 IIYPLSRSCS GPSVPITVPL DKCIPILIGS VEYHCSTNPP TKAARLVPHQ
451

B

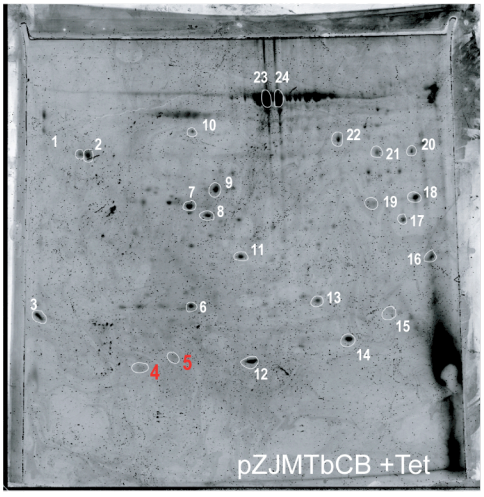

4A: VSG

Match to: **1VSGA** Score: **190**
variant surface glycoprotein (N-terminal domain), chain A – T. brucei

1 AAEKGFKQAF WQPLCQVSEE LDDQPKGALF TLQAAASKIQ KMRDAALRAS
51 IYAEINHGTN RAKAAVIVAN HYAMKADSGL EALKQTLSSQ EVTATATASY
101 LKGRIDEYLN LLLQTKESGT SGCMMDTSGT NTVTKAGGTI GGVPCKLQLS
151 PIQPKRPAAT YLGKAGYVGL TRQADAANNF HDNDAECRLA SGHNTNGLGK
201 SGQLSAAVTM AAGYVTVANS QTAVTVQALD ALQEASGAAH QPWIDAWKAK
251 KALTGAETAE FRNETAGIAG KTGVTKLVEE ALLKKKDSEA SEIQTELKKY
301 FSGHENEQWT AIEKLISEQP VAQNLVGDNQ PTKLGELEGN AKLTTILAYY
351 RMETAGKFEV LT

5A: VSG

Match to: **1VSGA** Score: **288**
variant surface glycoprotein (N-terminal domain), chain A – T. brucei

1 AAEKGFKQAF WQPLCQVSEE LDDQPKGALF TLQAAASKIQ KMRDAALRAS
51 IYAEINHGTN RAKAAVIVAN HYAMKADSGL EALKQTLSSQ EVTATATASY
101 LKGRIDEYLN LLLQTKESGT SGCMMDTSGT NTVTKAGGTI GGVPCKLQLS
151 PIQPKRPAAT YLGKAGYVGL TRQADAANNF HDNDAECRLA SGHNTNGLGK
201 SGQLSAAVTM AAGYVTVANS QTAVTVQALD ALQEASGAAH QPWIDAWKAK
251 KALTGAETAE FRNETAGIAG KTGVTKLVEE ALLKKDSEA SEIQTELKKY
301 FSGHENEQWT AIEKLISEQP VAQNLVGDNQ PTKLGELEGN AKLTTILAYY
351 RMETAGKFEV LT

Figure 4.10.

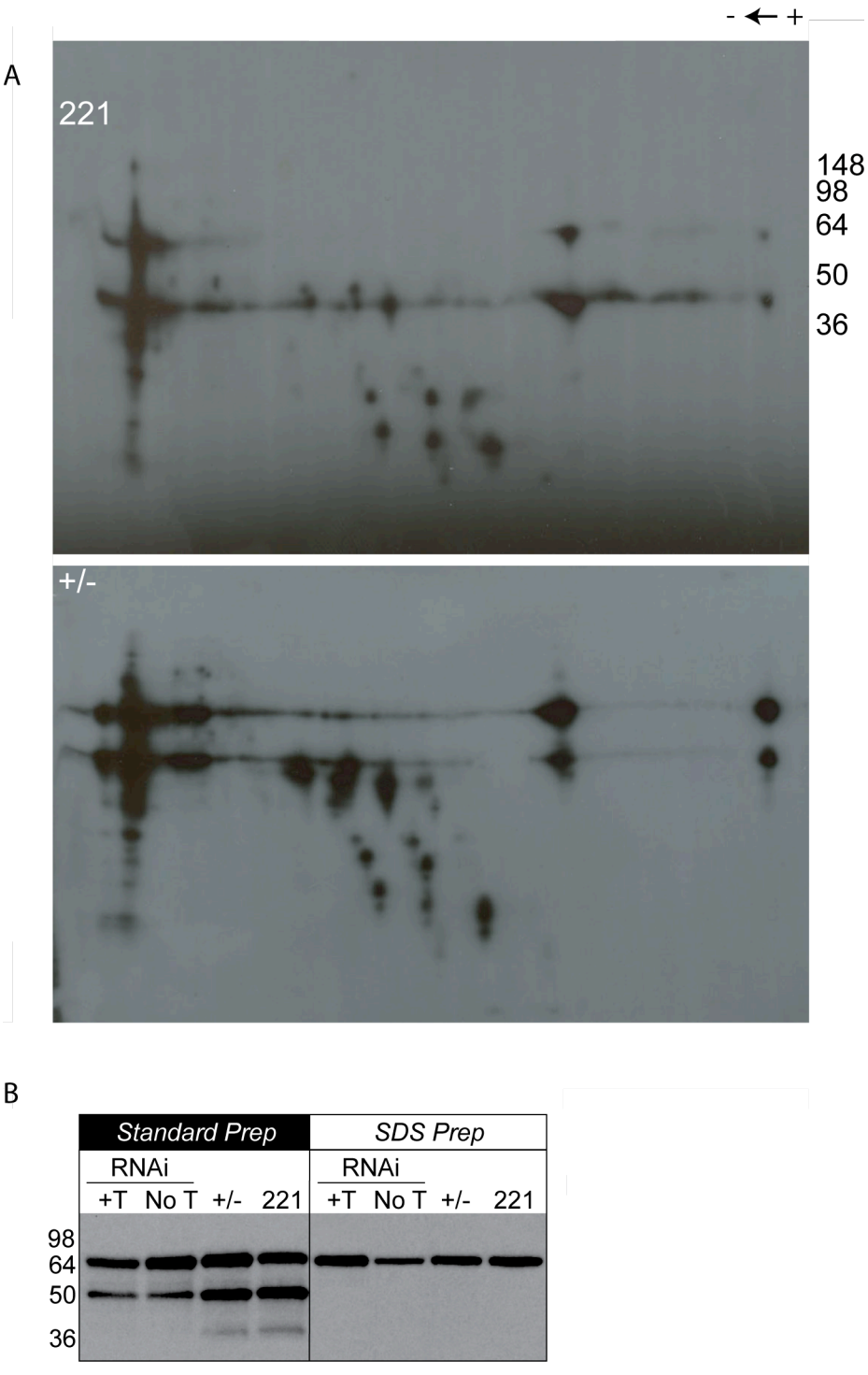
A
- ← +
221
148
98
64
50
36
+/-
B
Standard Prep
SDS Prep
RNAi
+T
No T
+/-
221
98
64
50
36

CONCLUSIONS AND FUTURE DIRECTIONS

CYSTEINE PROTEASES AND *T. BRUCEI*: REVIEW OF LITERATURE FROM 2003 TO THE PRESENT

Inhibition Studies

A great deal of research has been carried out in the past four and half years to identify selective cysteine protease inhibitors that can serve as drugs leads for new therapeutics to treat HAT. In 2003, Nkemgu *et al*. investigated the trypanocidal activities and inhibition efficacies of three commercially available cathepsin L inhibitors (104). In contrast to the diazomethyl ketone Z-Phe-Ala-CHN_2 that was used in Scory *et al.* (30), the inhibitors used in this study had more specific reactivity against Clan CA cysteine proteases (104). The inhibitors were 10-100 fold more potent than inhibitors previously tested (30,60,85) and, as with Z-Phe-Ala-CHN_2, treatment with the cysteine protease inhibitors was associated with an accumulation of undegraded transferrin in the parasite lysosome (30,104). Since it is the major cysteine protease in *T. brucei* and localizes to the lysosome, Nkemgu *et al.* concluded that rhodesain is the critical target of the inhibitors (104). However, they also acknowledged a lack of correlation between trypanocidal activity and inactivation rates of rhodesain produced by the inhibitors (104), an observation that could be explained by the presence of other critical cysteine protease targets and the lack of absolute inhibitor specificity.

In 2004, thiosemicarbazones were investigated as parasiticidal compounds against the major cysteine proteases from *T. brucei* (*i.e.* rhodesain), *Trypanosoma cruzi* (*i.e.* cruzain), and *Plasmodium falciparum* (falcipain) and against the parasites themselves (159). Thiosemicarbazones are a class of small molecules that had been previously

studied as antivirals and anticancer therapeutics and, more recently, as parasiticidal agents against *T. cruzi* and *P. falciparum* (159). They were also shown to inhibit the *T. cruzi* protease, cruzain (160). In the 2004 study, a library of thiosemicarbazones were synthesized by taking into account structure-activity relationships identified in the cruzain inhibition study (159,160). When the library was screened against the three parasite-derived proteases and appropriate parasites, several themicarbazones were found to be effective against both the enzymes and parasites (159). However, not all the most parasiticidal compounds were effective against the proteases (159). The authors concluded that, since several of the compounds were effective at killing all the three tested parasites with limited toxicity in mice, thiosemicarbazones represent valid drug leads for protozoan parasites (159). Not long after this report, Fujii *et al.* discovered even more potent thiosemicarbazone inhibitors of rhodesain and cruzain, although the inhibitors had only modest potency against falcipain-2 (161). Fujii *et al.* designed their compounds based on the thiosemicarbazone derivatives that were found to be most effective in Greenbaum *et al.* (159), but made modifications to an ethyl side chain (161). The authors conclude that the structure-activity relationship data obtained in this study will facilitate future design of lead optimization libraries of thiosemicarbazone inhibitors with potent trypanocidal activities (161).

Another class of cysteine protease inhibitors that have been shown to be effective inhibitors of rhodesain are aziridine-2,3-dicarboxylate derivatives (162). Prior to the study, inhibitors of this class were known to be effective against mammalian cathepsin L and B (162). When tested against recombinant rhodesain and *T. brucei brucei* in culture, Vicik *et al.* found that most of the compounds inhibited the enzyme at micromolar

concentrations and that a sub-set of these had trypanocidal activity equivalent to the late-stage HAT drug eflornithine (162). They conclude that the most promising compounds tested were the Leu-Pro-containing dibenzyl derivatives, since they are effective inhibitors of rhodesain and are the least cytotoxic to host-derived macrophages when used at trypanocidal concentrations (162). As follow-up, the authors plan to investigate potential for host toxicity and efficacy of these compounds in an animal model of infection (162).

A novel approach to identifying compounds that kill *T. brucei* in culture was taken in 2006 when Mackey *et al.* used a high-throughput approach screen to identify FDA-approved and clinical candidate drugs that are cytotoxic to *T. brucei* (19). The rationale for the screen was two fold: drugs that have already been approved for other uses (or are in late-stage clinical development) will not require the same costly approval processes as novel drugs and a method for high-throughput whole-cell screening of drugs will allow for large libraries to be screened rapidly and efficiency (19). A total of 2160 drugs were screened using an ATP-bioluminescense assay that was adapted to a high-throughput screening format, yielding 35 hits from seven different drug categories (19). Although the screen was not targeted at cysteine proteases (and none of the hits were known cysteine protease inhibitors), it is worth pointing out the high-throughout approach taken by Mackey *et al.* could be applied in the future to screen libraries of cysteine protease inhibitors again *T. brucei*.

Finally, in a soon-to-be-published study, *Mallari et al.*[8] report the effectiveness of a series of purine-derived nitrile compounds designed to target tbcatB (Mallari, in press). Mallari *et al.* hypothesized that the purine nitrile scaffold might have improved potency over other established cysteine protease inhibitor scaffolds by virtue of the fact that *T. brucei* purine-scavenging mechanisms may aid delivery of the inhibitors into the parasite (Mallari, in press). They found that the compounds killed *T. brucei* with a high degree of selectivity and, further, they provide a predictive model for the trypanocidal activity that is based primarily on potency against TbcatB (Mallari, in press).

Functional Insights

In 2003, Triggs *et al.* implicated cysteine proteases in the degradation of mis-folded VSG proteins, by treating *T. brucei* that express VSG lacking a glycosyl-phospatidylinosotiol (GPI) anchor (163) with the potent cysteine protease inhibitor FMK024 (118). FMK024-like inhibitors had previously been shown to inhibit rhodesain/brucipain (30,56). FMK024-treatment lead to an accumulation of GPI-minus protein in the lysosome, implying that lysosomal cysteine proteases are responsible for VSG turnover (118).

In 2006, Nikolskaia *et al.* used the cysteine protease inhibitors K11777 (49) and CA074 to study the ability of *T. brucei gambiense and T. brucei brucei* to traverse the blood-brain barrier (BBB) (122). *T. b. gambiense* had already been shown to cross an *in vitro* model system of the BBB (created using human brain microvascular endothelial cells (BMECs)) more efficiently than *T. b. brucei* (164). Using the BBB model system, the authors showed that the brucipain-rich supernatants could enhance crossing by *T. b.*

[8] Jeremy P. Mallari, Anang A. Shelat, Theresa C. O'Brien, Aaron Kosinski, Conor R. Caffrey, Michele Connelly, James H. McKerrow, and R. Kiplin Guy. Development of potent purine-derived nitrile inhibitors of the trypanosomal protease tbcatB. *Journal of Medicinal Chemistry*. In press.

brucei and that K11777, but not CA074, cancels the enhancement (122). CAO74 is a selective inhibitor of tbcatB, while K11777 inhibits both brucipain/rhodesain and tbcatB. They also found that K11777-treatment abolishes calcium fluxes that are required for the parasites to cross the model BBB (122). Taking into consideration that *T. b. gambiense* express much higher levels of cathepsin L-like protease than *T. b. brucei*, the authors conclude that brucipain may act as a critical mediator of *T. b. gambiense* BBB traversal (122).

As a follow-up their 1999 study (30), Scory *et al.* examined the effect of the diazomethyl ketone cysteine protease inhibitor Z-Phe-Ala-CHN_2 on *T. brucei* morphology, cell division, and protein content. The researchers found that treatment with the inhibitor leads to an increase in cell mass and lysosomal enlargement, followed by parasite death (124). Parasites also took on a "stumpy-like" morphology and most were not dividing, suggesting that the inhibitor induced cell cycle arrest (124). Ultrastructural analysis lead to the proposition that accumulation of undegraded lysosomal proteins could not alone account for the organelle's enlargement or parasite's overall greater protein content, since the lysosomes of treated parasites were no more electron dense than controls (124). However, an osmotic enlargement would not be expected to have a more dense appearance. Scory *et al.* conclude that Z-Phe-Ala-CHN_2 treatment leads to a depletion of essential nutrients required for DNA synthesis, which, in turn, results in cell cycle arrest and triggers differentiation of *T. brucei* from long-slender to short-stumpy bloodstream forms (124). Since exposure to the inhibitor *in vivo* results in a 92% decrease in cysteine protease activity (30), the authors implicate rhodesain as the critical target in their study (124). However, given that tbcatB-deficiency results in similar

phenotypic effects (117) (Chapters 1 and 3), and that rhodesain may be a substrate of tbcatB (Chapter 4), it is perhaps more likely that the cathepsin B-like protease is the critical target.

Rhodesain Substrate Specificity

Two independent studies have been carried out to determine the substrate specificity profile of recombinant rhodesain. In the first study, Gosalia *et al*. formatted a 722-member library of fluorogenic protease substrates with the general format Ac-Ala-X-X-(Arg/Lys)-coumarin on a microarray for high-throughput substrate specificity profiling (165). They determined the specificity of rhodesain, along with 13 other serine and 10 other cysteine proteases (165). They found that rhodesain has a strong preference for hydrophobic and aromatic residues (Leu, Val, Phe, Try) in the P2 position, and has a broad specificity for non-acidic residues in the P3 position (165). Using a different approach, Choe *et al*. confirmed the results obtained by Gosalia *et al.* and expanded the profile to include a survey at the P1 and P4 positions (97). They used positional scanning synthetic combinatorial library (PS-SCL) containing 160,000 tetrapeptide substrates, which together represent a complete randomization of the P1, P2, P3, and P4 positions with 20 amino acids, to profile 13 papain-like (Clan CA) cysteine proteases, including rhodesain (97)[9]. Like human cathepsins, rhodesain had a strong preference for arginine or lysine or at P1. The S2 subsite appeared to be the predominant specificity-defining factor (97) and rhodesain had a preference for hydrophobic and aromatic residues (again, Phe, Trp, Tyr, and Leu) at P2. Rhodesain also had a relatively broad specificity at P3 and P4, resembling human cathepsins L and V (97).

[9] This is the same method that was used to determine the substrate specificity of tbcatB (see Chapter 3).

Natural Cysteine Protease Inhibitors of *T. brucei*

In 2001, a novel endogenous protein cysteine protease inhibitor was identified in *T. cruzi* (166). Given the trivial name "chagasin", this inhibitor was effective against the major cysteine protease in *T. cruzi*, cruzain, as well as papain, but lacked significant homology with the members of the known classes of natural cysteine protease inhibitors like the cystatins (166). Soon after, a gene fragment encoding chagasin-like proteins was identified in *T. brucei* (167). In 2003, Sanderson *et al.* further characterized this cysteine protease inhibitor, along with homologs in *Leishmania mexicana*, *Leishmania major*, and the bacterium *Pseudomonas aeruginosa*, and found that all of these proteins inhibited papain-like cysteine proteases (168). Their results imply that there is a common evolutionary origin for bacterial and protozoan chagasin-like cysteine protease inhibitors (168).

More recently, researchers discovered that the pro-peptide of cruzain itself is a potent cysteine protease inhibitor (169). Reis *et al.* demonstrate that the full-length recombinant pro-domain of rhodesain effectively and selectively inhibits both cruzain and brucipain (169). Interestingly, the prodomain did not inhibit papain or human cathepsins S, K, or B, but it did inhibit human cathepsins V (moderately) and F (efficiently) (169).

Kanaji *et al.* reported that a member of the serpin family of protease inhibitors is an effective inhibitor of rhodesain (170). While most serpins target chymotrypsin-like serine proteases, some inhibit papain-like cysteine proteases. Squamous cell carcinoma antigen 1 (SCCA1) is a member of the later group, and the authors had shown previously that SCCA1 is induced by mediators of a Th2-type immune response (170).

Additional Cysteine Proteases in *T. brucei*

Although research concerning cysteine proteases in *T. brucei* has predominantly focused on papain-like (Clan CA, family C1) cysteine proteases, members of other families and clans have been identified.

Calpains are calcium-dependent, non-lysosomal cysteine proteases of the Clan CA, family C2. In 2005, Ersfeld *et al.* reported the identification of 18 calpain-like genes in *T. brucei*, along with an additional 27 genes in *L. major*, and 24 genes in *T. cruzi* (171). In characterizing the gene sequences, the authors found a conserved protease domain in most, while a few genes completely lacked a protease domain and were more similar to other kinetoplastid calpain-related proteins (171). Interestingly, all of the sequences lack the C-terminal calmodulin-like calcium-binding domain that is typical of mammalian calpains (171). The authors conclude that the highly modular structure of the protozoan calpains and calpain-like proteins reflects diverse cellular functions (171).

Metacaspases are subset of caspases, sharing the protease classification of Clan CD, family 14, but are unique to plants, fungi, and protozoa (172). In 2006, Helms *et al.* investigated the hypothesis that *T. brucei* metacaspases are mediators of programmed cell death by studying the expression, localization, and function of MCA2, MCA3, and MCA 4 in cultured parasites (173). The authors found that all three enzymes are essential in bloodstream form parasites (although their loss may be compensated for by alternative mechanisms) and co-localize with RAB11 positive recycling endosomes (173). However, they also determined that metacaspase-deficiency does not effect VSG recycling processes or degradation of internalized anti-VSG antibody, indicating that the *T. brucei* metacaspases have a function that is independent of known RAB11-associated

recycling processes (173). Clearly, additional research is needed to identify the function(s) of these proteases and determine whether they, in fact, play a role in programmed cell death.

CONCLUSIONS AND FUTURE DIRECTIONS FOR RESEARCH

The data presented in the preceding chapters indicate that *T. brucei* cathepsin B (tbcatB) is essential for *T. brucei* survival in culture ((117), Chapter 1) and in experimentally-infected mice (Chapter 2). Even modest knockdown of tbcatB activity by RNAi leads to parasite death under these *in vitro* and *in vivo* conditions and, although not lethal, *TBCATB* heterozygosisity impairs *T. brucei* growth in culture (Chapter 3). TbcatB-deficiency leads to a marked phenotype, with parasites exhibiting swollen flagellar pockets (Chapter 3), most likely the result of a block in endocytosis. TbcatB-deficiency is also associated with the accumulation of host and parasite proteins, including host transferrin, *T. brucei* p67, and rhodesain, indicating that the cysteine protease is required for their degradation (Chapter 1, 3, & 4). In the case of transferrin, accumulation in both knockdown and heterozygous knockout parasites proves that tbcatB is required for degradation of this key host protein (Chapter 1 and 3). Substrate specificity data (Chapter 3) and *in vitro* degradation assays (Chapter 4), performed using recombinant tbcatB, lend support to the hypothesis that a key function for tbcatB is the degradation of transferrin. Furthermore, data obtained in an iron starvation assay, along with the discovery that transferrin receptor expression is upregulated in tbcatB-deficient parasites, suggests that the lethality of tbcatB-deficiency may be caused by iron starvation. However, a number of important questions remain concerning tbcatB and its

role in promoting the survival and pathogenicity of *T. brucei*. The following offers a discussion of future directions for research to address questions arising from the research presented here and, more generally, to contribute to our understanding of cysteine protease function in *T. brucei*.

TbcatB localization- Immunoelectron microscopy analysis indicated that tbcatB localizes to lysosomal vesicles (Chapter 3). However, immunofluorescence (IFA) microscopy experiments failed to localize the enzyme to lysosomal compartments (Chapter 4). Rather, antiserum to tbcatB that was raised against recombinant enzyme expressed in *E. coli*, labeled an unidentified structure in the posterior tip of the parasite at or near the flagellar pocket (Chapter 4). Several approaches can be taken to determine whether the tbcatB antiserum labeling was accurate. First, new antibodies can be made to recombinant tbcatB from *P. pastoris*. For specific antibodies to be produced, the recombinant enzyme would be produced free of glycosylation sites, since previous attempts with the glycsolyated form of the enzyme failed to produce specific antibodies in rabbits and mice. For co-localization studies by IFA, new antibodies will need to be made in both mice and rabbits, since many of the cellular markers available for *T. brucei* are of mouse or rabbit origin and two primary antibodies from the same animal species cannot be used simultaneously. Alternatively, a *T. brucei* strain that expresses fluorescently-tagged tbcatB would be useful for co-localization, as well as trafficking, studies. Lastly, questions concerning tbcatB's localization could be addressed by developing a protocol for MNA-substrate localization in *T. brucei*. Key co-localization experiments that can be carried out by IFA once suitable antibodies, transgenic GFP-tbcatB *T. brucei*, and/or MNA-substrate localization are available are tbcatB with

rhodesain, transferrin, transferrin receptor (Tf-R), p67, and early and recycling endosomes.

Rhodesain as a potential substrate of tbcatB- Substrate specificity data for recombinant tbcatB suggests that the enzyme may process or even activate rhodesain. To address this question, an *in vitro* degradation assay should be set-up with recombinant rhodesain that has been pre-inhibited with an irreversible cathepsin L-like protease inhibitor, such as DCG-O4 (133). If recombinant tbcatB can cleave the enzyme, it would support the hypothesis that rhodesain is, in fact, a substrate. If this is the case, it would be important to determine the N-terminal sequence to see if it matches what is predicted from tbcatB substrate specificity data. A related, but more time-consuming, experiment would be to express a fluorescently-tagged version of rhodesain in *T. brucei* that cannot auto-activate and see whether tbcatB-deficiency (either in a tbcatB RNAi of TBCATB$^{+/-}$ strain) has an effect on the protein's localization or on overall protein degradation.

P67 as a potential substrate of tbcatB- The *T. brucei* lysosomal glycomembrane protein, p67, has been shown to accumulate in tbcatB-deficient parasites (Chapter 3) and may therefore represent a substrate of tbcatB. P67 is known to undergo various processing steps from the time that it is synthesized until is arrives in the lysosome (69). To investigate the hypothesis that tbcatB is involved in these processing events, Western blot analysis should be carried out to compare p67 profiles for control and tbcatB-deficient parasites. It will be important to compare results from standard lysate preparations and lysates prepared with the immediate addition of SDS to the cell, followed by boiling. Protease inhibitors could also be used in the standard lysate preparations to prevent non-

native lysis, although appropriate concentration of the inhibitors would have to be experimentally determined.

TbcatB trafficking- Immunelectron microscopy studies indicate that tbcatB is improperly trafficked in tbcatB RNAi knockdowns. The development of a transgenic *T. brucei* strain that expresses fluorescently-tagged tbcatB would aid in determining the route trafficked by tbcatB from the Golgi apparatus to its final destination(s). If developed in the pZJMTbCB strain, or if used in conjunction with cysteine proteases inhibitors, additional information about the trafficking of tbcatB could be obtained. Adding a construct for inducible expression of tbcatB in the *T. brucei* RNAi strain could also be helpful in understanding tbcatB trafficking, although the inducible expression systems that have been developed require the same drug, tetracycline, that is used to induce RNAi.

Transferrin degradation and the role of tbcatB iron acquisition- Multiple lines of evidence point to a role for tbcatB in transferrin degradation. Pal *et al*. have used a live cell assay to follow to transferrin endocytosis and degradation (135) and this assay could be used to identify and later recover transferrin degradation products from *T. brucei*. Presumably, these degradation products would have molecular weights and N-terminal sequences consistent with those predicted for tbcatB. *In vitro* transferrin degradation experiments should also be optimized in order to generate purified cleavage products that are suitable for sequencing and, thus, can be compared with degradation products obtained from *T. brucei* in culture.

However, these studies alone will not rule out the possibility that tbcatB activates rhodesain and that rhodesain then carries out the bulk of transferrin degradation. Additional information is required concerning tbcatB's ability to activate rhodesain, as

well as the rhodesain's role in transferrin degradation. The cysteine protease inhibitors used in previous studies (30,104) could have inhibited both enzymes and a good deal of rhodesain activity remained in parasites (117). Selective inhibitors for rhodesain and tbcatB would be extremely useful in determining whether rhodesain and tbcatB are both required for transferrin degradation.

One hypothesis for the lethality of tbcatB-deficiency proposed by this work is that tbcatB is required for the acquisition of iron from transferrin. In response to iron starvation induced by culturing *T. brucei* in media containing dog serum, tbcatB-deficient parasites upregulate expression of the transferrin receptor (Chapter 3). This upregulation leads to an accumulation of the receptor at the flagellar pocket (Chapter 3). This response could be explained if tbcatB plays a role in iron release by cleaving transferrin. To investigate this possibility radioactively-labeled iron could be loaded onto transferrin molecules and used in pulse-chase assays to determine the rate of iron release in tbcatB-deficient parasites. If iron is retained in the tbcatB-deficient parasites, it can be inferred that tbcatB plays a direct role in iron release.

TbcatB specific inhibitors- The most important conclusion that can be made from the work presented here is that tbcatB is a logical target for drug development. Future studies should focus on identifying cysteine protease inhibitors that are selective for tbcatB and can serve as drug leads. These efforts might also provide selective inhibitors as tools to be used to address the questions discussed above. Nevertheless, their real promise lies in aiding the development of a new chemotherapy to treat Human African Trypanosomiasis

REFERENCES

1. Organization, W. H. (Disease) Human African Trypanosomiasis: The Disease. In.
2. Organization, W. H. (2006). African Trypanosomiasis (Sleeping Sickness): Fact Sheet No. 259.
3. Organization, W. H. (2004) The World Health Report: 2004: Changing History. In.
4. Hajduk, S. L., Hager, K. M., and Esko, J. D. (1994). Human high density lipoprotein killing of African trypanosomes. *Annu Rev Microbiol*. **48**, 139-162
5. Hager, K. M., Pierce, M. A., Moore, D. R., Tytler, E. M., Esko, J. D., and Hajduk, S. L. (1994). Endocytosis of a cytotoxic human high density lipoprotein results in disruption of acidic intracellular vesicles and subsequent killing of African trypanosomes. *J Cell Biol*. **126**(1), 155-167
6. Vanhamme, L., Paturiaux-Hanocq, F., Poelvoorde, P., Nolan, D. P., Lins, L., Van Den Abbeele, J., Pays, A., Tebabi, P., Van Xong, H., Jacquet, A., Moguilevsky, N., Dieu, M., Kane, J. P., De Baetselier, P., Brasseur, R., and Pays, E. (2003). Apolipoprotein L-I is the trypanosome lytic factor of human serum. *Nature*. **422**(6927), 83-87
7. Kennedy, P. G. (2004). Human African trypanosomiasis of the CNS: current issues and challenges. *J Clin Invest*. **113**(4), 496-504
8. Roditi, I., and Clayton, C. (1999). An unambiguous nomenclature for the major surface glycoproteins of the procyclic form of Trypanosoma brucei. *Mol Biochem Parasitol*. **103**(1), 99-100
9. Organization, W. H. (Drugs) Human African trypanosomiasis, Drugs. In.

10. Immtech Pharmaceuticals, I. (2007, pipeline) Pipeline: Pafuramidine maleate (DB289). In. *Webpage*

11. University of North Carolina, C. H. U. (2000). Bill and Melinda Gate Foundation awards $15.1 million to treat African sleeping sickness, leishmaniasis. *Press release 12.18.00*.

12. Immtech Pharmaceuticals, I. (2007, oct press). Immtech Announces Interim Analysis in Phase III African Sleeping Sickness Trial. *Press release 10.4.07*.

13. Immtech Pharmaceuticals, I. (2007, jun press). US FDA Grants Orphan Drug Status to Immtech's Pafuramidine for Treatment of African Sleeping Sickness. *Press release 6.18.07*.

14. Docampo, R., and Moreno, S. N. (2003). Current chemotherapy of human African trypanosomiasis. *Parasitol Res*. **90 Supp 1**, S10-13

15. Fairlamb, A. H. (2003). Chemotherapy of human African trypanosomiasis: current and future prospects. *Trends Parasitol*. **19**(11), 488-494

16. Renslo, A. R., and McKerrow, J. H. (2006). Drug discovery and development for neglected parasitic diseases. *Nat Chem Biol*. **2**(12), 701-710

17. Berriman, M., Ghedin, E., Hertz-Fowler, C., Blandin, G., Renauld, H., Bartholomeu, D. C., Lennard, N. J., Caler, E., Hamlin, N. E., Haas, B., Bohme, U., Hannick, L., Aslett, M. A., Shallom, J., Marcello, L., Hou, L., Wickstead, B., Alsmark, U. C., Arrowsmith, C., Atkin, R. J., Barron, A. J., Bringaud, F., Brooks, K., Carrington, M., Cherevach, I., Chillingworth, T. J., Churcher, C., Clark, L. N., Corton, C. H., Cronin, A., Davies, R. M., Doggett, J., Djikeng, A., Feldblyum, T., Field, M. C., Fraser, A., Goodhead, I., Hance, Z., Harper, D., Harris, B. R.,

Hauser, H., Hostetler, J., Ivens, A., Jagels, K., Johnson, D., Johnson, J., Jones, K., Kerhornou, A. X., Koo, H., Larke, N., Landfear, S., Larkin, C., Leech, V., Line, A., Lord, A., Macleod, A., Mooney, P. J., Moule, S., Martin, D. M., Morgan, G. W., Mungall, K., Norbertczak, H., Ormond, D., Pai, G., Peacock, C. S., Peterson, J., Quail, M. A., Rabbinowitsch, E., Rajandream, M. A., Reitter, C., Salzberg, S. L., Sanders, M., Schobel, S., Sharp, S., Simmonds, M., Simpson, A. J., Tallon, L., Turner, C. M., Tait, A., Tivey, A. R., Van Aken, S., Walker, D., Wanless, D., Wang, S., White, B., White, O., Whitehead, S., Woodward, J., Wortman, J., Adams, M. D., Embley, T. M., Gull, K., Ullu, E., Barry, J. D., Fairlamb, A. H., Opperdoes, F., Barrell, B. G., Donelson, J. E., Hall, N., Fraser, C. M., Melville, S. E., and El-Sayed, N. M. (2005). The genome of the African trypanosome Trypanosoma brucei. *Science*. **309**(5733), 416-422

18. Subramaniam, C., Veazey, P., Redmond, S., Hayes-Sinclair, J., Chambers, E., Carrington, M., Gull, K., Matthews, K., Horn, D., and Field, M. C. (2006). Chromosome-wide analysis of gene function by RNA interference in the african trypanosome. *Eukaryot Cell*. **5**(9), 1539-1549

19. Mackey, Z. B., Baca, A. M., Mallari, J. P., Apsel, B., Shelat, A., Hansell, E. J., Chiang, P. K., Wolff, B., Guy, K. R., Williams, J., and McKerrow, J. H. (2006). Discovery of trypanocidal compounds by whole cell HTS of Trypanosoma brucei. *Chem Biol Drug Des*. **67**(5), 355-363

20. Vanhamme, L., Pays, E., McCulloch, R., and Barry, J. D. (2001). An update on antigenic variation in African trypanosomes. *Trends Parasitol*. **17**(7), 338-343

21. Alberts. *Molecular Biology of the Cell.* (1994) 4th Edition.

22. Gull, K. (2003). Host-parasite interactions and trypanosome morphogenesis: a flagellar pocketful of goodies. *Curr Opin Microbiol*. **6**(4), 365-370

23. Field, M. C., and Carrington, M. (2004). Intracellular membrane transport systems in Trypanosoma brucei. *Traffic*. **5**(12), 905-913

24. Michels, P. A., Bringaud, F., Herman, M., and Hannaert, V. (2006). Metabolic functions of glycosomes in trypanosomatids. *Biochim Biophys Acta*. **1763**(12), 1463-1477

25. Cross, G. A. (2002) Trypanosoma brucei culture commentary. In.

26. Overath, P., Czichos, J., and Haas, C. (1986). The effect of citrate/cis-aconitate on oxidative metabolism during transformation of Trypanosoma brucei. *Eur J Biochem*. **160**(1), 175-182

27. Bouteille, B., Millet, P., Enanga, B., Mezui Me, J., Keita, M., Jauberteau, M. O., Georges, A., and Dumas, M. (1998). [Human African trypanosomiasis, contributions of experimental models]. *Bull Soc Pathol Exot*. **91**(2), 127-132

28. Masocha, W., Rottenberg, M. E., and Kristensson, K. (2006). Minocycline impedes African trypanosome invasion of the brain in a murine model. *Antimicrob Agents Chemother*. **50**(5), 1798-1804

29. Troeberg, L., Chen, X., Flaherty, T. M., Morty, R. E., Cheng, M., Hua, H., Springer, C., McKerrow, J. H., Kenyon, G. L., Lonsdale-Eccles, J. D., Coetzer, T. H., and Cohen, F. E. (2000). Chalcone, acyl hydrazide, and related amides kill cultured Trypanosoma brucei brucei. *Mol Med*. **6**(8), 660-669

30. Scory, S., Caffrey, C. R., Stierhof, Y. D., Ruppel, A., and Steverding, D. (1999). Trypanosoma brucei: killing of bloodstream forms in vitro and in vivo by the cysteine proteinase inhibitor Z-phe-ala-CHN2. *Exp Parasitol*. **91**(4), 327-333

31. GeneDB. Trypanosoma brucei GeneDB. In.

32. Clayton, C. E. (1999). Genetic manipulation of kinetoplastida. *Parasitol Today*. **15**(9), 372-378

33. Wirtz, E., Hoek, M., and Cross, G. A. (1998). Regulated processive transcription of chromatin by T7 RNA polymerase in Trypanosoma brucei. *Nucleic Acids Res*. **26**(20), 4626-4634

34. Ramos, J. L., Martinez-Bueno, M., Molina-Henares, A. J., Teran, W., Watanabe, K., Zhang, X., Gallegos, M. T., Brennan, R., and Tobes, R. (2005). The TetR family of transcriptional repressors. *Microbiol Mol Biol Rev*. **69**(2), 326-356

35. Wirtz, E., Leal, S., Ochatt, C., and Cross, G. A. (1999). A tightly regulated inducible expression system for conditional gene knock-outs and dominant-negative genetics in Trypanosoma brucei. *Mol Biochem Parasitol*. **99**(1), 89-101

36. Shi, H., Djikeng, A., Mark, T., Wirtz, E., Tschudi, C., and Ullu, E. (2000). Genetic interference in Trypanosoma brucei by heritable and inducible double-stranded RNA. *Rna*. **6**(7), 1069-1076

37. Ngo, H., Tschudi, C., Gull, K., and Ullu, E. (1998). Double-stranded RNA induces mRNA degradation in Trypanosoma brucei. *Proc Natl Acad Sci U S A*. **95**(25), 14687-14692

38. Wang, Z., Morris, J. C., Drew, M. E., and Englund, P. T. (2000). Inhibition of Trypanosoma brucei gene expression by RNA interference using an integratable vector with opposing T7 promoters. *J Biol Chem*. **275**(51), 40174-40179

39. Morris, J. C., Wang, Z., Drew, M. E., Paul, K. S., and Englund, P. T. (2001). Inhibition of bloodstream form Trypanosoma brucei gene expression by RNA interference using the pZJM dual T7 vector. *Mol Biochem Parasitol*. **117**(1), 111-113

40. Balana-Fouce, R., and Reguera, R. M. (2007). RNA interference in Trypanosoma brucei: a high-throughput engine for functional genomics in trypanosomatids? *Trends Parasitol*. **23**(8), 348-351

41. Louis, J. M., Ishima, R., Torchia, D. A., and Weber, I. T. (2007). HIV-1 protease: structure, dynamics, and inhibition. *Adv Pharmacol*. **55**, 261-298

42. Warren, J. D., Woodward, D. L., and Hargreaves, R. T. (1977). 4-Substituted semicarbazones of mono- and dichlorobenzaldehydes as antihypertensive agents. *J Med Chem*. **20**(11), 1520-1521

43. Sajid, M., and McKerrow, J. H. (2002). Cysteine proteases of parasitic organisms. *Mol Biochem Parasitol*. **120**(1), 1-21

44. Rawlings, N. D., Tolle, D. P., and Barrett, A. J. (2004). MEROPS: the peptidase database. *Nucleic Acids Res*. **32**(Database issue), D160-164

45. Rosenthal, P. J., Lee, G. K., and Smith, R. E. (1993). Inhibition of a Plasmodium vinckei cysteine proteinase cures murine malaria. *J Clin Invest*. **91**(3), 1052-1056

46. Olson, J. E., Lee, G. K., Semenov, A., and Rosenthal, P. J. (1999). Antimalarial effects in mice of orally administered peptidyl cysteine protease inhibitors. *Bioorg Med Chem*. **7**(4), 633-638

47. Wasilewski, M. M., Lim, K. C., Phillips, J., and McKerrow, J. H. (1996). Cysteine protease inhibitors block schistosome hemoglobin degradation in vitro and decrease worm burden and egg production in vivo. *Mol Biochem Parasitol*. **81**(2), 179-189

48. Engel, J. C., Doyle, P. S., Hsieh, I., and McKerrow, J. H. (1998). Cysteine protease inhibitors cure an experimental Trypanosoma cruzi infection. *J Exp Med*. **188**(4), 725-734

49. Engel, J. C., Doyle, P. S., and McKerrow, J. H. (1999). [Trypanocidal effect of cysteine protease inhibitors in vitro and in vivo in experimental Chagas disease]. *Medicina (B Aires)*. **59 Suppl 2**, 171-175

50. Barr, S. C., Warner, K. L., Kornreic, B. G., Piscitelli, J., Wolfe, A., Benet, L., and McKerrow, J. H. (2005). A cysteine protease inhibitor protects dogs from cardiac damage during infection by Trypanosoma cruzi. *Antimicrob Agents Chemother*. **49**(12), 5160-5161

51. Doyle, P. S., Zhou, Y. M., Engel, J. C., and McKerrow, J. H. (2007). A cysteine protease inhibitor cures chagas' disease in an immunodeficient-mouse model of infection. *Antimicrob Agents Chemother*. **51**(11), 3932-3939

52. Abdulla, M. H., Lim, K. C., Sajid, M., McKerrow, J. H., and Caffrey, C. R. (2007). Schistosomiasis mansoni: novel chemotherapy using a cysteine protease inhibitor. *PLoS Med*. **4**(1), e14

53. Letch, C. A., and Gibson, W. (1981). Trypanosoma brucei: the peptidases of bloodstream trypanosomes. *Exp Parasitol*. **52**(1), 86-90

54. North, M. J., Coombs, G. H., and Barry, J. D. (1983). A comparative study of the proteolytic enzymes of Trypanosoma brucei, T. equiperdum, T. evansi, T. vivax, Leishmania tarentolae and Crithidia fasciculata. *Mol Biochem Parasitol*. **9**(2), 161-180

55. Lonsdale-Eccles, J. D., and Mpimbaza, G. W. (1986). Thiol-dependent proteases of African trypanosomes. Analysis by electrophoresis in sodium dodecyl sulphate/polyacrylamide gels co-polymerized with fibrinogen. *Eur J Biochem*. **155**(3), 469-473

56. Lonsdale-Eccles, J. D., and Grab, D. J. (1987). Lysosomal and non-lysosomal peptidyl hydrolases of the bloodstream forms of Trypanosoma brucei brucei. *Eur J Biochem*. **169**(3), 467-475

57. Mottram, J. C., North, M. J., Barry, J. D., and Coombs, G. H. (1989). A cysteine proteinase cDNA from Trypanosoma brucei predicts an enzyme with an unusual C-terminal extension. *FEBS Lett*. **258**(2), 211-215

58. Eakin, A. E., Bouvier, J., Sakanari, J. A., Craik, C. S., and McKerrow, J. H. (1990). Amplification and sequencing of genomic DNA fragments encoding cysteine proteases from protozoan parasites. *Mol Biochem Parasitol*. **39**(1), 1-8

59. Pamer, E. G., Davis, C. E., Eakin, A., and So, M. (1990). Cloning and sequencing of the cysteine protease cDNA from Trypanosoma brucei rhodesiense. *Nucleic Acids Res*. **18**(20), 6141

60. Troeberg, L., Morty, R. E., Pike, R. N., Lonsdale-Eccles, J. D., Palmer, J. T., McKerrow, J. H., and Coetzer, T. H. (1999). Cysteine proteinase inhibitors kill cultured bloodstream forms of Trypanosoma brucei brucei. *Exp Parasitol*. **91**(4), 349-355

61. Mbawa, Z. R., Gumm, I. D., Shaw, E., and Lonsdale-Eccles, J. D. (1992). Characterisation of a cysteine protease from bloodstream forms of Trypanosoma congolense. *Eur J Biochem*. **204**(1), 371-379

62. Caffrey, C. R., Hansell, E., Lucas, K. D., Brinen, L. S., Alvarez Hernandez, A., Cheng, J., Gwaltney, S. L., 2nd, Roush, W. R., Stierhof, Y. D., Bogyo, M., Steverding, D., and McKerrow, J. H. (2001). Active site mapping, biochemical properties and subcellular localization of rhodesain, the major cysteine protease of Trypanosoma brucei rhodesiense. *Mol Biochem Parasitol*. **118**(1), 61-73

63. Pamer, E. G., Davis, C. E., and So, M. (1991). Expression and deletion analysis of the Trypanosoma brucei rhodesiense cysteine protease in Escherichia coli. *Infect Immun*. **59**(3), 1074-1078

64. Troeberg, L., Pike, R. N., Morty, R. E., Berry, R. K., Coetzer, T. H., and Lonsdale-Eccles, J. D. (1996). Proteases from Trypanosoma brucei brucei. Purification, characterisation and interactions with host regulatory molecules. *Eur J Biochem*. **238**(3), 728-736

65. Pamer, E. G., So, M., and Davis, C. E. (1989). Identification of a developmentally regulated cysteine protease of Trypanosoma brucei. *Mol Biochem Parasitol*. **33**(1), 27-32

66. Mbawa, Z. R., Gumm, I. D., Fish, W. R., and Lonsdale-Eccles, J. D. (1991). Endopeptidase variations among different life-cycle stages of African trypanosomes. *Eur J Biochem*. **195**(1), 183-190

67. Grab, D. J., Wells, C. W., Shaw, M. K., Webster, P., and Russo, D. C. (1992). Endocytosed transferrin in African trypanosomes is delivered to lysosomes and may not be recycled. *Eur J Cell Biol*. **59**(2), 398-404

68. Grab, D. J., Shaw, M. K., Wells, C. W., Verjee, Y., Russo, D. C., Webster, P., Naessens, J., and Fish, W. R. (1993). The transferrin receptor in African trypanosomes: identification, partial characterization and subcellular localization. *Eur J Cell Biol*. **62**(1), 114-126

69. Brickman, M. J., and Balber, A. E. (1994). Transport of a lysosomal membrane glycoprotein from the Golgi to endosomes and lysosomes via the cell surface in African trypanosomes. *J Cell Sci*. **107 (Pt 11)**, 3191-3200

70. Alexander, D. L., Schwartz, K. J., Balber, A. E., and Bangs, J. D. (2002). Developmentally regulated trafficking of the lysosomal membrane protein p67 in Trypanosoma brucei. *J Cell Sci*. **115**(Pt 16), 3253-3263

71. Mutomba, M. C., and Wang, C. C. (1998). The role of proteolysis during differentiation of Trypanosoma brucei from the bloodstream to the procyclic form. *Mol Biochem Parasitol*. **93**(1), 11-22

72. Knowles, G., Black, S. J., and Whitelaw, D. D. (1987). Peptidase in the plasma of mice infected with Trypanosoma brucei brucei. *Parasitology*. **95 (Pt 2)**, 291-300

73. Nwagwu, M., Okenu, D. M., Olusi, T. A., and Molokwu, R. I. (1988). Trypanosoma brucei releases proteases extracellularly. *Trans R Soc Trop Med Hyg*. **82**(4), 577

74. Boutignon, F., Huet-Duvillier, G., Demeyer, D., Richet, C., and Degand, P. (1990). Study of proteolytic activities released by incubation of trypanosomes (Trypanosoma brucei brucei) in pH 5.5 and pH 7.0 phosphate/glucose buffers. *Biochim Biophys Acta*. **1035**(3), 369-377

75. Huet, G., Richet, C., Demeyer, D., Bisiau, H., Soudan, B., Tetaert, D., Han, K. K., and Degand, P. (1992). Characterization of different proteolytic activities in Trypanosoma brucei brucei. *Biochim Biophys Acta*. **1138**(3), 213-221

76. Okenu, D. M. N., and Opara, K. N. (1996). *Trypanosoma brucei*:properties of extracellularly released proteases. *J Parasitic Dis*. (20), 23-28

77. Opara, K. N., Uwem, F.E., & Okenu, D.M.N. (1994). The effect of of chloroquine on the proteins released by *Trypanosoma brucei*. *Nig J Parsitol*. (15), 145-169

78. Okenu, D. M., Opara, K. N., Nwuba, R. I., and Nwagwu, M. (1999). Purification and characterisation of an extracellularly released protease of Trypanosoma brucei. *Parasitol Res*. **85**(5), 424-428

79. Lonsdale-Eccles, J. D., Mpimbaza, G. W., Nkhungulu, Z. R., Olobo, J., Smith, L., Tosomba, O. M., and Grab, D. J. (1995). Trypanosomatid cysteine protease activity may be enhanced by a kininogen-like moiety from host serum. *Biochem J*. **305 (Pt 2)**, 549-556

80. Bishop, J. R., Shimamura, M., and Hajduk, S. L. (2001). Insight into the mechanism of trypanosome lytic factor-1 killing of Trypanosoma brucei brucei. *Mol Biochem Parasitol*. **118**(1), 33-40

81. Coppens, I., Levade, T., and Courtoy, P. J. (1995). Host plasma low density lipoprotein particles as an essential source of lipids for the bloodstream forms of Trypanosoma brucei. *J Biol Chem*. **270**(11), 5736-5741

82. Robertson, C. D., North, M. J., Lockwood, B. C., and Coombs, G. H. (1990). Analysis of the proteinases of Trypanosoma brucei. *J Gen Microbiol*. **136**(5), 921-925

83. Shaw, E. (1990). Cysteinyl proteinases and their selective inactivation. *Adv Enzymol Relat Areas Mol Biol*. **63**, 271-347

84. Kornblatt, M. J., Mpimbaza, G. W., and Lonsdale-Eccles, J. D. (1992). Characterization of an endopeptidase of Trypanosoma brucei brucei. *Arch Biochem Biophys*. **293**(1), 25-31

85. Caffrey, C. R., Scory, S., and Steverding, D. (2000). Cysteine proteinases of trypanosome parasites: novel targets for chemotherapy. *Curr Drug Targets*. **1**(2), 155-162

86. McKerrow, J. H., Engel, J. C., and Caffrey, C. R. (1999). Cysteine protease inhibitors as chemotherapy for parasitic infections. *Bioorg Med Chem*. **7**(4), 639-644

87. Du, X., Hansell, E., Engel, J. C., Caffrey, C. R., Cohen, F. E., and McKerrow, J. H. (2000). Aryl ureas represent a new class of anti-trypanosomal agents. *Chem Biol*. **7**(9), 733-742

88. Caffrey, C. R., Schanz, M., Nkemngu, N. J., Brush, M., Hansell, E., Cohen, F. E., Flaherty, T. M., McKerrow, J. H., and Steverding, D. (2002). Screening of acyl hydrazide proteinase inhibitors for antiparasitic activity against Trypanosoma brucei. *Int J Antimicrob Agents*. **19**(3), 227-231

89. Hertz-Fowler, C., Ersfeld, K., and Gull, K. (2001). CAP5.5, a life-cycle-regulated, cytoskeleton-associated protein is a member of a novel family of calpain-related proteins in Trypanosoma brucei. *Mol Biochem Parasitol*. **116**(1), 25-34

90. Szallies, A., Kubata, B. K., and Duszenko, M. (2002). A metacaspase of Trypanosoma brucei causes loss of respiration competence and clonal death in the yeast Saccharomyces cerevisiae. *FEBS Lett*. **517**(1-3), 144-150

91. Rossi, A., Deveraux, Q., Turk, B., and Sali, A. (2004). Comprehensive search for cysteine cathepsins in the human genome. *Biol Chem*. **385**(5), 363-372

92. Field, M. C., Allen, C. L., Dhir, V., Goulding, D., Hall, B. S., Morgan, G. W., Veazey, P., and Engstler, M. (2004). New approaches to the microscopic imaging of Trypanosoma brucei. *Microsc Microanal*. **10**(5), 621-636

93. Hill, K. L., Hutchings, N. R., Russell, D. G., and Donelson, J. E. (1999). A novel protein targeting domain directs proteins to the anterior cytoplasmic face of the flagellar pocket in African trypanosomes. *J Cell Sci*. **112 Pt 18**, 3091-3101

94. Salter, J. (2001). Characterization of the protease that facilitates schistosome infection. *Thesis (doctoral in Biomedical Sciences) University of California, San Francisco*.

95. Harris, J. L., Peterson, E. P., Hudig, D., Thornberry, N. A., and Craik, C. S. (1998). Definition and redesign of the extended substrate specificity of granzyme B. *J Biol Chem*. **273**(42), 27364-27373

96. Mathieu, M. A., Bogyo, M., Caffrey, C. R., Choe, Y., Lee, J., Chapman, H., Sajid, M., Craik, C. S., and McKerrow, J. H. (2002). Substrate specificity of schistosome versus human legumain determined by P1-P3 peptide libraries. *Mol Biochem Parasitol*. **121**(1), 99-105

97. Choe, Y., Leonetti, F., Greenbaum, D. C., Lecaille, F., Bogyo, M., Bromme, D., Ellman, J. A., and Craik, C. S. (2006). Substrate profiling of cysteine proteases using a combinatorial peptide library identifies functionally unique specificities. *J Biol Chem*. **281**(18), 12824-12832

98. Barrett, A. J., Tolle, D. P., and Rawlings, N. D. (2003). Managing peptidases in the genomic era. *Biol Chem*. **384**(6), 873-882

99. Ward, W., Alvarado, L., Rawlings, N. D., Engel, J. C., Franklin, C., and McKerrow, J. H. (1997). A primitive enzyme for a primitive cell: the protease required for excystation of Giardia. *Cell*. **89**(3), 437-444

100. McKerrow, J. H. (1999). Development of cysteine protease inhibitors as chemotherapy for parasitic diseases: insights on safety, target validation, and mechanism of action. *Int J Parasitol*. **29**(6), 833-837

101. Selzer, P. M., Pingel, S., Hsieh, I., Ugele, B., Chan, V. J., Engel, J. C., Bogyo, M., Russell, D. G., Sakanari, J. A., and McKerrow, J. H. (1999). Cysteine protease inhibitors as chemotherapy: lessons from a parasite target. *Proc Natl Acad Sci U S A*. **96**(20), 11015-11022

102. Shaw, E. (1988). Peptidyl sulfonium salts. A new class of protease inhibitors. *J Biol Chem*. **263**(6), 2768-2772

103. Lalmanach, G., Boulange, A., Serveau, C., Lecaille, F., Scharfstein, J., Gauthier, F., and Authie, E. (2002). Congopain from Trypanosoma congolense: drug target and vaccine candidate. *Biol Chem*. **383**(5), 739-749

104. Nkemgu, N. J., Grande, R., Hansell, E., McKerrow, J. H., Caffrey, C. R., and Steverding, D. (2003). Improved trypanocidal activities of cathepsin L inhibitors. *Int J Antimicrob Agents*. **22**(2), 155-159

105. van den Hoff, M. J., Christoffels, V. M., Labruyere, W. T., Moorman, A. F., and Lamers, W. H. (1995). Electrotransfection with "intracellular" buffer. *Methods Mol Biol*. **48**, 185-197

106. Meara, J. P., and Rich, D. H. (1996). Mechanistic studies on the inactivation of papain by epoxysuccinyl inhibitors. *J Med Chem*. **39**(17), 3357-3366

107. Bogyo, M., Verhelst, S., Bellingard-Dubouchaud, V., Toba, S., and Greenbaum, D. (2000). Selective targeting of lysosomal cysteine proteases with radiolabeled electrophilic substrate analogs. *Chem Biol*. **7**(1), 27-38

108. Illy, C., Quraishi, O., Wang, J., Purisima, E., Vernet, T., and Mort, J. S. (1997). Role of the occluding loop in cathepsin B activity. *J Biol Chem*. **272**(2), 1197-1202

109. Goulet, B., Baruch, A., Moon, N. S., Poirier, M., Sansregret, L. L., Erickson, A., Bogyo, M., and Nepveu, A. (2004). A cathepsin L isoform that is devoid of a signal peptide localizes to the nucleus in S phase and processes the CDP/Cux transcription factor. *Mol Cell*. **14**(2), 207-219

110. Barrett, A. J., Kembhavi, A. A., Brown, M. A., Kirschke, H., Knight, C. G., Tamai, M., and Hanada, K. (1982). L-trans-Epoxysuccinyl-leucylamido(4-guanidino)butane (E-64) and its analogues as inhibitors of cysteine proteinases including cathepsins B, H and L. *Biochem J.* **201**(1), 189-198

111. Shi, G. P., Munger, J. S., Meara, J. P., Rich, D. H., and Chapman, H. A. (1992). Molecular cloning and expression of human alveolar macrophage cathepsin S, an elastinolytic cysteine protease. *J Biol Chem*. **267**(11), 7258-7262

112. Woodward, R., and Gull, K. (1990). Timing of nuclear and kinetoplast DNA replication and early morphological events in the cell cycle of Trypanosoma brucei. *J Cell Sci*. **95 (Pt 1)**, 49-57

113. Crouch, S. P., Kozlowski, R., Slater, K. J., and Fletcher, J. (1993). The use of ATP bioluminescence as a measure of cell proliferation and cytotoxicity. *J Immunol Methods*. **160**(1), 81-88

114. Turk, D., Podobnik, M., Popovic, T., Katunuma, N., Bode, W., Huber, R., and Turk, V. (1995). Crystal structure of cathepsin B inhibited with CA030 at 2.0-A resolution: A basis for the design of specific epoxysuccinyl inhibitors. *Biochemistry*. **34**(14), 4791-4797

115. Eakin, A. E., Mills, A. A., Harth, G., McKerrow, J. H., and Craik, C. S. (1992). The sequence, organization, and expression of the major cysteine protease (cruzain) from Trypanosoma cruzi. *J Biol Chem*. **267**(11), 7411-7420

116. Nobrega, O. T., Santos Silva, M. A., Teixeira, A. R., and Santana, J. M. (1998). Cloning and sequencing of tccb, a gene encoding a Trypanosoma cruzi cathepsin B-like protease. *Mol Biochem Parasitol*. **97**(1-2), 235-240

117. Mackey, Z. B., O'Brien, T. C., Greenbaum, D. C., Blank, R. B., and McKerrow, J. H. (2004). A cathepsin B-like protease is required for host protein degradation in Trypanosoma brucei. *J Biol Chem*. **279**(46), 48426-48433

118. Triggs, V. P., and Bangs, J. D. (2003). Glycosylphosphatidylinositol-dependent protein trafficking in bloodstream stage Trypanosoma brucei. *Eukaryot Cell*. **2**(1), 76-83

119. Lecordier, L., Walgraffe, D., Devaux, S., Poelvoorde, P., Pays, E., and Vanhamme, L. (2005). Trypanosoma brucei RNA interference in the mammalian host. *Mol Biochem Parasitol*. **140**(1), 127-131

120. Hamadien, M., Bakhiet, M., and Harris, R. A. (2000). Interferon-gamma induces secretion of trypanosome lymphocyte triggering factor via tyrosine protein kinases. *Parasitology*. **120 (Pt 3)**, 281-287

121. Livak, K. J., and Schmittgen, T. D. (2001). Analysis of relative gene expression data using real-time quantitative PCR and the 2(-Delta Delta C(T)) Method. *Methods*. **25**(4), 402-408

122. Nikolskaia, O. V., de, A. L. A. P., Kim, Y. V., Lonsdale-Eccles, J. D., Fukuma, T., Scharfstein, J., and Grab, D. J. (2006). Blood-brain barrier traversal by African trypanosomes requires calcium signaling induced by parasite cysteine protease. *J Clin Invest*. **116**(10), 2739-2747

123. Rawlings, N. D., Tolle, D.P. & Barrett, A.J. (2004) *MEROPS*: the Peptidase Database (Release 7.90). In.

124. Scory, S., Stierhof, Y. D., Caffrey, C. R., and Steverding, D. (2007). The cysteine proteinase inhibitor Z-Phe-Ala-CHN2 alters cell morphology and cell division

activity of Trypanosoma brucei bloodstream forms in vivo. *Kinetoplastid Biol Dis*. **6**, 2

125. Steverding, D. (2000). The transferrin receptor of Trypanosoma brucei. *Parasitol Int*. **48**(3), 191-198

126. Kelley, R. J., Alexander, D. L., Cowan, C., Balber, A. E., and Bangs, J. D. (1999). Molecular cloning of p67, a lysosomal membrane glycoprotein from Trypanosoma brucei. *Mol Biochem Parasitol*. **98**(1), 17-28

127. Mussmann, R., Janssen, H., Calafat, J., Engstler, M., Ansorge, I., Clayton, C., and Borst, P. (2003). The expression level determines the surface distribution of the transferrin receptor in Trypanosoma brucei. *Mol Microbiol*. **47**(1), 23-35

128. Buttle, D. J., Murata, M., Knight, C. G., and Barrett, A. J. (1992). CA074 methyl ester: a proinhibitor for intracellular cathepsin B. *Arch Biochem Biophys*. **299**(2), 377-380

129. Berman, H. M., Westbrook, J., Feng, Z., Gilliland, G., Bhat, T. N., Weissig, H., Shindyalov, I. N., and Bourne, P. E. (2000). The Protein Data Bank. *Nucleic Acids Res*. **28**(1), 235-242

130. Rice, P., Longden, I., and Bleasby, A. (2000). EMBOSS: the European Molecular Biology Open Software Suite. *Trends Genet*. **16**(6), 276-277

131. Obenauer, J. C., Cantley, L. C., and Yaffe, M. B. (2003). Scansite 2.0: Proteome-wide prediction of cell signaling interactions using short sequence motifs. *Nucleic Acids Res*. **31**(13), 3635-3641

132. Bradford, M. M. (1976). A rapid and sensitive method for the quantitation of microgram quantities of protein utilizing the principle of protein-dye binding. *Anal Biochem*. **72**, 248-254

133. Greenbaum, D., Medzihradszky, K. F., Burlingame, A., and Bogyo, M. (2000). Epoxide electrophiles as activity-dependent cysteine protease profiling and discovery tools. *Chem Biol*. **7**(8), 569-581

134. Loeb, C. R., Harris, J. L., and Craik, C. S. (2006). Granzyme B proteolyzes receptors important to proliferation and survival, tipping the balance toward apoptosis. *J Biol Chem*. **281**(38), 28326-28335

135. Pal, A., Hall, B. S., Jeffries, T. R., and Field, M. C. (2003). Rab5 and Rab11 mediate transferrin and anti-variant surface glycoprotein antibody recycling in Trypanosoma brucei. *Biochem J*. **374**(Pt 2), 443-451

136. Kabiri, M., and Steverding, D. (2000). Studies on the recycling of the transferrin receptor in Trypanosoma brucei using an inducible gene expression system. *Eur J Biochem*. **267**(11), 3309-3314

137. Mussmann, R., Engstler, M., Gerrits, H., Kieft, R., Toaldo, C. B., Onderwater, J., Koerten, H., van Luenen, H. G., and Borst, P. (2004). Factors affecting the level and localization of the transferrin receptor in Trypanosoma brucei. *J Biol Chem*. **279**(39), 40690-40698

138. van Luenen, H. G., Kieft, R., Mussmann, R., Engstler, M., ter Riet, B., and Borst, P. (2005). Trypanosomes change their transferrin receptor expression to allow effective uptake of host transferrin. *Mol Microbiol*. **58**(1), 151-165

139. Gerrits, H., Mussmann, R., Bitter, W., Kieft, R., and Borst, P. (2002). The physiological significance of transferrin receptor variations in Trypanosoma brucei. *Mol Biochem Parasitol*. **119**(2), 237-247

140. Brooks, D. R., Tetley, L., Coombs, G. H., and Mottram, J. C. (2000). Processing and trafficking of cysteine proteases in Leishmania mexicana. *J Cell Sci*. **113 (Pt 22)**, 4035-4041

141. Mottram, J. C., Frame, M. J., Brooks, D. R., Tetley, L., Hutchison, J. E., Souza, A. E., and Coombs, G. H. (1997). The multiple cpb cysteine proteinase genes of Leishmania mexicana encode isoenzymes that differ in their stage regulation and substrate preferences. *J Biol Chem*. **272**(22), 14285-14293

142. Hall, B., Allen, C. L., Goulding, D., and Field, M. C. (2004). Both of the Rab5 subfamily small GTPases of Trypanosoma brucei are essential and required for endocytosis. *Mol Biochem Parasitol*. **138**(1), 67-77

143. Garcia-Salcedo, J. A., Perez-Morga, D., Gijon, P., Dilbeck, V., Pays, E., and Nolan, D. P. (2004). A differential role for actin during the life cycle of Trypanosoma brucei. *Embo J*. **23**(4), 780-789

144. Allen, C. L., Goulding, D., and Field, M. C. (2003). Clathrin-mediated endocytosis is essential in Trypanosoma brucei. *Embo J*. **22**(19), 4991-5002

145. Kelley, R. J., Brickman, M. J., and Balber, A. E. (1995). Processing and transport of a lysosomal membrane glycoprotein is developmentally regulated in African trypanosomes. *Mol Biochem Parasitol*. **74**(2), 167-178

146. de Meester, F., Shaw, E., Scholze, H., Stolarsky, T., and Mirelman, D. (1990). Specific labeling of cysteine proteinases in pathogenic and nonpathogenic Entamoeba histolytica. *Infect Immun*. **58**(5), 1396-1401

147. Bangs, J. D., Brouch, E. M., Ransom, D. M., and Roggy, J. L. (1996). A soluble secretory reporter system in Trypanosoma brucei. Studies on endoplasmic reticulum targeting. *J Biol Chem*. **271**(31), 18387-18393

148. Kilmartin, J. V., Wright, B., and Milstein, C. (1982). Rat monoclonal antitubulin antibodies derived by using a new nonsecreting rat cell line. *J Cell Biol*. **93**(3), 576-582

149. Tu, X., and Wang, C. C. (2005). Pairwise knockdowns of cdc2-related kinases (CRKs) in Trypanosoma brucei identified the CRKs for G1/S and G2/M transitions and demonstrated distinctive cytokinetic regulations between two developmental stages of the organism. *Eukaryot Cell*. **4**(4), 755-764

150. Field, H., Farjah, M., Pal, A., Gull, K., and Field, M. C. (1998). Complexity of trypanosomatid endocytosis pathways revealed by Rab4 and Rab5 isoforms in Trypanosoma brucei. *J Biol Chem*. **273**(48), 32102-32110

151. Jeffries, T. R., Morgan, G. W., and Field, M. C. (2001). A developmentally regulated rab11 homologue in Trypanosoma brucei is involved in recycling processes. *J Cell Sci*. **114**(Pt 14), 2617-2626

152. Balber, A. E., and Frommel, T. O. (1988). Trypanosoma brucei gambiense and T. b. rhodesiense: concanavalin A binding to the membrane and flagellar pocket of bloodstream and procyclic forms. *J Protozool*. **35**(2), 214-219

153. Brickman, M. J., Cook, J. M., and Balber, A. E. (1995). Low temperature reversibly inhibits transport from tubular endosomes to a perinuclear, acidic compartment in African trypanosomes. *J Cell Sci*. **108 (Pt 11)**, 3611-3621

154. Wehland, J., and Willingham, M. C. (1983). A rat monoclonal antibody reacting specifically with the tyrosylated form of alpha-tubulin. II. Effects on cell movement, organization of microtubules, and intermediate filaments, and arrangement of Golgi elements. *J Cell Biol*. **97**(5 Pt 1), 1476-1490

155. Huete-Perez, J. A., Engel, J. C., Brinen, L. S., Mottram, J. C., and McKerrow, J. H. (1999). Protease trafficking in two primitive eukaryotes is mediated by a prodomain protein motif. *J Biol Chem*. **274**(23), 16249-16256

156. Engstler, M., Pfohl, T., Herminghaus, S., Boshart, M., Wiegertjes, G., Heddergott, N., and Overath, P. (2007). Hydrodynamic flow-mediated protein sorting on the cell surface of trypanosomes. *Cell*. **131**(3), 505-515

157. Tsuji, S., Kato, H., Matsuoka, Y., and Fukushima, T. (1984). Molecular weight heterogeneity of bovine serum transferrin. *Biochem Genet*. **22**(11-12), 1145-1159

158. Delcroix, M., Medzihradsky, K., Caffrey, C. R., Fetter, R. D., and McKerrow, J. H. (2007). Proteomic analysis of adult S. mansoni gut contents. *Mol Biochem Parasitol*. **154**(1), 95-97

159. Greenbaum, D. C., Mackey, Z., Hansell, E., Doyle, P., Gut, J., Caffrey, C. R., Lehrman, J., Rosenthal, P. J., McKerrow, J. H., and Chibale, K. (2004). Synthesis and structure-activity relationships of parasiticidal thiosemicarbazone cysteine protease inhibitors against Plasmodium falciparum, Trypanosoma brucei, and Trypanosoma cruzi. *J Med Chem*. **47**(12), 3212-3219

160. Du, X., Guo, C., Hansell, E., Doyle, P. S., Caffrey, C. R., Holler, T. P., McKerrow, J. H., and Cohen, F. E. (2002). Synthesis and structure-activity relationship study of potent trypanocidal thio semicarbazone inhibitors of the trypanosomal cysteine protease cruzain. *J Med Chem*. **45**(13), 2695-2707

161. Fujii, N., Mallari, J. P., Hansell, E. J., Mackey, Z., Doyle, P., Zhou, Y. M., Gut, J., Rosenthal, P. J., McKerrow, J. H., and Guy, R. K. (2005). Discovery of potent thiosemicarbazone inhibitors of rhodesain and cruzain. *Bioorg Med Chem Lett.* **15**(1), 121-123

162. Vicik, R., Busemann, M., Gelhaus, C., Stiefl, N., Scheiber, J., Schmitz, W., Schulz, F., Mladenovic, M., Engels, B., Leippe, M., Baumann, K., and Schirmeister, T. (2006). Aziridide-based inhibitors of cathepsin L: synthesis, inhibition activity, and docking studies. *ChemMedChem*. **1**(10), 1126-1141

163. McDowell, M. A., Ransom, D. M., and Bangs, J. D. (1998). Glycosylphosphatidylinositol-dependent secretory transport in Trypanosoma brucei. *Biochem J*. **335 (Pt 3)**, 681-689

164. Grab, D. J., Nikolskaia, O., Kim, Y. V., Lonsdale-Eccles, J. D., Ito, S., Hara, T., Fukuma, T., Nyarko, E., Kim, K. J., Stins, M. F., Delannoy, M. J., Rodgers, J., and Kim, K. S. (2004). African trypanosome interactions with an in vitro model of the human blood-brain barrier. *J Parasitol*. **90**(5), 970-979

165. Gosalia, D. N., Salisbury, C. M., Ellman, J. A., and Diamond, S. L. (2005). High throughput substrate specificity profiling of serine and cysteine proteases using solution-phase fluorogenic peptide microarrays. *Mol Cell Proteomics*. **4**(5), 626-636

166. Monteiro, A. C., Abrahamson, M., Lima, A. P., Vannier-Santos, M. A., and Scharfstein, J. (2001). Identification, characterization and localization of chagasin, a tight-binding cysteine protease inhibitor in Trypanosoma cruzi. *J Cell Sci*. **114**(Pt 21), 3933-3942

167. Rigden, D. J., Mosolov, V. V., and Galperin, M. Y. (2002). Sequence conservation in the chagasin family suggests a common trend in cysteine proteinase binding by unrelated protein inhibitors. *Protein Sci*. **11**(8), 1971-1977

168. Sanderson, S. J., Westrop, G. D., Scharfstein, J., Mottram, J. C., and Coombs, G. H. (2003). Functional conservation of a natural cysteine peptidase inhibitor in protozoan and bacterial pathogens. *FEBS Lett*. **542**(1-3), 12-16

169. Reis, F. C., Costa, T. F., Sulea, T., Mezzetti, A., Scharfstein, J., Bromme, D., Menard, R., and Lima, A. P. (2007). The propeptide of cruzipain--a potent selective inhibitor of the trypanosomal enzymes cruzipain and brucipain, and of the human enzyme cathepsin F. *Febs J*. **274**(5), 1224-1234

170. Kanaji, S., Tanaka, Y., Sakata, Y., Takeshita, K., Arima, K., Ohta, S., Hansell, E. J., Caffrey, C., Mottram, J. C., Lowther, J., Donnelly, S., Stack, C., Kadowaki, T., Yamamoto, K., McKerrow, J. H., Dalton, J. P., Coombs, G. H., and Izuhara, K. (2007). Squamous cell carcinoma antigen 1 is an inhibitor of parasite-derived cysteine proteases. *FEBS Lett*. **581**(22), 4260-4264

171. Ersfeld, K., Barraclough, H., and Gull, K. (2005). Evolutionary relationships and protein domain architecture in an expanded calpain superfamily in kinetoplastid parasites. *J Mol Evol*. **61**(6), 742-757

172. Mottram, J. C., Helms, M. J., Coombs, G. H., and Sajid, M. (2003). Clan CD cysteine peptidases of parasitic protozoa. *Trends Parasitol*. **19**(4), 182-187

173. Helms, M. J., Ambit, A., Appleton, P., Tetley, L., Coombs, G. H., and Mottram, J. C. (2006). Bloodstream form Trypanosoma brucei depend upon multiple metacaspases associated with RAB11-positive endosomes. *J Cell Sci*. **119**(Pt 6), 1105-1117

UCSF LIBRARY RELEASE

Publishing Agreement

It is the policy of the University to encourage the distribution of all theses and dissertations. Copies of all UCSF theses and dissertations will be routed to the library via the Graduate Division. The library will make all theses and dissertations accessible to the public and will preserve these to the best of their abilities, in perpetuity.

I hereby grant permission to the Graduate Division of the University of California, San Francisco to release copies of my thesis or dissertation to the Campus Library to provide access and preservation, in whole or in part, in perpetuity.

12/12/07

Author Signature

Date